筑　波　大　学

博　士　（医学）　学　位　論　文

Novel dominant screening scheme identified mutations of the *Sim1* and *Mc4r* genes in obese pedigrees

（新規の優性遺伝スクリーニング法による、
肥満マウス家系における ***Sim1*** および ***Mc4r***
遺伝子変異の同定）

2016

筑波大学大学院博士課程人間総合科学研究科

Md. Sarowar Hossain

Acknowledgement

Regarding the outcome of this thesis, I take an opportunity to express my sincere gratitude, profound thankfulness, deep appreciation, indebtedness and heartfelt reverence to my supervisor Prof. Masashi Yanagisawa M.D. Ph.D., Director, World Premier International Research Center (WPI), International Institute for Integrative Sleep Medicine (IIIS), Center for Behavioral Molecular Genetics (FIRST), University of Tsukuba, Japan, for his keen supervision, authoritative guidance, valuable suggestions, generous help, proper direction and untold patience during the entire period of the research project.

I also indebted and best regarded to a great extent with a sincere gratitude and profound thankfulness to my co-supervisor Prof. Hiromasa Funato M.D. Ph.D., World Premier International Research Center (WPI), International Institute for Integrative Sleep Medicine (IIIS), Center for Behavioral Molecular Genetics (FIRST), University of Tsukuba, Japan for his active supervision, special guidance and wise advices.

I express my special gratitude and indebtedness to Shigeharu Wakana Ph.D., Team leader, Technology and Development Team for Mouse Phenotype Analysis, Japan Mouse Clinic, RIKEN Bio Resource Center (BRC), Japan for his precise guidance, wise advice, and kind co-operation during the course of my research work.

I take the opportunity to express my best regards and gratefulness to Dr. Chika Miyoshi, Dr. Tomoyuki Fujiyama, Dr. Hideki Kaneda, Dr. Tomohiro Suzuki, Dr. Ikuo Miura, Dr. Makito Sato, Dr. Kumar Vivek, Dr. Joseph S. Takahashi for their affection, sympathy, valuable suggestions and co-operation throughout the period of my research work.

I thankfully acknowledge my indebtedness and gratitude to Fuyuki Asano, Aya Ikkyu, Satomi Kanno, Noriko Hotta, Miyo Kakizaki, Takato Honda, Staci J. Kim, Haruna Komiya, Kimio Kobayashi, for spending time out of their busy schedule during my research work and to Dr. Muratani for supporting the whole-exome sequencing for this study.

I appreciate the great assistance rendered by the all members of World Premier International Research Center (WPI), International Institute for Integrative Sleep Medicine (IIIS), Yanagisawa/ Funato laboratory, Technology and Development Team for Mouse Phenotype Analysis, Japan Mouse Clinic, RIKEN Bio Resource Center (BRC), Japan for their cordial co-operation.

I express my gratefulness to my parents, my wife and all the members of my family and relatives for their moral and endurance hardship, affection and blessings that have enabled me to accomplish this study.

Finally, I would like to express my sincere and heartiest thank to all of the supporter of this research grant [The Ministry of Education, Culture, Sports, Science and Technology (MEXT), The Funding Program for World-Leading Innovative R&D on Science and Technology (FIRST program), The Japan Society for the Promotion of Science (JSPS). The Uehara Memorial Foundation and a research grant from the Takeda Science Foundation, Technology and Development Team for Mouse Phenotype Analysis, Japan Mouse Clinic, RIKEN Bio Resource Center (BRC), Japan].

(Md. Sarowar Hossain)

論 文 概 要

目　　的：

われわれの研究室では、睡眠覚醒制御に関わる新規遺伝子を同定するために５０００匹以上のランダム点突然変異マウスのスクリーニングを実施してきた。その過程で、変異マウスの中に顕著な肥満を呈するものが少数認められた。これらの変異マウスは、化学変異原であるエチルニトロソウレアを投与した雄と野生型雌との交配で得られたマウスであるため、遺伝子変異が肥満を惹き起こしたとすれば、その遺伝子変異は肥満を惹き起こす優性変異と考えられる。しかしながら、これまでランダム点突然変異マウスのスクリーニングによって、肥満を惹起する劣性変異はいくつか報告があるものの、優性変異については報告がない。

これまで、肥満マウスの優性スクリーニングが成功していない理由として、次の２つが考えられる。１）変異を導入するストレインとカウンターストレイン間の量的形質座位（quantitative trait locus）の影響のために、肥満家系の樹立や表現型に基づく遺伝子型の類推が困難である。２）肥満マウスは妊孕性が低下するため、肥満家系の樹立と維持が困難である。また、フォワード・ジェネティクス一般の大きな欠点は time-consuming であることであり、研究が順調に進展した場合でも遺伝子を同定するまでに数年以上の時間がかかるという問題がある。

われわれの優性スクリーニングの研究では、変異ストレインとカウンターストレインとして C57BL/6（B6)サブストレインである B6J と B6N を用いているため、量的形質 座位の影響は無視できる。また、次世代作成には自然交配ではなく体外受精を行いているので、妊孕性の低いマウス家系も維持できる。さらに、次世代シーケンス技術の進展により全エクソームシーケンスを用いた変異同定が可能となったことによる全工程の時間短縮が可能となった。このように、われわれのスクリーニングスキームでは、肥満の優性変異スクリーニン

グ遂行における障壁がクリアされていることから、スクリーニングで見出された肥満マウスの次世代を作成し、肥満の優性スクリーニングを実施した。

研究の目的は２つある。１つは、我々の優性スクリーニングスキームの有効性検討である。過去に成功していない肥満の優性スクリーニングに成功すれば、我々のスクリーニングスキームが有用なものであり、肥満以外の表現型にも援用できる可能性を示唆する。もう１つの目的は、優性に肥満を惹起する遺伝子変異の同定である。この遺伝子がこれまでエネルギー代謝への関与が知られていないものである場合、肥満形成に関与する新たな分子を同定することになる。

対象と方法：

８－１０週齢の雄 B6J マウスにエチルニトロソウレアを２回腹腔内投与した。その後１０週以上経過して、妊孕性が回復した後に、野生型雌マウス卵と体外受精を行った。次世代マウスの３割以上が肥満を示した場合に、遺伝性があると判定した。肥満家系の N2 世代マウス（B6J を B6N に２回戻し交配）を用いて、連鎖解析を行った。連鎖解析には最近公表された B6J と B6N 間の一塩基多型データを用いた。全エクソームシーケンスはつくば i-Laboratory に委託した。マウスの体重、血糖、インスリン、レプチンを測定した。また、視床下部より RNA を調整し、定量的 PCR により視床下部の神経ペプチドの定量をおこなった。SIM1 と ARNT2 による転写活性を検討するため、ルシフェラーゼアッセイを行った。

結　　果：

ランダム点突然変異を持つマウスの中から、１０、１８、２８週齢において最も肥満したマウスを合計１３匹選んだ。体外受精によって次世代を作成したところ、１３家系のうち２家系で約半数の個体が肥満を示した。他の家系には、肥満の遺伝は認められなかった。遺伝性の肥満を示す２家系の連鎖解析を行ったところ、１０番染色体と１８番染色体に連鎖が認められた。全エクソームシーケンスにより、１０番染色体上の連鎖領域に Sim1 遺伝子の変異

が、１８番染色体上の連鎖領域に Mc4r 遺伝子の変異が認められた。遺伝子変異は SIM1 蛋白質 PAS ドメイン内のアミノ酸置換をもたらし、変異型 SIM1 蛋白質はルシフェラーゼアッセイにおいて転写活性を全く示さなかった。一方、Mc4r 遺伝子の遺伝子変異は、第一膜貫通ドメイン直前に終止コドンをもたらす。

Sim1 ヘテロ変異、Mc4r ヘテロ変異、高脂肪食誘導性肥満という機序の異なる肥満モデルマウスの視床下部において、摂食行動やエネルギー代謝に関与する神経ペプチドの発現を検討したが、肥満モデルごとに全く異なる傾向であった。

考　　察：

C57BL/6 サブストレインを使用することで、はじめて肥満の優性スクリーニングに成功した。家系の樹立から遺伝子変異の同定まで、実質的に２年程度であった。見出した遺伝子変異は Sim1 と Mc4r であり、どちらも機能欠失型の変異である。過去の報告から Sim1 と Mc4r とも haploinsufficiency によって肥満を呈することが知られており、今回見出した遺伝子変異が肥満の原因になると考えられる。見出された遺伝子はいずれもエネルギー代謝において重要な役割を持つことが知られている遺伝子である。エネルギー代謝に関与する多くの遺伝子がすでに知られていることから、新たなエネルギー代謝制御遺伝子を見つけることはかなり難しそうである。

結　　論：

C57BL/6 サブストレイン、体外受精、全エクソームシーケンスを組み合わせたフォワード・ジェネティクス研究は感度が良く、家系の維持が安定している。肥満以外の表現型への応用が可能である。

Abstract

Purpose:

In order to identify a gene essential for a defined biological phenomena, forward genetic strategy acts as one of the most influential approaches and enables us to understand the genetic basis of human biology and disease, when applied in model animals such as fruit fly and mouse. The forward genetic strategy that is a phenotype-driven and hypothesis-free approach, will help to identify novel genes which may play a crucial role in the target behaviors. The forward genetic study demonstrates its strength in research areas in which a gene-targeting approach would not work because of the redundant and compensatory regulation of target phenotypes. Although the forward genetics is usually a time-consuming project, which usually takes more than five years from the phenotype screening to identify a candidate gene mutation, the recent advance in DNA sequencing technology have been sped up the process from the linkage analysis to identified candidate mutations.

In order to identify novel genes regulating sleep/wakefulness, our laboratory has been undertaken a large-scale forward genetic screen of sleep abnormalities. Through the screening, we found several mutagenized mice that showed severe obesity. Since we were looking for dominant phenotypes, severe obesity of these mice could be inheritable in a dominant manner. Although there had been no successful dominant screening for obesity, we hypothesized that two major reasons of no success are: 1) the quantitative trait locus between the mutagenized mice strain and counter strain may make the effect of mutations obscure, 2) mice with severe obesity usually exhibit a very low fertility so that it is very difficult to establish and keep dominantly obese pedigrees. One of the two major characteristics of our forward genetic scheme is the use of C57BL/6 (B6) substrains, B6J and B6N for the mutagenized and counterstrains. B6J and B6N are very similar in metabolic phenotypes consistent with a close phylogenetic distance, which is suitable to detect the metabolic effect

of mutations reliably. Another characteristic is the routine use of in vitro fertilization, which enables us to establish and keep pedigrees of mice that show low fertility in natural breeding. Thus, our dominant screening scheme may overcome the issues that led to abort dominant screening of obesity in the past studies.

The purpose of the current study was two-fold; i) to evaluate the efficiency and reproducibility of our new forward genetic scheme by conducting the dominant screening of obesity, 2) to identify the gene mutation that causes obesity in a dominant inheritance. If the identified gene is a novel player in the homeostasis of energy metabolism, the mutant mice may afford a new genetic model for the human metabolic syndrome, as well as new insights into the pathophysiology of obesity.

Material and methods:

In parallel with examining the sleep/wakefulness abnormalities we have dominantly screened the same ENU mutagenized mice for obesity using C57BL/6 substrains. Initially, intraperitoneal injection of ENU was given to the wild-type male C57BL/6J mice at 8-10 weeks of age. After a sterile period (10-11 weeks) the injected males were crossed (IVF) with C57BL/6J or C57BL/6N wild-type female to produce G1/F1 progeny. Phenotypic screens of G1/F1 progeny were routinely carried out. The phenodeviant F1 male mice were again mated (IVF) with C57BL/6N wild-type females to produce N2 progeny. The N2 progeny was then subjected to the inheritance testing of obesity and linkage analysis. Further, by whole exome sequencing as well as direct sequencing the mutation of candidate gene of the established pedigrees was identified. Subsequently, assay of transcriptional activity, metabolic characterization and quantitation of hypothalamic gene expression was performed to observe the role of candidate gene mutation.

Result:

In this dominant screening, total thirteen G1/F1 obese male were selected to establish obesity pedigrees. Among them, we have established two obese pedigrees. Linkage analysis of one obese pedigree showed a single LOD score peak on the chromosome 18. In this case, we found a single nucleotide substitution of *Mc4r* gene in obese mutant mice, which results in a premature stop codon in the first transmembrane domain of *Mc4r* protein. Linkage analysis of another obese pedigree exhibited a single peak of LOD score on chromosome 10. Through the whole exome sequencing and direct sequencing, we found a single nucleotide substitution of the *Sim1* gene, which causes a nonsynonymous change of a well-conserved residue in the PAS A domain, crucial for functional dimer formation with *Arnt2*. As predicted, We further confirmed using luciferase assay that the mutant *Sim1* protein lacks transcriptional activity. Therefore, through the metabolic assay both of the obese pedigrees showed a strong correlation with the human and mice having heterozygous in *Mc4r* or *Sim1* gene. Because both *Sim1* and *Mc4r* are expressed in the hypothalamus, a regulatory center of feeding and energy metabolism, we examined hypothalamic gene expression of *Sim1* mutant and *Mc4r* mutant mice, and further compared with those of high-fat diet-induced obesity (DIO) mice. All three obese mice showed decrease in *Avp* mRNA. Both *Sim1* mutant and DIO mice had a lower level of *Agrp* mRNA. The *Sim1* mutant mice exhibited decreased level of *Orexin, Oxytocin* and *Trh1* mRNAs Whereas, DIO mice showed a decrease in *Pacap* and *Ghrh* mRNAs. These findings confirm that the crucial roles of *Sim1* and *Mc4r* in maintaining energy homeostasis and substantiate the sensitivity of our forward genetic screening as well.

Discussion:

Through the dominant screening of obesity using B6 substrains, we have established two obese pedigrees. One pedigree showed mutation in *Mc4r* gene and another showed mutation in *Sim1* gene. To the best of our knowledge, this is the first successful dominant screening of

obesity. One of the main reasons of the successful dominant screening may be the use of B6 substring as the mutagenized and counter strains. Since B6J and B6N have the almost same genetic background and there is no significant QTL between them regarding body weight, the phenotypic change exhibited a very well correlation with the presence of mutation in the *Mc4r* and *Sim1*.

Since obesity strongly affects the fertility, it is very difficult to produce the next generation by natural mating between the obese mice. Thus, in vitro fertilization is required to obtain offspring of obese mice. After the heritable test of obesity phenotype, a linkage analysis and subsequent whole exome sequencing enabled us to identify the candidate gene mutations in the obese mice. Further, a direct sequencing confirms the presence of mutations in the *Mc4r* and *Sim1* genes in *Obese-10* pedigree and *Obese-13* pedigree, respectively.

The founders of the *Obese-10* and *Obese-13* pedigrees were the most obese mice among all 5000 G1/F1 males. Thus, a strong phenotype that negates the fluctuation of body weight due to other correlated factors is necessary for the successful dominant screening for obesity. Therefore, it would be very difficult to succeed in dominant screening if the obesity caused by mild or moderate effect of genetic mutation or by the strong effect of other correlated factors.

The metabolic phenotypes of *Obese-10* and *Obese-13* pedigrees were consistent with those of heterozygous *Mc4r* or *Sim1* deficient mice, respectively. Further, the decreased transcriptional activity of SIM1(136K) protein found with a luciferase assay demonstrates that the loss of function of SIM1 protein may render *Obese-13* mutant mice overweight. Finally, the quantitation of hypothalamic gene expressions of these obese mutant pedigrees along with diet-induced obesity mice exhibits distinct gene expression patterns in the hypothalamus.

Conclusion:

This dominant screening of obesity in ENU-mutagenized mice successfully established two obese pedigrees and identified the candidate genes. Thus, this dominant screening strategy using C57BL/6 substrains would be a very applicable method in obesity screening or in any research area to identify the candidate gene that affects a variety of behavioral and metabolic phenotypes.

Table of contents

Contents **Page No.**

Contents

List of tables

Chapter 1.
Introduction and review of literature

1.1. Factors affecting the efficiency of forward genetic screening using mice

1.1.1. General introduction of screening of randomly mutagenized mice

Forward genetics:

The term forward genetic encompasses several means of identifying the genotype that is responsible for a phenotype. Forward genetic comprises of assortment a biological process, produces mutant population, screen for mutant with a preferred phenotype, map and clone the gene responsible for the phenotype[1]. Forward genetic approach starts with an ask on behalf of particular biological characteristic disease (e.g. obesity), and to know about the responsible gene that supports the produced occurrence[1] and is very useful in identifying molecular maps of the pathways controlling basic biological functions of a given trait[2]. To understand the genetic basis of human biology and disease using any model animals such as fruit fly and mice, the forward genetic approach is acting as an one of the most influential methods in the mordern era[1].

The forward genetic is opposite of reverse genetics. The reverse genetics contribute to analyze the phenotype of an organism following the disruption of a known gene. The strategies of reverse genetic involve in direct manipulation of specific genes, either by targeting mutagenesis or transgenesis. This strategy is driven by the manipulation of DNA. It also proceeds from a simple molecular change to the complex effects of that change by investigating the functional consequences of a specific mutation in the context of the whole organism[2]. Both of the strategies are complementary and extensively used in all model organisms.

History of forward genetic approach:

In earlier genetic studies, the house mouse *Mus musculus* was originally used[3]. A variety of visible phenotypes such as obesity[4] observed in the house mouse were found to be caused by spontaneous mutations. But, the use of spontaneous mutations to examine the function of genes had some limitations, due to low spontaneous mutation rate in mouse germ cells ($5x10^{-6}$ per locus)[5]. In 1927, the X-rays were first used to induce heritable mutations capability to induce mutations at a rate 20 times higher (13×10^{-5} to 50×10^{-5}) than that of spontaneous mutation[6]. The X-ray mutagenesis causes a wide variety of chromosomal rearrangements, such as deletions, inversion, translocations, that affect multiple genes. After it several chemicals such as procarbazine, triethylenemlamine, chlorambucil etc. have been used for their ability to generate mutagenesis with a greater frequency in germ cells in several model organisms, but they also exhibit some problems of genetic lesions associated with early or late spermatogensis[6,7]. It soon became clear that physical or chemical means of inducing mutations must be necessary in order to examine the function of all of the genes in the mouse genome more quickly. In 1979, Russell's group at the Oakridge National Laboratory first used ENU in the mouse to induce mutation and found that ENU is the most powerful mutagen of spermatogonia in mice[8]. The rate of inducing mutations by the ENU was at a frequency of up to 150×10^{-5} per locus[6,9,10]. These findings, considered as a milestone in mouse genetics, for the generation of new mouse mutants. In the 1980s, geneticists began to embrace the technique of ENU mutagenesis in a large scale, using ENU in a region-specific screen[11]. Therefore, several research groups are engaged in genetic screens using ENU mutagenesis with a high proficiency in the recent era. By the use of forward genetic approach the recent advances in DNA sequencing technology have been sped up in identifying disease causing mutations in mutagenized mice[1].

N-ethyl-N-nitrosourea (ENU) mutagenesis:

The synthetic alkylating chemical agent N-ethyl-N-nitrosourea (ENU)[12] is toxic and carcinogenic to the cells, potent mutagen, and primarily affects spermatogonial stem cells. The most powerful mutagenic effect of ENU is widely used for mutagenesis in mice. It does not require any metabolic processing for its activation[13]. ENU induces random point mutations in the spermatogonial stem cells at a frequency of ~$150x10^{-5}$ per locus in mice[8]. ENU transfers its ethyl group to oxygen and nitrogen reactive sites of the nucleotides[14]. The transferred ethyl group constitutes a DNA adduct that results in heritable mutations during cell proliferation and DNA replication[15]. During replication ENU causes mispairing and base pair substitutions in DNA[10,16]. Most of the ENU-induced mutations are single base pair substitutions that cause missense errors, as well as the other mutations like splice site errors, and nonsense mutations[17]. Approximately, 70% to 85% of all ENU-induced nucleotide substitutions are assessed to be either A-T to T-A transversions or A-T to G-C transitions[14,18,19]. On the other hand, the G-C to C-G transversion event is rarely seen[20]. Some amino acid changes will be under represented due to the low frequency of G-C to C-G transversions. However, the evidence from the prevalent successful use of ENU mutagenesis that these preferences have so far limit the successful identification of new mutant models over the past three decades[21]. ENU is usually administered by intraperitoneal injections to adult male mice. It has largely been elucidated that the doses and injection regimes of ENU play an important role in the most efficient induction of heritable mutations in different strains of mice[22–24].

A typical treatment schedule might comprise at the most common dosage (two/three weekly i.p. injection at 80-100 mg/kg) for an adult male mouse. However, the optimum dose and regime vary according to the strain of mouse being used[25]. Generally, ENU creates an average of 60 coding changes per sperm, which would correspond to approximately one

mutation per 700,000 bp of the target DNA sequence[19,26]. As ENU is toxic and carcinogenic, so an increase in dose may result in a higher mutation load but it may cause a reduction in the viability of the mouse reproductivity[23,25].

Dominant vs recessive screen:

The phenotype-driven approach of forward genetics is considered as unbiased, because it makes no assumptions with regard to the genetic basis or cause of a particular disease. In the phenotype-driven screens of the mouse, the chemical mutagen ethyl nitrosourea (ENU) has been used as a principle mutagenesis strategy. The success of screening depends on the optimal selection of a number of considerations in ENU mutagenesis, such as breeding strategy, ENU dose, mouse strain and method of phenotypic detection, which are often dictated by the phenotype or disease that one wishes to examine[27]. One of the first choices a researcher must make is whether to perform a dominant or recessive screen. In a dominant screen, a phenotype must be detected when only one copy of the mutant gene is present; whereas, a recessive screen allows for the identification of genetic mutations that are inherited in a recessive fashion. The decision of whether to perform a dominant or recessive screen is frequently decided by the type of disease one wishes to examine, but the advantages and disadvantages of each type of screen must also be considered[27].

In the dominant screening of ENU-mutagenesis strategy, the chemical mutagen ethylnitrosourea (ENU) is generally administered to male (G_0 male), where the mutagen ENU acts most effectively on spermatogonial stem cells and generate mutation. This mutagenized male (G_0 male) is then bred with wild-type female and transmits the ENU-induced mutations to the G1 progeny (the counter strain is same as G_0 males) or F1 progeny (the counter strain is different than G_0 males) (Fig. 3a). In order to get a large number of candidate mutants, the maximum number of G1/F1 progeny is necessarily produced and the primary phenotype screen is conducted the G1/F1 population as thoroughly as possible. The detection rate of

mutants depends upon the number, type and accuracy of the phenotypic parameters, environmental and genetic background and observation period[28]. Then the linkage analysis or subsequent mapping is performed using N2 progeny. Dominant screens have a simple breeding scheme requiring a small number of animals than the recessive screening[27].

A recessive screen comprises of a three-generation breeding scheme to get homozygous mutations in a proportion of the resultant G3 offspring, and can be conducted in at least two ways. G_0 males are bred to wild-type females to produce G1 progeny and then G1 males are crossed to wild-type females to produce G2 progeny. G2 females can either be crossed to other G2 males from the same pedigree (intercross) or they can be crossed to their fathers (backcross) (Fig. 1). In either case G3 progeny is produced. G3 animals are then screened for a particular phenotype[5,27]. In a recessive backcross, some litters will have 25% of pups affected, whereas other litters will have no affected animals. Recessive screens, however, are complex, require an intensive animal caretaking and large breeding facilities when compared to dominant screens[5,27].

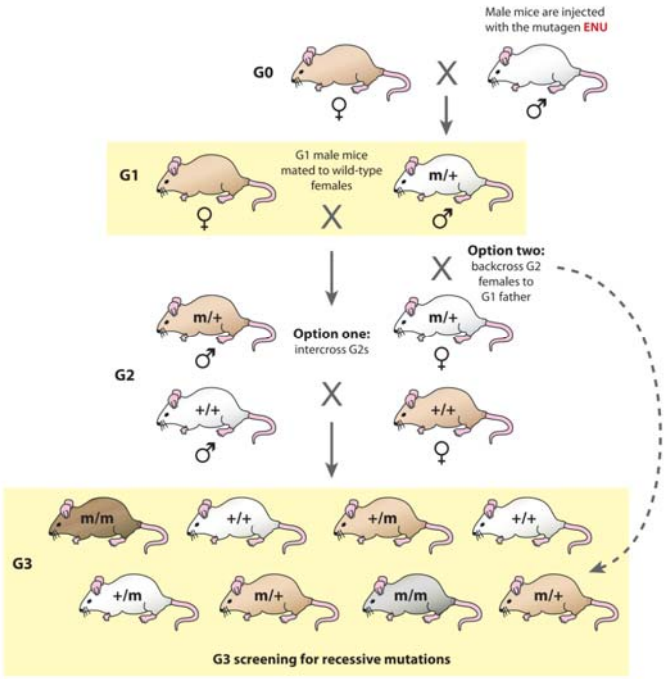

Figure 1. Recessive screening of ENU-mutagenized mice[27]

1.1.2. Linkage analysis and mouse strain

The term linkage can be elucidated as the tendency for genes and the genetic markers to be inherited collectively due to their location near one another on the same chromosome. Linkage analysis is a great tool to recognize the chromosomal location of disease genes. It is a study to aim at establishing linkage between genes based on the observation that reside physically close on a chromosome and linked during meiosis[29]. Linkage analysis exerts the mapping of the chromosomal location of disease by testing the co-segregation of marker alleles with the disease phenotypes. It is a classic method to explore the genetic determinants of disease[30]. Linkage mapping, also named as positional cloning, which involved in systematic scanning of the entire DNA contents of various family members affected by the disorder using frequently spaced, polymorphic DNA segments whose exact position is known[31]. From the beginnings as a model organism for research, mouse plays the s excellent role in genetic studies. Mice have a short generation time, has a well-characterized genome, which is similar to humans, deliver large progenies and breed year round and easy to maintain[5]. Compared to the other mammalian species mouse has the ability to tolerate inbreeding well. Due to the polymorphic variations, inbred mouse strains provide a defined genetic background reducing variability[27]. The mouse genome was the first mammalian genome to be sequenced after the human genome in 2000[32] and almost about ninety-nine percent of genome identity and gene functions are observed between mice and humans[33]. For the first time, the mouse genome to be sequenced was a mix of different strains of mouse (129S1/SvImJ, 129X1/SvJ, A/J, C57BL/6 and DBA/2J), while in 2002, the C57Bl/6J mouse strain was fully sequenced[33]. The mouse genome is relatively easy to manipulate and the pathogenic consequences of genetic mutations in mouse is parallel to the humans pathogenic consequences[27]. Mouse models of human disease, thus allow for in-depth biological studies that are not possible in humans[5].

The mating mouse strain plays an important role to generate linkage in a QTLs. Because, linkage analysis can be carried out between a single marker locus and a putative disease locus or across a set of markers consisting of a small number of markers or even all markers on a given chromosome. The parent mice must be heterozygous at each of two loci to be informative for linkage otherwise, an insufficient information will be produced to distinguish recombinant from non-recombinant events in offspring[34]. The different characteristic effects of different QTLs between the mutagenized and backcross strains may confound the mapping of the mutant locus and sometimes lower the statistical control in detecting mutant locus based on LOD score[35]. Generally, a mutagenized strain and a counter strain are identical in their genomic DNA except for 4-6 single nucleotide polymorphisms per chromosome. But, the availability of polymorphic marker is necessary in a linkage analysis. Recently a number of polymorphic markers such as microsatellites and SNPs between inbred mouse strains are available. Generally, the ENU-treated C57BL/6J (B6J) mice used to cross with DBA/2J[36], BALB/c[37] or C3H/He[38,39] mice. These inbred strains possess more than 5,000,000 genetic variations relative to the B6J strain[40]. On the other hand, the C57BL/6N (B6N) strain, a B6 substrain, which has approximately 17,000 genetic variants relative to B6J mice with only 108 non-synonymous coding changes[41]. The list of available SNPs (Single nucleotide polymorphisms) between the C57BL/6J and C57BL/6N mice strains helps to use these mice strains in forward genetic screening. Thus, a successful quantitative trait loci (QTLs) between the screening strain treated with (ENU), and the counter strain used for the backcross is somehow depends upon the uses of mating mouse strain. However, each inbred mouse strain exhibits a characteristic profile of body weight regulation and energy metabolism in a same feeding condition[42,43] under the influence of QTLs[44].

1.1.3. Fertility and in vitro fertilization (IVF)

Fertility is the natural capability to produce progeny. Human fertility is affected by various factors. By reducing the spermatogenesis obesity strongly and adversely affect the male fertility. The frequency of obesity is rapidly rising in worldwide which affects both women and men, where, male obesity is an issue of serious concern in case of infertility[45]. The prevalence of obesity has also raised tremendously in the women of reproductive age. Female obesity affects the ovulation. The excessive fat delays time to pregnancy (TTP) causing poorer embryo development, and in effects on the endometrium. The obesity epidemic has been accompanied by a potential rise in male infertility, which has been endorsed to hormonal disturbances and compromised semen parameters[46].

Besides, in vitro fertilization is a kind of assisted reproductive technology through which the fertilization process is done by manually combining of sperm and egg in the laboratory dish and the embryo is then transferred to the uterus. Recently, in vitro fertilization is one of the most extensively used interventions for the condition of infertility[47]. In parallel with the human, a strong relationship between obesity and infertility was found in mice also[48]. In that case the production of progeny using natural mating between obese male and female is difficult. Instead, a routine use of in vitro fertilization is favorable to generate the next generation in case of obesity phenotype.

1.1.4. Candidate gene approach vs whole exome sequencing

The candidate gene approach is an important tool for studying complex genetic diseases. It is composed of the following aspects to explore genetic influences on a complex trait. (1) Preparation of hypotheses and identification of candidate genes having a role in the etiology of the disease. (2) Detection of genetic variants with functional changes or non-functional variants, which is linked disequilibrium with positive polymorphisms. (3) Genotype the variants in a population. (4) Assessment of the correlation between those variables and the

phenotypes[49]. The correlations between genetic variants and trait differences can be examined by the genetic association studies on a population scale[50]. To identify the genes responsible for mendelian diseases the linkage analyses and positional cloning have been successfully used in the past two decades. However, linkage study could not show a successful result in identifying diseases related gene in complex diseases characterized by heterozygous phenotypes, a variety of biological pathways or functional variety of genes with a small contribution. Whereas, the candidate gene approach exerts its effects as a promising alternative approach[49]. In the candidate gene approach, after choosing a candidate gene and suitable polymorphism, the investigators commonly test the role of the gene in a sample of randomly chosen subjects of the disease in comparison with the control group of the litter mates[51]. A combination of candidate gene approach and linkage mapping plays as a most applicable method of identifying disease genes to date. The candidate gene approach exerts firm advantages over positional cloning or linkage mapping and is applicable in quick determination of genetic variants with the disorder as well as in identifying the genes having modest effect[31].

Whole exome sequencing is a method used for sequencing of all the expressed genes in a genome or exome. It is a widely used targeted high-throughput DNA sequencing technology, which encodes and sequences the protein coding portion of DNA (known as exons)[52]. It can identify the genetic variation with a high effectiveness, but less costs in comparing to the whole-genome sequencing. It is widely applicable in identifying the Mendelian and other common diseases associated with genetic variations[53]. In order to sequence of massive numbers of different DNA strands at once a large number of equivalent DNA-sequencing systems are available. These technologies play a major role in developing of our understandings in medical genetics, hasten health-improvement projects, and guiding to a fully understood personalized medicine in the near future[54]. To the complement of the

other sequencing methods, the whole-exome sequencing is now progressively used to identify novel genes by comparing exomes and also to find mutations in genes already known to cause disease from patients with similar features. The whole-exome sequencing is a powerful application of the next-generation technology for determining the variations of all exons or coding regions, of known genes. It provides exposure of more than 95% of the exons, that contains 85% of disease-causing mutations in many disease-predisposing SNPs throughout the genome. The whole-exome sequencing has been used to distinguish more than 150 genes, and this statistics is rising rapidly[54].

1.2. Forward genetic screening for obesity

1.2.1. General introduction of obesity

Obesity:

Obesity can be defined as the increased fat mass to an amount that is harmful to health. According to world health organization (WHO) the overweight as well as obesity is defined as abnormal or excessive fat accumulation that provides a threat to an individual's health. Since 1980 worldwide obesity has more than doubled. According to WHO about 42 million children under the age of 5 were overweight or obese in 2013. Besides, more than 1.9 billion adults (18 years and older) were overweight, among them more than 600 million were obese in 2014. Statistically, about 39% of adults were overweight and 13% were obese in the year of 2014. Overweight and obesity acts as a major risk factor for a number of chronic diseases. In addition to the developing countries, overweight and obesity also considerably on the rise in middle income as well as low income countries, particularly in urban settings. (http://www.who.int/mediacentre/factsheets/fs311/en/).

Prevalence of obesity:

The obesity prevalence has increased significantly in a single generation among adults and especially, children. The prevalence of obesity has been increased drastically, with diverse

regional patterns and distinct variations throughout countries in the levels and trends in overweight and obesity in the past three decades[55]. A high prevalence affects nearly all rich countries and is rapidly increasing among more rich populations of poorer countries. The burdens of ill health put greater burdens on families and social support services, on health services and lessen the output of national economies[56]. In 2010, overweight and obesity were estimated worldwide to cause 4% of disability-adjusted life-year, 4% of years of life lost and 3·4 million deaths[57]. Worldwide, the prevalence of overweight and obesity combined rose by 47·1% for children and 27·5% for adults between 1980 and 2013. The number of overweight and obese individuals amplified from 857 million in 1980, to 2·1 billion in 2013[55].

Consequences of obesity:

Obesity causes and intensify many health consequences resulting from the extra fat mass or increased free fatty acids and enlarged fat cells secreted peptides. The diseases obstructive sleep apnea[58] and osteoarthritis of large and small joints[59] are associated with increased fat mass. The enlarged fat cells secreted adipocytokines are correlated with type 2 diabetes mellitus[60,61], cholelithiasis[62], nonalcoholic fatty liver disease and nonalcoholic steatohepatitis[63], coronary heart disease[64], hypertension [65] and sometimes certain forms of cancer[66,67]. Obesity acts as a cardiovascular risk factor for children, which is predictive as of adult cardiac risk and even causes premature death[68]. Childhood obesity is broadly correlated with heart disease, surpassing undernutrition and infectious diseases[69]. A number of population studies have shown considerable evidence that obesity shortens the duration of life[70–74].

Causes of obesity:

Several factors are responsible to cause obesity. The excessive food or energy intake and a lack of physical activity play a major role to cause obesity[75]. The genetics, psychiatric illness or medical reasons also act as a great reason to cause obesity[76]. Besides, the easily accessible

and palatable diet, increased reliance on cars, and mechanized manufacturing increasing rates of obesity at a public level[77–79]. In addition the following possible matters also contribute to the recent increase of obesity: endocrine disruptors, insufficient sleep, decreased variability in ambient temperature, increased use of medications that can cause weight gain, smoking, proportional increases in ethnic and age groups that tend to be heavier, epigenetic risk factors, pregnancy at a later age, natural selection for higher BMI, and assortative mating leading to increase concentration of obesity risk factors[80]. Further, there also some other factors supporting the influence of these mechanisms on the increased prevalence of obesity.

Genetic determinants of obesity:

Among the various potential causes for obesity the certain genetic conditions play a major role to cause obesity. The genome-wide association studies already have been identified a number of genetic variants, those are associated with obesity[81]. Molecular genetic studies has been identified a few numbers of candidate genes for human obesity. Mutation of these candidate genes develops the excessive body weight, but the causal mutations are rare and unable to expose the current obesity epidemic. Each of the single gene variant has only a minute influence on the body weight, but the genetic propensity to the common obesity is most likely has a polygenic basis[82]. Besides of the common variants, FTO and MC4R, new loci, such as GNPDA2T, KCTD15, MEM18, MTCH2, NEGR1 and SH2B1 have been identified[81]. The (GWAS) study can offer the new opportunities for the genetic study of the complex obesity disease. The genetic determinants strongly influence in people with severe and early-onset obesity as well as some unfavorable clinical consequences (Fig. 2)[83].

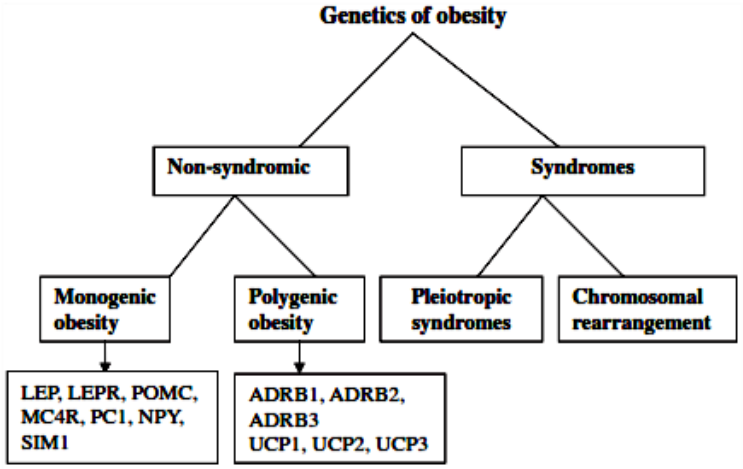

Figure 2. Genetics of obesity[83]

1.2.2. History of forward genetic screening for obesity

In 1949, a strain of obese offspring was found at the Jackson Laboratory by the study of a non-obese mouse colony. This result suggests for the presence of a mutation (ob/ob) in a hormone regulating hunger and energy expenditure in the obese mice[4]. In the 1960s, at the Jackson Laboratory a second mutation (db/db) causing obesity as a similar phenotype was identified, exhibiting diabetes and obesity[84]. After the seminal discovery of leptin in (ob/ob) mice in 1994 and leptin receptor in db/db mice in 1995 through the forward genetic studies on recessive mice[85], the application of forward genetic approach has been widely used to identify the molecular network of gene associated with obesity and energy homeostasis. Subsequently, the forward genetic study using ENU mutagenized mice, have found the obesity-causing mutations in the *Mc4r*[39,86], *leptin*[37] and *leptin receptor*[87] genes through the recessive inheritance. However, there was no evidence of finding dominant heritable traits related to obesity using a successful dominant screening of forward genetic approach.

1.3. Leptin and hypothalamic neuron network

Leptin:

Leptin is a 167-amino-acid peptide which is generated from adipose tissue. The level of leptin in the systemic circulation is directly proportional to the amount of body fat and fluctuate within the changes of caloric intake, thereby signaling the quantity of stored energy[88]. Generally, leptin exerts its effect centrally by interacting with various neuronal pathways particularly in the hypothalamus of brain, through orexigenic and anorexigenic neuropeptides and regulate food intake. In the arcuate nucleus of the hypothalamus, leptin activates *pro-opiomelanocortin* (*Pomc*) and cocaine- and amphetamine-regulated[88] transcript (CART), to suppress appetite, and inhibits *Agouti-related peptide (Agrp)* and *Neuropeptide Y(Npy),* both of which are generally stimulate appetite[89,90]. In the lateral hypothalamus area, leptin decreases the expression of the orexigenic peptides *Melanin-concentrating hormone (Mch)*[91] and *Orexin*[92]. Besides, of controlling the energy intake through the central regulation of appetite and satiety, leptin also regulates energy expenditure possibly through the suppression of *Mch*[93]. On the other hand, mutations or deficiency in the gene encoding the leptin receptor exhibit severe early-onset obesity associated with hyperphagia[94,95] and administration of leptin reduces the obesity in leptin deficient mice[96] and in leptin deficient humans[97].

Insulin:

Insulin is a kind of peptide hormone that secrets from the pancreatic beta cells. Insulin secrets for short term depending upon the blood glucose level on the other hand, in response to the adiposity level, insulin secrets for a long tern[98]. Insulin has a strong impact in regulating glucose homeostasis and lipid metabolism and central administration of insulin inhibits food intake and decreases body weight[99]. The action of insulin is mediated by the insulin receptor (InsR), which is expressed in several areas of the CNS including the hypothalamus. Insulin

strongly expressed in *Pomc* and *Agrp* neurons of the ARC and contributes in the regulation of glucose homeostasis, food intake and body weight[89,100–102]. In the hypothalamus insulin regulates the AMPK signaling pathway to energy balance[103]. The brain-specific deletion of Insulin receptor in mice exhibited diet sensitive obesity associated with increased food intake[104] and central administration of insulin regulates feeding behavior. The selective ablation of insulin receptor in *Agrp* or *Pomc* neurons does not show any effect on food intake or body weight, but, the transgenic deletions of insulin receptor in *Agrp* or *Pomc* neurons have an impact on glucose metabolism representing the importance of insulin action in the regulation of glucose homeostasis on the *Agrp* and *Pomc* neurons[101].

Proopiomelanocortin (Pomc):

The *Pomc* neurons are found in the arcuate nucleus of the hypothalamus and nucleus tractus solitarius of the brain stem and involve in the regulation of food intake as well as energy expenditure[105]. In the hypothalamic arcuate nucleus, leptin and insulin acts in activating *Pomc* neurons[89,90,106]. The activated *Pomc* neuron releases α-MSH, which binds with *Mc4r* gene and decrease food intake and increase energy expenditure[107,108]. Activation of hypothalamic nicotinic acetylcholine receptors (alpha-3 and beta-4) leads to activates *Pomc* neurons. The activated *Pomc* neurons subsequently activate the melanocortin-4 receptors and decreases food intake in mice[109]. On the other hand, *Pomc* deficiency exhibits early-onset obesity associated with hyperphagia due to the lack of melanocortin-4 receptors activation[110].

Agouti-related peptide (Agrp):

The neuropeptide *Agrp* is synthesized in *NeuropeptideY* containing *Agrp/Npy* neuron located in the ventromedial part of the arcuate nucleus in the hypothalamus[111]. *Agrp* co-expresses with *Neuropeptide Y* and increases appetite as well as decreases energy expenditure and metabolism[112,113]. Intracerebroventricularly (ICV) administration or transgenically expression

of *Agrp* causes hyperphagia. Thus, the activated *Agrp* promotes food intake and positive energy balance by antagonizing *Mc4r* genes located in PVN[112,114,115]. Moreover, insulin and leptin inhibit *Agrp* expression and regulates food intake and energy expenditure[106]. Since *Agrp* neurons are inhibited by insulin and leptin thus, they are activated by the decline of insulin and leptin signalings[116]. The hypothalamic *Agrp* neurons also express the neurotransmitter GABA, *Npy* as well as many other molecules, having vital functions in a physiologic circuit[117].

NeuropeptideY (Npy):

NeuropeptideY (Npy) is an amino acid peptide that produced in various parts of the brain, especially in the hypothalamic arcuate nucleus[118]. *Npy* exerts its functions through the five highly conserved NeuropeptideY receptors. It is one of the most potent orexigenic neuropeptides. *Npy* coexpress with *Agrp* an endogenous antagonist of the *Mc4r* to exert orexigenic effects in increasing food intake as well as storage of energy as fat[112,115]. However, *Npy* is inhibited by insulin and leptin in the hypothalamus and decrease food intake[119,120]. As the *Npy* neurons are inhibited by insulin and leptin thus, the decline of insulin and leptin signaling demonstrates to activate *Npy* to exert its orexigenic action[116]. Injection of *Npy* into the hypothalamus of rats increase food intake and decreases energy expenditure[121]. Therefore, *Npy* on repeated administration leads to obesity[121,122]. On the other hand, genetic knockout of *Npy* reduces hyperphagia and obesity in *ob/ob* mice[123].

Melanin concentrating hormone (Mch):

Mch is an orexigenic hypothalamic peptide originated from the pituitary gland. Though *Mch* expressing neurons are mainly located in the lateral hypothalamus and zona incerta but, the neurons project widely throughout the brain[124,125]. In the regulation of food intake as well as energy homeostasis *Mch* plays an important role. *Mch* deficient mice exhibit a characteristics of hypophagia and lean body weight with increased metabolic activity[126–128]. Whereas,

transgenic mice which overexpress *Mch* shows a characteristics of obesity and resistance to insulin[129]. The *Mch* overexpression in hypothalamus also found in the leptin deficient *ob*/*ob* mice exhibits characteristics of hyperphagia and centrally administration of *Mch* promotes food intake and weight gain[130].

***Orexin/hypocretin* neuropeptide:**

Orexin is a neuropeptide (*prepro-orexin* mRNA) found in the neurons within and around the lateral and posterior hypothalamus of the brain[131]. In parallel with the regulation of arousal and wakefulness *Orexin* also regulates appetite behavior. The central administration of *Orexin* peptides in rats exhibit a positive stimulation of food consumption[131]. The orexigenic peptides not only act within hypothalamic centers, but are also capable to regulate food intake through their activities at extra-hypothalamic centers, such as in the regions of brain's endogenous reward circuitry[132,133]. *Orexin* enhances the hunger for food, and other functions those correlated with the enhancement hunger production. By suppressing the inhibitory feedback *Orexin* also acts to increase meal size[134].

***Oxytocin* neuropeptide:**

Oxytocin is a type of peptide hormone generally produced from the parvocellular paraventricular nucleus (pPVN) as well as magnocellular neurons in both the supraoptic nucleus (SON) and PVN. *Oxytoxin* also produced in the anterior hypothalamus, medial amygdala, medial preoptic area, bed nucleus of the stria terminalis (BNST) and in the periphery[135–137]. In the neural circuits *Oxytocin* plays a major role in appetite along with social behavior, anxiety or stress[138,139] as well as in the regulation of body weight[140,141]. Animal studies revealed that *Oxytocin* control the body weight[142,143] by inhibiting the appetite, particularly for carbohydrates and sugar[140,144]. The diet induced obese mice show functional abnormalities in *Oxytocin* systems. Injections of Oxytocin receptor antagonist in wild-type mice increase the consumption of sucrose over fat[145]. Whereas, Oxytocin receptor

deficient animals develop late onset obesity[146,147] and increased consumption of sweet solutions in compared with wild-type animals[148] and the administration of *Oxytocin* exhibit weight loss[149].

Growth hormone releasing hormone (Ghrh):

Ghrh is a kind of peptide hormone, which produced in the arcuate nucleus of the hypothalamus[150]. The neurosecretory nerve terminals of arcuate neurons, releases *Ghrh* that carried out to the anterior pituitary gland by the hypothalamo-hypophyseal portal system. In the anterior pituitary gland it stimulates the growth hormone-releasing hormone receptor promotes for *Growth hormone (Gh)* secretion[151,152].

Thyrotropin releasing hormone (Trh):

Trh is a hormone generally produced in the paraventricular nucleus of the hypothalamus and acts as a key regulator of hypothalamic-pituitary-thyroid axis[153]. *Trh* is also found in many other brain loci outside of the hypothalamus as well as in various nonneuronal tissues such as heart, reproductive organs and gastrointestinal tract[154]. *Trh* mainly regulates the thyroid-stimulating hormone secretion for the maintenance of thyroid hormone homeostasis[155]. Besides, *Trh* also regulates the release of several other hormones such as Insulin, *Vasopressin*, *Growth hormone* and Prolactin[156,157]. *Trh* plays an important role in the CNS in the regulation of energy homeostasis[153]. Central administration of *Trh* or agonist of *Trh* exhibits a significant reduction of food intake in models of stress-induced feeding, hungry rats or in normal rodents[158–163]. Subcutaneously administration of *Trh* in rat also exhibits increases water intake and body temperature, but decreases food intake[164]. *Trh* indirectly affects in energy homeostasis[165] and in upregulation of locomotor activity[166,167]. *Trh* inhibits *Mch* neurons by synaptic inhibition of local GABA neurons and reduces the *Trh* mediated food intake[168].

Arginine vasopressin (Avp):

The *Arginine vasopressin* is a neuropeptide hormone found in the paraventricular nucleus (PVN) of the hypothalamus and in the supraoptic nucleus (SON) of the brain[169]. The primary functions of *Avp* are to regulate the retention of water in the body and high concentrations *Avp* raise blood pressure by constriction of blood vessels[170,171]. *Peripheral* administration of *Arginine vasopressin* in goat reduces cumulative food intake in a dose-dependent manner. This hypophagic effect of *Avp* was reversed by both a V_1-receptor antagonist and an alpha-adrenergic antagonist. *Avp* also exhibits stress-induced anorexia[172].

Pituitary adenylate cyclase activating polypeptide (Pacap):

Pituitary adenylate cyclase activating polypeptide (Pacap) is a hypophysiotropic hormone involved in adenohypophyseal hormone release[173] as well as a neuropeptide expresses in the central and peripheral nervous systems[174] and numerous tissues in vertebrates[175]. In the neuroendocrine control of food intake *Pacap* exerts an important role. Besides, it exhibits an anorexigenic effect on the regulation of satiety. Intracerebroventricular (ICV) administration of *Pacap* decrease food intake in mouse[176], rats[177,178], Chick[179] and goldfish[180]. The results suggest that *Pacap* has an impending effect on the regulation of food intake.

Corticotropin releasing hormone (Crh):

The *Crh* is a peptide, which is secreted in the PVN of hypothalamus[181], in placenta and in a number of peripheral tissues. *Crh* serves as an integrator of adaptive responses to stress, gastrointestinal function, inflammatory processes, cardiovascular processes, and influences food intake[182]. *Crh* and its related peptides regulate feeding behavior and stress responses in vertebrates, including fish, amphibians, birds and mammals[183]. Intracerebroventricular (ICV) administration of *Crh* in the goldfish exerts an anorexigenic action[180] that can be inhibited by *Crh* receptor antagonists[183].

Somatostatin (Sst):

Somatostatin is a peptide hormone that is found in periventricular and paraventricular (PVN) nucleus, ventromedial, arcuate nucleus and in the brainstem of the nucleus of the solitary tract (NTS)[184,185]. *Somatostatin* binding with Somatostatin receptors regulates the endocrine system and inhibits the secretion of several secondary hormones such as insulin and glucagon secretion (http://www.britannica.com/science/somatostatin). Injection of *Somatostatin* or Somatostatin agonist intracerebroventricularly (ICV) into the brain increased food intake in rats at low dose[186–188]. However, at higher doses injection of *Somatostatin* decreased food intake in mice and rats[162,187,189,190]. The decrease food intake at higher doses may be due to the occurrence of other competing behavioral changes and peripheral circulation leakage[191] where the peptide exhibits inhibitory effects[192]. Whereas, activation of *Somatostatin* signaling in brain by ICV injection of stable *Somatostatin* agonists at low doses strongly increases food intake in rodents and non-mammalian species[193].

***Melanocortin-4 receptor (Mc4r)* gene:**

The MC4R is encoded by 333-amino acid protein having single exon and found to be expressed primarily in the brain[194]. The Mc4r gene belongs to the large super family of G-protein coupled receptors having the common structural feature of seven transmembrane spanning protein domains[195]. Mutations in the *Mc4r* gene account for obesity cases. A common variant of the *Mc4r* gene causing increased appetite and decreased satiety are distributed in the population and results the risk for increased weight gain. MC4R belongs to the large super family of G protein-coupled seven transmembrane receptors (GPCRs), whose subtypes are identified so far couples in a stimulatory manner to adenylate cyclase[196]. The *Mc4r* gene is widely distributed in the brain, predominantly in hypothalamus concerned in appetite as well as body weight regulation[197,198]. There are different melanocortin pathways that regulate food intake and energy expenditure[199]. The endogenous agonist α-melanocyte

stimulating hormone (αMSH), a peptide derived from Pomc and an antagonist Agrp[106] modulates *Mc4r* signaling. On the other hand, an adipocyte-derived hormone, leptin activates Pomc resulting in increased secretion of α-MSH and deactivates Agrp neurons in the arcuate nucleus of the hypothalamus[200,201]. The suppression of *Mc4r* signaling by *Agrp* or synthetic antagonists increase food intake and diminish the hypophagic response to leptin, as well as activation of *Mc4r* by αMSH or synthetic peptide agonists reduce food intake[202,203]. In mice, the regulation of firing activity of neurons from the PVN by α-MSH, and Agrp can be mediated independently of G-α-s signaling by ligand-induced coupling of Mc4r to the closure of inwardly rectifying potassium channel Kir7.1. Furthermore, *Agrp* is a biased agonist that by binding to *Mc4r* hyperpolarizes neurons and opening Kir7.1 and inhibits α-MSH binding. As a result, Kir7.1 signaling shows a melanocortin-mediated regulation of energy homeostasis within the PVN[204]. The paraventricular hypothalamus Mc4r-expressing neurons act as a functional target for orexigenic arcuate nucleus *Agrp* expressing neuron and explicit to lateral parabrachial nucleus satiety-promoting circuit, the activation of which encodes positive valence in calorically depleted mice[205].

***Single minded1 (Sim1)* gene:**

The Sim1 gene encodes the bHLH-PAS (basic helix-loop-helix–Per Arnt Sim) structural protein domain[206] and form subgroups of bHLH super family of transcription factors. By the presence of bHLH and PAS domain Sim1 gene acts as a critical transcriptional factor and strongly expressed in the development of the PVN[207]. By using the PAS domain wild-type *Sim1* gene bind with *Arnt2* to form a hetero-dimer and exert a strong transcriptional activity for functioning in the development of the hypothalamus[208]. The human *Sim1* and *Sim2* genes exert a strong homology with mouse *Sim1* and *Sim2* in the amino-terminal part of the protein in which the conserved bHLH (basic helix-loop-helix), PAS (Per-Arnt-Sim) and PAC (PAS associated C-terminal) domains are located. PAS domain serves as a potent protein-protein

interaction interface and regulation of the dimerization activity of the bHLH domain to induce the transcription of target genes[209,210].

Sim1 gene is allied with human monogenic obesity and chromosomal aberrations in *Sim1* locus results in hyperphagic obesity in human[211,212]. *Sim1* gene is necessary for the development of the paraventricular nucleus of the hypothalamus (PVH), medial amygdala, supraoptic nucleus (SON) and nucleus of the lateral olfactory tract (NLOT)[199,207,213]. The PVH is the critical regulator of appetite, energy expenditure and body weight. The PVN, supraoptic hypothalamic nuclei and anterior paraventricular nuclei are responsible for the production of multiple neuropeptides, including *Oxytocin, Vasopressin, Trh and Somatostatin* etc. These neuropeptides have been implicated in energy balance in experimental models[214,215]. The role of *Sim1* gene is not limited to the formation of the PVN or its projections only. In regulating body weight it also plays an important role in the leptin–melanocortin–oxytocin pathway[215] where, the *Oxytocin* may exert a tonic stimulatory effect on nucleus tractus solidarius (NTS) neurons to reduce the amount of meal[216,217]. *Sim1* haploinsufficiency affects the anterior periventricular nucleus expressing, *Oxt, Avp, Trh, Crh* and *Sst* by and mediate the hyperphagic obesity of *Sim1* deficient mice. The *Oxt* mRNA was drastically reduced in the hypothalamus of *Sim1* deficient mice in compared with controls[216]. The neurotransmitter *glutamate* also exhibits a critical role to mediate the function of *Mc4rs* on *sim1* neurons in regulating both energy expenditure and food intake[218]. The deficiency of *Sim1* gene exhibited increased hypothalamic *Pomc* level, but showed and impaired action of melanocortin-mediated anorexia and decrease activation of paraventricular nucleus neurons. This result suggested that *Sim1* functions downstream of the *Mc4r* in *Sim1* heterozygous mouse[219]. In supporting with this evidence it also stated that, overexpression of *Sim1* partially rescued the A^y, and diet induced obesity of the A^y mouse by the normalization of food intake, but has little or no effect on their energy expenditure[219]. Conditional deletion of

Sim1 with Cre93 and Cre159 generated a strong phenotype that exhibited a significant decrease of *Oxytocin, Mc4r* and *Sim1* mRNAs expression with the development of early onset of obesity[215]. Tamoxifen induced neural inactivation of *Sim1* gene in mice showed decreased expression of PVN neuropeptides, especially *Oxytocin*, *Vasopressin*, *Crh* and *Trh* but no change in energy expenditure. It also revealed that the survival of PVN neurons does not depend on *Sim1* expression. The results confirm the previous evidence that *Sim1* regulates body weight by acting both physiologically as well as developmentally[220].

Chapter 2.
Research plan and objectives

In order to identify a gene essential for a defined biological phenomena, forward genetic strategy acts as one of the most influential approaches and enables us to understand the genetic basis of human biology and disease, when applied in model animals[1] such as fruit fly and mouse. Among the various sources of generating phenotypic variation the chemical mutagen N-ethyl-N-nitrosourea (ENU) performs as a powerful mutagen for spermatogonial cells of mouse and widely using in generating mutagenesis of mice[8,221–223]. There have been many research areas in which candidate gene approach would not work because the loss of function effects caused by gene targeting are often masked by the redundant and compensatory regulation of target phenotypes. The forward genetic strategy that is phenotype driven and hypothesis-free approach, will help to find out novel genes which may play a crucial role in the target behaviors of phenotypes.

The major obstacle of the forward genetics is that it usually takes more than five years from the phenotype screening to identify a candidate gene mutation. However, the recent advance in DNA sequencing technology have been sped up the process from the linkage analysis to identified candidate mutations. A key to successful forward genetic study is the similarity in genome DNA between a mutagenized strain and counter strain. Since C57BL/6 (B6) substrains have the almost same genetic background[40,224], B6J and B6N are ideal strains for forward genetic study. Hence, by the combination of using B6 substrains, routine use of in vitro fertilization and whole exome sequencing is a better way for new gene discovery.

In order to examine the sleep/wakefulness abnormalities in randomly mutagenized mice, our laboratory has been undertaken a large-scale forward genetic screen of sleep abnormalities. Throughout the screening of more than 5,000 mutagenized

G1(C57BL/6JxB6J)/F1(B6JxB6N) males we have found several mice that exhibited with an obvious obesity phenotype. Although several genes such as *leptin* and *Mc4r*[39,85,86] have been found to be mutated through the recessive screening for obesity, there has been no successful dominant obesity screening, which may be due to the significant QTL effects between the mutagenized and counter strains on body weight and the low fertility of obese mice. However, our screening scheme may overcome these obstacles by the use of B6 substrains and a routine use of in vitro fertilization. Thus, we started a forward genetic study for obesity.

The purpose of the current study was two fold; i) to evaluate the efficiency and reproducibility of our new forward genetic scheme by conducting the dominant screening of obesity, 2) to identify the gene mutation that causes obesity in a dominant inheritance. If the identified gene is a novel player in the homeostasis of energy metabolism, the mutant mice may afford a new genetic model for the human metabolic syndrome, as well as new insights into the pathophysiology of obesity.

Chapter 3.
Materials and methods

3.1. Animals and mutagenesis strategy[225]

The mice were kept singly in the cages at 23-25°C with free access to water and normal diet under a 12 h-12 h light-dark cycle. The experimental procedures were carried out under the guideline of RIKEN Bioscience Technology Center in 'Outline for conducting animal experiments' (Issued August 1999, revised October 2001) and also with the guidance of animal resource center of University of Tsukuba, Japan. The stock male mice were supplied from CLEA Japan, Inc. The ENU (Sigma-Aldrich) was injected intraperitoneally to the wild-type male C57BL/6J mice at 8-10 weeks of age with 85-100 mg/kg body weight twice at weekly intervals. After a sterile period (10-11 weeks) the injected males were mated (IVF) with C57BL/6J or C57BL/6N wild-type female to produce G1/F1 progeny. Phenotypic screens of G1/F1 progeny were routinely carried out. The phenodeviant F1 male mice were again mated with C57BL/6N wild-type females to produce N2 progeny (Fig. 3a). The N2 progeny was then used for the inheritance testing of obesity and mapping[36,38].

3.2. Screening method for heritability of obesity[225]

In order to examine the sleep/wakefulness abnormalities, we have screened more than 5000 randomly ENU mutagenesis G1/F1 mice. In parallel with examining the sleep/wakefulness abnormalities we also have dominantly screened the same randomly mutagenized group of mice for obesity. At the age of 12 weeks, G1/F1 male mice were implanted an EEG/EMG electrode under isoflurane anesthesia and then examined for sleep/wakefulness abnormalities. In this study, total thirteen obese male G1/F1 mice were selected to generate N2 progeny via in vitro fertilization method. The body weight of the N2 mice was measured weekly from the age of 10 weeks to 26 weeks and bi-weekly from the age of 28 weeks to 34 weeks. The N2 progeny was examined for heritability of obesity and linkage analysis. If the body weight at

least 30% of N2 progeny exhibit similar obesity to their founder mouse, then the obesity phenotype was considered as heritable. Besides, the body weight of the N3 mice of *Obese-10* and *Obese-13* was measured weekly from the age of 6 weeks to 11 weeks.

3.3. Linkage analysis[225]

In order to perform the linkage analysis, tissue was collected from the N2 mice by tail cutting. The genomic DNA was isolated and purified by using a DNeasy Blood & Tissue kit (Qiagen). Through the use of custom Taqman genotyping assay to determine the SNPs of each N2 mice. The assay was performed by Applied Biosystems 7900HT followed by Fast Real-Time PCR System and controlled by TaqMan Genotyper (Thermo Fisher) as well as SDS2.2.2 software.Based on the polymorphism data between C57BL/6J and C57BL/6N mice the custom probes were designed[41]. The J/qtl software (Jackson Laboratory) was used to perform QTL analysis. For this linkage analysis total 93 markers (Table 1) have been used for whole chromosomes. Among them, 6 SNPs markers were used in the region of chromosome10, and 4 SNPs markers were used in the region of chromosome18. In order to locate the association between phenotype and genotype the strain distribution patterns (SDPs) were constructed according to the descending order of body weight (from high body weight to lower body weight) of sample N2 mice using the body weight of 18 weeks and 26 weeks.

Table-1: List of SNPs markers for linkage analysis:

Chr	Position	Rs number	B6J/B6N	Forward primer (5'-3')	Reverse Primer (5'-3')
Chr1	3597640	rs32685032	A/T	CCCACACCCCATAATACTGACATAT	AGTCTAATTTCATTCTCAGCCATTGGT
Chr1	42424440	rs31362610	T/C	TGGCTTTCTCTTATATACTTTCCGATGTG	GCAAACTCTGCCCATATGACTTAGT
Chr1	61228463	rs13475886	T/C	TGGAGGAGTCAGGAAGAGAAAGG	CTGGCCAAGACAGAATTAAGGAGAA
Chr1	131282938	rs6327099	T/C	AGTAGGGTTTTGTATTGGCTTAGTTTGTT	GAGGTAGATGGATTGTGGTTTAGCT
Chr1	165062830	rs6341208	A/T	AACATGCTGACTCCTCGATTGTAAA	TGATCGTTCTGATTGTTGAAATCCCTTT
Chr1	196072469	rs242712390	C/A	CCAAATTTCAGGAGTGATGCATTCAG	TCTATCTGCAAAGAACCTCTCATACCT
Chr2	7991482	rs13476337	A/T	CAGGATCCAAGCTTACTGACTCAT	GTGAAATTGATGACTCTCAAAATGAAGGT
Chr2	44998528	rs33488914	A/G	GCAAGCGCATTGATGTTTTCATAGT	ACTCAGCTGGGAGACTTCCT

Chr	Position	Rs number	B6J/B6N	Forward primer (5'-3')	Reverse Primer (5'-3')
Chr2	78639333	rs33162749	C/T	TCTACTCTCCAGTTCAACAGTGGTA	GACACAGGCTTAACATGAGTATGGT
Chr2	105914300	rs227312316	G/A	GCCTTAAAGTTTACAAAAAGCATGCCATA	CAAAACAAAAGATTACATATAGAAATAT TGAGAACGAACT
Chr2	138305756	rs13476801	T/C	GAATGTGACATTATGTTCATATTCATAATT AAATTTATTCCTTTT	CCTCAATCTACAGTCAGGCCAAATT
Chr2	178997069	rs29673978	C/T	GATCTTGGCAATGTATGAGGGATGA	GCACTTAACAGTCTCAGCATTAGCT
Chr3	5370727	rs13476956	C/T	CAGATTCATCTTCCTGCTAGACACA	TCCTAGATTACATATTTTCATAATTGA TAACTTTCTGCAT
Chr3	27139753	rs237712466	T/G	GTCACCGAGCATGTGTAAACC	GCGGAAACTCACAAATCTTCATCTT
Chr3	73922455	rs31154737	A/T	ATCCAAGCTCTGAATTGACCCATT	CTGGCCCTTTCACACATCTCA
Chr3	107273295	rs31321678	A/G	CCTGCAAATTGTGCTCTGGAAA	GTGGTGGTCTTTGCCTCTGT
Chr3	151882540	rs31594267	A/C	TCTTGCCTCCGACCATGAAATG	TCAGCAGTTTTATCTTAGTCAGGTTTCAA
Chr4	6301848	rs32143059	G/A	AGCTCATGTTGATATGAAAAATAAATT CTTAAAAAGGATT	ACATTTTATTAAAAATCATTAGAGTTCTA TGTCTTGGGT
Chr4	28249560	rs13477622	T/C	TGAAGGTCTCCATTGCCACATG	CAGTGAATATTCCTAATATAAGTGAAGCTGGTT
Chr4	65605269	rs13477746	T/C	CCTTCTCCAATCCATTTCTCACTGT	AATCTGATAATATAGCTATTATAAAAAAT GTAGTGTGCCA
Chr4	110323003	rs245725397	C/T	GAGCAGTCCATCTTGTATATTGGAACA	AACGGAAAGCCAGTGTAACCTAAA
Chr4	155284926	rs6397070	T/C	AGTGTCCCTTGTGTCCAATGAAA	TCCAAAGCTCTCTTGCCTTGAG
Chr5	4547791	rs247844351	C/T	GCCGAATGGCATAGCAGAATT	CTGGATGGCGTCAGAGTTTCT
Chr5	41153028	rs33508711	C/T	GAATCTGTGATCGCTACCTGTATCC	AAGAGAAAAAGGAGCCTTTGTGAGA
Chr5	71133300	rs13478320	C/A	GATACTGTTGTAGTCATTTCAGGAAACCA	GATGTTTCTGGTTCTTTGAGAGATGC
Chr5	92510104	rs33249065	A/G	ACCAAGGCACAAAAAAACCCAATTT	TGGCAGATGTGTGTTTGATAGCT
Chr5	117909356	rs3662161	A/G	ACCAAGGCATAGCATAGCATAGC	GTAAAAGCACCTGTATTGGGTTTGG
Chr5	150428596	rs33208334	T/C	AACATGGCCATAACCAACTGTACT	GGCTCTGCAGTAAGCACTTGTTATA
Chr6	6183941	rs30450019	A/G	AGGCAGCTGTTAAATGCTAGCT	GCAAATCAGAAAGGTGGGAAAGAGA
Chr6	44236335	rs30892442	A/C	TGTTCGACAATTCTGACTGAGCTC	AGTGTGCTATACAACAAAGACAATCGT
Chr6	67237174	rs6157367	T/A	CTACTCTTAAAGCAGTCCTGTCACT	TCTCTTACTTTTTTGACTATGGATAAATGGCT
Chr6	117420898	rs13478995	C/G	AGCAATCAGAGGAGGAAGAACCT	GCACCTCACATTTCTCTTCTACCA
Chr6	141021111	rs235068709	G/T	GCGGTCTCACCATATTGTCCTA	CAGTTGTATGGCTGGAGATGCTT
Chr7	6929448	rs242748489	G/A	CCATCTTCCTCATGAAGAATATTAAGCTACA	CGGATCTCATGATGTGTCCCTTTTA
Chr7	38216957	rs31221380	A/C	TCTGCCTCTCTTTTCTCCTATTCCT	CCCGTTTGACTGAAAAGCACAATAT
Chr7	78961795	rs32060039	C/G	GGAAGCGTGGGCTCCTC	TGCAATGCTTTTCCTGGAGTAACTT
Chr7	110121823	rs243575509	C/T	CTTTCAGCCCTTGAGGCAATG	TGCTCATCCTCTTCTCCTATGCA
Chr7	136179208	rs13479522	A/G	CTGTCCCATCTGTTGAGAAGCA	GTAAGATGTGCACTCAGCATTGAC
Chr8	10521755	rs13479605	C/A	GCATGTGCATGGGCTTTAATTAAGT	CTGACAGTCACTGGCTTCCT
Chr8	30207547	rs13479672	T/C	AATGATATGCACCACAGCACTCT	GCACTATTGCTAAGGGAAACGGATT
Chr8	77477256	rs32729089	T/A	CTACCCTATGTCAGGTGTTTTCATCA	GGGTGAGGTATTTGTGGTCTGTTA
Chr8	94031516	rs33601490	T/C	CTTGGTGCTATGGCTTTAAAAGGTT	CCTCAGATGTCTTACTCATAACAAGCT

Chr	Position	Rs number	B6J/B6N	Forward primer (5'-3')	Reverse Primer (5'-3')
Chr8	126154896	rs32577205	A/G	GGAGGAGTCTCTAATTGCTTTTATGGT	GGGACTTTGTGATCACATCTAGCTT
Chr9	6238770	rs33672596	A/A	GTGCACACATGAACCTGACAAA	GGCCCCCTAATTATCATTGATCATACA
Chr9	30964211	rs13480122	T/C	ACAAAGCAGAGAGAGGCTGTAC	AGATCCCAGACCTCGGTGAG
Chr9	52593224	rs29644859	T/G	AGTGCTCTACAGTGCAAGAAATTGA	GTCTCCTGACTCTTAAGAATGGCAAT
Chr9	85132792	rs260373537	T/C	TCAAGGTTCCTTCTGCCCATAAAAT	GAGGACTGAAATGGATTCTAACAGGAAA
Chr9	119550616	rs30431245	T/C	CAGGCTTGAGAGCAGTGGTATTTAT	GGCAGAAAGGAAGTTTAAGGAGAGA
Chr10	5315765	rs50477269	A/G	CTCTAAGTTTCCAGAAGGCAAAAGC	AGACACTCTGTGCACTTAGAGATTCT
Chr10	33372829	rs13480575	T/C	GCAGTCTCTGAAGGTCATTTTACCA	TCTCCTTGAAGGTTGCTGATCAC
Chr10	57472268	rs13480619	T/C	TTTGACAACAGGCTTCCTACTCTTT	TGGGCTTGTCCTAGTTTGAAAAGT
Chr10	80258110	rs13459122	T/A	GGCAGCAACAATGTGTGAGATG	CTCTGTCTTGTGATGACCTCTGT
Chr10	108815683	rs13480759	C/T	GGTTTTCTTGGCTTTTGTCTTCTGT	CGTGGAGGGATTAGAAGACACTT
Chr10	126196231	rs236992510	G/A	CCTCATCAACCACTCCAAGGT	CTCCTGAATTCTGCATCCAGTGA
Chr11	4408733	rs3659787	G/A	GCATGGTTCTAGCGCACGAA	CAACCCTGGTTGCACAAATGAG
Chr11	28247415	rs259140591	C/T	ACATAAGTGGTTTTCCCAGAATTATTTTTTATTTTCTT	AAGGTGCTTCAGTATAAATAGATTTTTTTTTAAAT
Chr11	47930884	rs13481014	T/C	TCTTACATGTTTTTATAATCTCCAGTGCATAATGT	GCGAGACAAGTATTTCCTGATACTTATGTAT
Chr11	79065732	rs13481117	G/T	AATCTTCCTTCTACCCCACCCA	GAGGTCATGAGGTCAAGATTGTTCT
Chr11	120168102	rs49027247	T/C	GGGAAGCCCATTGTAGAAGTATCAG	GGCTCCCAGGCAAGGT
Chr12	7460524	rs29142759	A/G	GTACATAAGTGCTTTTCCTGGACACT	CTTTGCAGGTAGAGTTCTAAGAACTATGAATT
Chr12	35152831	rs29487143	G/C	TGGTTCTATGCTTCAGTGTATTGCA	ATTCCATTTATTACATATGCAAAATGTTCATCGT
Chr12	63868521	rs29133146	A/C	GCTGTGGCTTGCTCTAGGA	CCCCTCACCGAAGATGCTT
Chr12	86986287	rs13481569	G/A	TGGGTGCGCTGTTTCAGATT	GCTGGAATATTGAATGGCTTGGTTT
Chr12	108071865	rs13481634	A/C	GCTGGACATGTTGCTTCTCACA	GAGCACCTGTCTCCAGCAT
Chr13	3427897	rs30039194	A/A	TCGCAACCCCAGCTCTTG	ACCAGTCTCTCAATCCAACATGTG
Chr13	41538155	rs3722313	T/C	TGCCTGCTCTGCCTTCTC	GGAGACAGGTGAAGAGTGAGGAA
Chr13	77550367	rs29802434	G/C	TCAGCGATACCCCATGTTAAAATCA	GAAGACAAATACTGAGAGGCAAAGAGT
Chr13	101979187	rs3702296	A/G	CCCATGTTATGGACTCAAGGAGTAG	TCTTTACGCCTGCTTCCTCAATAAG
Chr14	10769899	rs31187642	G/A	GGAAAGCAGGAAGCCAAGACA	TGTTAGAGCAGATGGGAGGTTACT
Chr14	37292635	rs31133670	A/G	ATTTCTGAAGTATGACCCGTATTACAACTC	CAATTCTACATTTTATAGAGTAAAAAGAGAGAAAAATCTGG
Chr14	74815528	rs30264676	T/A	CTATGGCAAAAGGGAAGTGCAAAT	TTGTCACAACTGTCTTCCTTTCTGT
Chr14	100024215	rs31059846	A/G	TCACCGTGAGTGGGCATTC	TGCTTAAGACCTTTACCATGCATCTT
Chr14	124508019	rs31233932	C/T	GCGTCAATCTACTCATGGTAAGGATATT	TCAGTCTTCTCAGTCCCTAATGCTA
Chr15	9686848	rs257670740	T/C	AAAATAACCCTAGAATTAACTTCCTGTCTTCAG	CCTTGCTTCAAAGCATACTCTTCCA
Chr15	30543322	rs261563123	C/T	GGTCTTGGGTGACTCTGTGAAAG	GGGAGTTTTTAGATCATTGACCTGTAGT
Chr15	71462981	rs31858887	T/C	TCATTTTATTTGGCATCTGCCATTAGC	TCAGCGTGGGAGTGAAATGATG

Chr	Position	Rs number	B6J/B6N	Forward primer (5'-3')	Reverse Primer (5'-3')
Chr15	97085796	rs31921278	A/G	TGTGTTAGCACTACAGTTGTTCATCA	GGAGTGGCTTTGAGATCATTTAGACA
Chr16	4207926	rs219190959	C/T	GCTTTAACAGTATGCAACCATTGGT	GGGCTGCACTGGTAACTCTTC
Chr16	17412172	rs4165065	T/C	CTCCTACAAACACCCTGAATGCT	AGAAGTATATCAGAGATGTTCATGAGATGGAA
Chr16	52740057	rs4187179	T/C	GTCTCCACGTCTGATGTCAAAGAG	GCTGAATGGTAGATTTACCAGCTGTA
Chr16	87819874	rs4214728	T/C	TGAAGCAGAAAGCAGTAACTTACCA	CTTTGTTTCCTTGACCACATTTTCCT
Chr17	5332903	rs4137196	T/C	GAATCTGATGCTGGCTGAATTGG	GTCCATGGCTGTTACTTCTAAGCA
Chr17	39307300	rs33334258	G/A	CAGTGGAATACTATTCAGATATGGAAAGAA AAGT	CTTTTAAGCCTGGATTACTACACTTTGG
Chr17	60459368	rs13483055	T/C	TGCTTGTGGCAGAAAGATCTAATCA	TGAAACTTCTCTGGACCTCCTCTT
Chr17	93798641	rs229426697	C/T	AAAATTTATGTAACAATAAAGAGGCTAATG TTTTGAATCT	TCTAGAGCTTTTAGGTGTGTTGTCAAG
Chr18	15408257	rs13483221	C/T	GCTGTCCAGTGCAAGAGTCA	ACCAACCTGGATGAGTCACATTTAG
Chr18	35366160	rs13483296	A/T	TGTACAGCTAATTTAGCTATTCTGCACAT	TGGTTGGTGCCCAGTACTTAAAA
Chr18	54774495	rs13483369	A/C	AGAAGCCCTGTCATGAAAATCACAT	GGGTGCCCCAAAATATTGTATGAAA
Chr18	84686237	rs29690544	T/C	ACCTTCAGGCAGTCCAGTACT	TCTCAGAGTTTCTCATCTTTAGGTGTACT
Chr19	9101495	rs31112038	G/C	CCGGTGGGACCTTCATTTCTAAAA	CCTAAGATGCCGTCATATACAAAGTCA
Chr19	16676708	rs30709918	T/C	GTTTACAAGTAACAGCAGGCAACAG	GTAAAACCTCCTGCATATCACTCTGA
Chr19	38079901	rs30953636	G/T	GTTTGCAAAGCCAGATTTTCTCCTA	GGTTCAGCAGGGTCCTTTGT
Chr19	50050644	rs3724876	G/T	TCAGGCTTAGTTTTTTTAATGTCAGGAGAT	CCTCAACGGAGCTTTGTCCTT

3.4. Whole-exome sequencing[225]

In order to perform the whole exome sequencing, tissue also was collected from the N2 mice by tail cutting. The genomic DNA was isolated and purified by using a DNeasy Blood & Tissue kit (Qiagen). According to the SeqCap EZ Developer Library kit (MM9 exome, cat#110624, Roche NimbleGen) from 500 ng of genomic DNA, the exome sequencing libraries were prepared. Sequencing of multiplexed library with 151x2 paired-end mode in NextSeq 500 sequencer (Illumina) was performed by i-Laboratory LLP sequencing platform (Tsukuba, Japan). Reads in FASTQ files were imported to CLC Genomics Workbench (Qiagen), trimmed by 1-base at 3' end, and mapped to the mm10 mouse reference which represents the C57BL/6J strain genome. Exome sequencing statistics were calculated for capture target region definition provided by SeqCap kit. Variant call was performed using

Basic Variant Detection tool where the potential variants were filtered against control mice variants. Nonsynonymous base substitutions and small InDels were identified based on ENSEMBLE transcript annotation. All of variants identified on chromosome 10 and chromosome 18 for each pedigree were verified by visual inspection of sequence tag alignment. The numbers of the total reads and of variants called of four obese mice from the *Obese-10* and *Obese-13* pedigrees were summarized in Table 1[225].

3.5. Mutation analysis and genotyping of mutant mice

3.5.1. Isolation and purification of DNA from mouse tissue and agarose gel

To isolate the DNA the tissue was collected from the sample mouse's tail/ear. The genomic DNAs were isolated by using QIAGEN DNeasy blood and tissue kit (QIAGEN). The isolated DNA was amplified by PCR reaction using specific primers. The amplification of the DNA was confirmed by running the amplified DNA sample through agarose gel electrophoresis (1.5 % gel, Run time 30 minutes at 100 volts). The amplified PCR products were purified using fast gene Gel/PCR extraction kit (Nippon genetics Europe GmbH, Germany).

3.5.2. Direct sequencing of DNA

For direct sequencing, the PCR products amplified from genomic DNAs were purified using a Fast Gene Gel/PCR extraction kit (Nippon Genetics). The sequencing reaction was performed using PCR products (purified) 50-100ng, forward and reverse primer 0.5 µl, big dye 1.0 µl, big dye terminator (v3.1) 1.5 µl and de-ionized water up to 20 µl. The reaction was initiated with hot start at 96°C for 1 min and followed by 25 cycles of 96°C for 30 Sec, 50°C for 15 Sec, 60°C for 4 min and finally holds at 4°C. The PCR sequenced product was then purified by using fast gene dye terminator removal kit (Nippon genetics Europe GmbH, Germany). Finally, the DNA sequencing was analyzed by using the ABI 3130 sequencers (Applied Biosystems, USA).

3.5.3. Detection of gene mutation by dCAPS assay[225]

To detect the *Mc4r* gene mutation through Derived Cleaved Amplified Polymorphic Sequences (dCAPS) assay, the genomic DNA was amplified using Mc4r S1 (5'-TCCACCCGGCTGACCACGATGGGA-3') and Mc4r AS2 (5'-GGCATCCGTATCCGTACTGT-3') and then digested with *Dde*I, which recognizes only the mutant *Mc4r* sequence. Electrophoresis on 2% gel showed a 353 bp band for the wild-type and 219 bp and 134 bp bands for the *Mc4r* mutant. The single nucleotide variant of the *Sim1* gene was also detected via the derived cleaved amplified polymorphic sequence (dCAPS) method using primers designed by dCAPS Finder 2.0 (http://helix.wustl.edu/dcaps/dcaps.html). Genomic DNA was amplified using Sim1 dCAPS S1 (5'-TCCACCCGGCTGACCACGATGGGA-3') and Sim1 dCAPS AS2 (5'-AAGGCTCAGGAGGAGAGAGG-3') to produce a *Fok*I recognition sequence, GGATG, specific to the wild-type *Sim1* sequence. PCR products were digested with *Fok*I and then separated via electrophoresis on 2.5% agarose gel. *Fok*I digestion of the *Sim1* heterozygous mutant genome resulted in 189 bp, 152 bp, and 37 bp bands, while *Fok*I digestion of the wild-type genome results in 152 bp and 37 bp bands.

3.6. Clinical biochemical test[225]

At the age of 12 weeks the blood samples (200 µl) were collected from the tail vein or orbital sinus of mice under anesthesia at the late light phase in a fed condition. The samples were then centrifuged to separate the serum from the blood and stored at -80ºC until use. According to the protocol of ultra sensitive mouse insulin/leptin (ELISA) kit (Morinaga institute of biological science, Inc. Yokohama, Japan) the serum insulin/leptin level was measured and the absorbance was measured by using ARVO^{TM} X5 2030 multi label reader (PerkinElmer, USA). The glucose level of mice was measured by collecting blood from the

tail vein using glucometer “Glu-test every” kits (Sanwa Kagaku Kenkyusho Co. Ltd. Japan) at the age of 9 weeks, at late light phase in a fed condition.

3.7. Luciferase assay

3.7.1. Plasmid construction[225]

Genomic cDNA of mice was synthesized from the hypothalamic tissues. Full-length mouse *Sim1* and *Arnt2* cDNAs were amplified from mouse hypothalamic cDNA, which was reverse-transcribed from mRNA prepared using a Prime Script RT kit (Takara). By the use of In-Fusion HD Cloning kit (Takara-Bio) these *Sim1* cDNA and *Arnt2* cDNA were then subcloned into pcDNA3.1 vector. Using KOD plus a mutagenesis kit (Toyobo) a single nucleotide substitution was introduced into *Sim1* cDNA to express SIM1(M143K). The Luciferase reporter plasmid 6xCMEAd2MLP-pGL3 vector was constructed by inserting a 6x CNS midline enhancer (CME) sequence of the Drosophila *toll4* gene[226] and TATA box into the upstream region of the firefly luciferase gene of the pGL3-basic (Promega) according to pML/6C-WT vector[227] using ligation reaction. The presence of the mutation in the sub-cloned vectors and also the WT sequence were checked and confirmed by direct sequencing using ABI 3130 Genetic Analyzer (Applied Biosystems, USA). All of the plasmid vectors were transformed into *DH5-α,* cultivated and finally purified to use.

3.7.2. Reporter assay of SIM1 transcriptional activity[225]

Luciferase assay was performed to observe the SIM1 transcriptional activity in cells transiently expressing WT or mutant SIM1. HEK293 cells were maintained and cultured in DMEM supplemented with penicillin/streptomycin and 10% fetal bovine. The cultured cells were plated in 24-well plates at a density of 50,000 cells per well. After 24 hours, cells were subjected for transient transfection with pcDNA3.1-*Sim1* (50, 150, 300 ng) or with pcDNA3.1-*Sim1(M143K)* (150, 300 ng), pcDNA3.1-*Arnt2* (150 ng), pML-6xCME-Luc (150 ng), and pRL-SV40 (40 ng) per well using Lipofectamine X (Life Technologies). By adding

pcDNA3.1 the total amount of transfected plasmids was adjusted to 640 ng in each well. Forty-eight hours post-transfection, the luciferase activity of the cells were assayed by using a Dual-Luciferase Reporter Assay System (Promega). Each assay was performed in triplicate and repeated three times. Firefly luciferase activity was normalized to the Renilla luciferase activity for each well[228].

3.8. Measurement of daily food intake and epididymal fat[225]

At the age of 8 weeks the N3 male mice were housed individually and supplied chow diet food (MF; Oriental Yeast). The mice were allowed one week for habituation of taking food from the food jar. After the one week habituation of food intake the amount of daily food intake was measured at every 24 hours in normal condition for seven consecutive days. At the age of 12 weeks of N3 mice we had dissected the intra-abdominal white adipose tissue (WAT)/epididymal fat and measured the weight of epididymal fat by electric balance.

3.9. Production of diet-induced obesity mice[225]

In order to the production of the diet induced obese mice, the C57BL/6 mice at 3 weeks of age were subjected to feed a high-fat diet (D12492; Research Diet). The high-fat diet provided 5.2 kcal/g (60% fat, 20% carbohydrate and 20% protein,) whereas, the low-fat diet, or normal chow, (MF; Oriental Yeast) provided 3.6 kcal/g (13% fat, 61% carbohydrate and 26% protein). These high fat diet feeding was continued up to the age of 9 weeks. After 9 weeks of being fed the high-fat diet, mice were sacrificed at ZT11.

3.10. Collection of tissue and preparation[225]

In order to measure the mRNA expression level of hypothalamic genes/neuropeptides the hypothalamic tissue was collected from N3 male mice. The mice were supplied chow diet food. At the age of 12 weeks the mice were deeply anesthetized with sodium pentobarbital (50 mg/kg body weight) and then sacrificed via cervical dislocation. The brain of the mice was rapidly removed and the medial hypothalamus was dissected on ice based on the

following boundaries: rostral, the optic chiasm; caudal, the mammillary bodies; 1 mm bilateral from the midline; and 1.5 mm dorsal of the ventral surface. This dissected tissue included the arcuate nucleus, ventromedial hypothalamic nucleus, dorsomedial hypothalamic nucleus, paraventricular hypothalamic nucleus, anterior hypothalamic area, and the medial half of the lateral hypothalamic area. After collection of the brain, it was rapidly stored under liquid nitrogen and finally stored at -80^{o}C up to use. This tissue was then used to isolate RNA using the RNeasy Lipid Tissue Mini kit (Qiagen, Chatsworth, CA). The isolated RNA also stored at -80^{o}C.

3.11. Quantitative RT-PCR analysis[225]

The cDNA synthesis by the using the isolated RNA with oligo dT primers and a Prime Script reverse transcriptase kit (TaKaRa). Then the real-time quantitative PCR reactions were performed with ViiA7 Real-Time PCR System (ThermoFisher) using SYBR GREEN PreMix Ex Taq (TaKaRa). In order to the quantitative RT-PCR analysis of the hypothalamic genes, the following PCR primers were used: *Agrp* forward, 5'-TCCCAGAGTTCCCAGGTCTA-3'; *Agrp* reverse, 5'-GCCAAAGCTTCTGCCTTCT-3'; *Avp* forward, 5'-AGGATGCTCAACA CTACGCTCT -3'; *Avp* reverse, 5'-ACTGTCTCAGCTCCATGTCAGA -3'; *Crh* forward, 5'-GAAAGGGAAAAGGCAAAAGAA-3'; *Crh* reverse, 5'-GTTAGGGGCGCTCTCTTCTC-3'; *Gapdh* forward, 5'-AGAACATCATCCCTGCATCC-3'; *Gapdh* reverse, 5'-CACATTGGGG GTAGGAACAC-3'; *Ghrh* forward, 5'-CTCTTTGTGATCCTCATCCTCAC-3'; *Ghrh* reverse, 5'-AGTTTCCTGTAGTTGGTGGTGAA-3'; *Mc4r* forward, 5'-GCCAGGGTACCAA CATGAAG-3'; *Mc4r* reverse, 5'-ATGAAGCACACGCAGTATGG-3'; *Mch* forward, 5'-TGC TGAGTCCACACAGGAAA-3'; *Mch* reverse, 5'-GCCAACATGGTCGGTAGACT-3'; *Npy* forward, 5'-TACTCCGCTCTGCGACACTA-3'; *Npy* reverse, 5'-TCACCACATGGAAGGG TCTT-3'; *Orexin* forward, 5'-GGGTATTTGGACCACTGCAC-3'; *Orexin* reverse, 5'-CCCA GGGAACCTTTGTAGAAG-3'; *Oxytocin* forward, 5'-GCCAGGAGGAGAACTACCTG-3';

Oxytocin reverse, 5'-CTCCGAGAAGGCAGACTCAG-3'; *Pacap* forward, 5'-CTATGGCTA TTGCTATGCACTCTG-3'; *Pacap* reverse, 5'-CAACCTGGGGAAGACTCATTTAG-3'; *Pomc* forward, 5'-AACCTGCTGGCTTGCATC-3'; Pomc reverse, 5'-TTTTCAGTCAGGGG CTGTTC-3'; *Sim1* forward, 5'-CCTCCATCCACAGAATCCAC-3'; *Sim1* reverse, 5'-TGATA CTGTTCGGTGCGGTA-3'; *Somatostatin* forward, 5'-CTCTGCATCGTCCTGGCTTT-3'; *Somatostatin* reverse, 5'-AAGTACTTGGCCAGTTCCTGTTT-3'; *Trh* forward, 5'-GAAGG TGCTGTGACTCCTGAC-3'; *Trh* reverse, 5'-ATCTAAGGCAGCACCAAGGTC-3'. The averages of *glyceraldehyde-3-phosphate dehydrogenase (GAPDH)* mRNA were used for normalization. A relative quantification method was employed for the quantification of target molecules by calculating the ratio between the amount of the target molecule and a reference molecule within the same sample, according to the manufacturer's protocol. The reactions were performed in duplicate and the results were averaged.

3.12. Statistical analysis[225]

The significance of differences between two groups was assessed by two tailed *t* test. Data of SIM1 luciferase assay were analyzed by one-way ANOVA followed by Tukey's post-hoc test. The body weight data were analyzed by one-way repeated ANOVA followed by Tukey's post-hoc test. The qPCR data were analyzed by two-tailed *t*-test with Bonferroni correction for multiple comparisons. Sample sizes were determined using R software based on the averages and standard deviations that were obtained from small scale experiments. The experimenters were blinded to genotypes and treatment assignments. Statistical analyses were performed using SPSS Statistics 22 (IBM) and R software. All data were tested for Gaussian distribution and variance. Homogeneity of variance was tested for using Levene's test[225]. The differences were considered as statistically significant if $P < 0.05$. Data were expressed as the means ± SEM.

Chapter 4.
Results

4.1. Screening strategy to establish obese pedigree[225]

In order to screen of randomly mutagenized mice for sleep/wake disorder, ENU was injected into C57BL/6J (B6J) wild-type male mice (G_o mice) and crossed with C57BL/6J (B6J) or C57BL/6N (B6N) wild-type female mice to produce G1/F1 mice. In parallel with sleep/wakefulness screening of these randomly mutagenized B6J/B6N G1/F1 male mice, we performed dominant screening for obesity by using the same mice (Fig. 3a). In this project, we have dominantly screened more than 5000 phenodeviant G1/F1 males. In this dominant screening of obesity, we have screened about 2500 mutagenized G1 mice. These G1 mice were produced by the in vitro fertilization (IVF) method, using the sperm of ENU-treated B6J male mice and egg of wild-type B6J female mice. In addition to the G1 mice, we also have screened about 2940 phenodeviant F1 mice. These F1 mice were produced by the in vitro fertilization (IVF) method, using the sperm of ENU-treated B6J male mice and egg of wild-type B6N female mice. At the age of 18 weeks, the body weight distribution of these mutagenized F1 mice (n=2940) seems skewed toward overweight (mean = 33.3 g, standard deviation = 3.76 g and skewness = 0.85, Fig. 3b).

Among the 5000 mutagenized G1/F1 mice, we have selected thirteen obese mice at several ages to include early-onset and late-onset obesity and performed dominant screening to establish the heritable obese pedigree. In this regard, we have chosen the five heaviest male mice by 18 weeks old, having body weight: 51 g, 48 g, 48 g, 46 g, and 46 g and the other five heaviest male mice by 28 weeks old, having body weight: 53 g, 51 g, 51 g, 51 g, and 50 g. We also have selected two obese mice by 32 weeks old, with high blood glucose levels having body weight and blood glucose: 52 g and 286 mg/dl, 53 g and 266 mg/dl. Besides, we have selected one mouse, which exhibited severe early-onset obesity, at the age of 10 weeks

having a body weight 47g. These thirteen obese male mice were then crossed with B6N wild-type female mice through in vitro fertilization to produce N2 progeny (Fig. 3a).

During the screening, the obesity phenotype was considered as heritable, if at least 30% of the progeny developed obesity same as in the obesity of founder mouse. As we searched the gene mutations which reproducibly cause dominant inheritance of obesity, thus the body of progeny below 30% was not allowed. Among the 13 pedigrees, two pedigrees, *Obese-10* and *Obese-13,* showed heritable obesity. The offspring of the other 11 pedigrees did not show obesity and high blood glucose. The F1 founder mouse of *Obese-13* pedigree having body weight 47 g at the age of 10 weeks, which was the most severe occurrence of early-onset obesity among all mice screened. Correspondingly, the F1 founder mouse of *Obese-10* pedigree, having body weight 51 g at 18 weeks old was the heaviest mouse at this age among all the mice screened, except for the F1 founder mouse of *Obese-13*. Consequently, the two founders of the heritable obese pedigrees were two most obese mice out of the 5000 mice screened. The inherited obesity characteristics of N2 mice were confirmed by measuring body weight (Fig. 6a,b and 10a,b). Linkage analysis of each pedigree exhibited a strong and single peak of LOD score. Subsequently, the direct sequence of candidate genes within the mapped regions led us to identify a single point mutation in *Mc4r* gene of the *Obese-10* pedigree and in *Sim1* gene of the *Obese-13* pedigree. Thus, among a total of 13 pedigrees, the *Obese-10* and *Obese-13* pedigrees, which were derived from a screening of the F1 mice, showed severe obesity at the N2 generation.

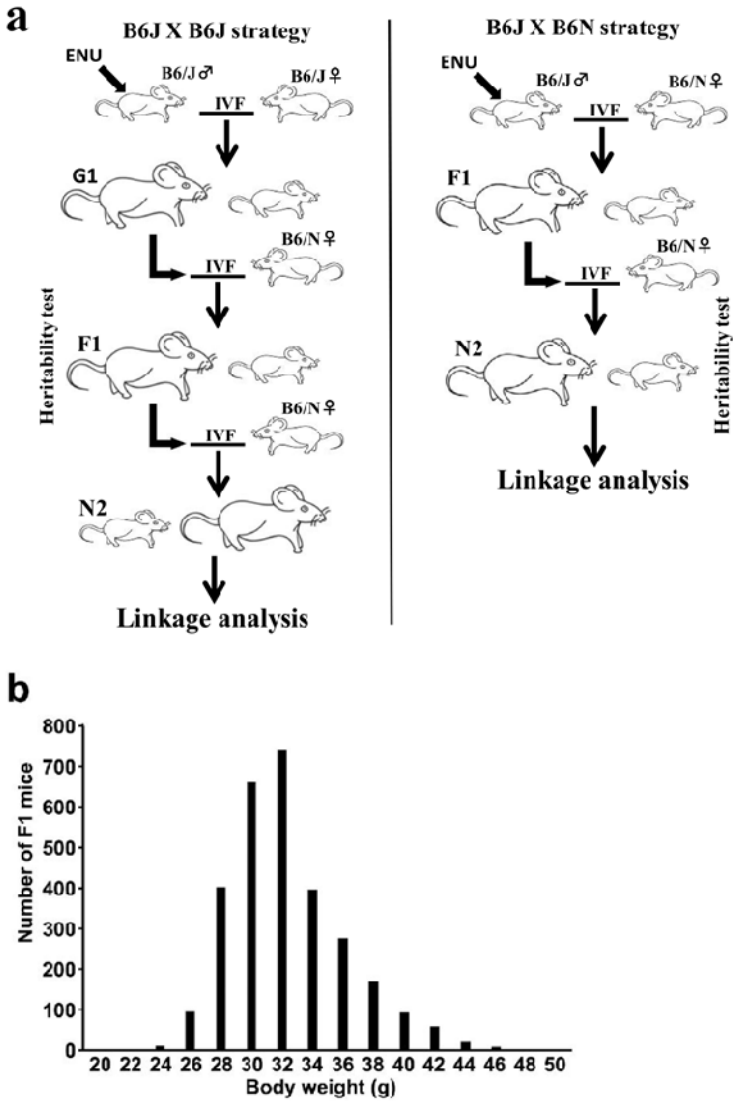

Figure 3. Obesity screening of randomly mutagenized mice[225].

(a) Ethylnitrosourea (ENU) was injected intraperitoneally to the C57BL/6J (B6J) males, which were crossed with C57BL/6J (B6J)/C57BL/6N (B6N) females to obtain the offspring (G1/F1 mice). The F1 mice were screened for obesity. By the use of sperm cells from an obese mouse the in vitro fertilization was performed with wild-type B6N eggs to obtain N2 mice, which was examined for heritable obesity. If the pedigree showed heritable obesity, N2 mice were further used for a linkage analysis. (b) The body weight histogram of all F1 mice screened at 18 weeks old. n = 2940.

4.2. *Sec63* mutation of the *Obese-13* pedigree[225]

We performed whole-exome sequencing using two severely obese N2 mice (Body weight 62.5 g and 60.6 g at the age of 26 weeks old) of the *Obese-13* pedigree as well as two severely obese N2 mice of the *Obese-10* pedigree (Table 1). The two *Obese-13* obese mice showed heterozygous non-synonymous mutations in the *Sec63* genes (Chr10: 42816394) along with *Sim1* (Chr10: 50908536) gene, whereas, the two obese mice of *Obese-10* pedigree did not. The mutant *Sec63* gene was located within the mapped region of chromosome 10 along with *Sim1* gene (Fig. 7c) and no additional non-synonymous mutations were found there. To further segregate the *Sec63* gene mutations for the obese phenotype, we performed direct sequencing of the *Sec63* genes of five obese mice, which had a chromosomal recombination between rs13480575 and rs13480619 (the fifth column in Fig. 7d) and of randomly selected five non-obese mice. All obese mice exhibited mutations in *Sec63* genes as well as in *Sim1* gene, but the non-obese mice did not have any mutations either in *Sim1 gene* or in *Sec63* gene. As a result, it was confirmed that, the mutations in the *Sim1* and *Sec63* genes were co-segregated due to its proximity. In one obese mouse that is devoid of the B6J/N haplotype (the second column from the last in Fig. 7d) did not show any mutations in the *Sim1* and *Sec63* genes. This result demonstrates that obesity in this mouse may be caused due to the effects of other gene mutations or by any other unknown factors. In the *Obese-13* pedigree, the mutation in the *Sec63* gene causes an isoleucine to methionine substitution at the residue 620. *Sec63* gene is highly conserved from yeast to man[229]. It acts as an important part of a protein complex that translocates a newly synthesized peptide into the endoplasmic reticulum and also allied with autosomal polycystic liver disease[230]. But, none of the obese mice of the *Obese-13* pedigree exhibited any cyst formation in the livers suggesting that the *Sec63* gene does not affect in causing obesity, but we can not avoid the possibility.

4.3. *Mc4r* mutation of the *Obese-10* pedigree

4.3.1. Identification of single point mutation on *Mc4r* gene in the *Obese-10* pedigree[225]

The body weight of the founder F1 male mouse of the *Obese-10* pedigree was 51 g at the age of 18 weeks. This phenodeviant F1 mouse was crossed with wild-type B6N female mice to produce N2 mice. Relative to the body weight distribution of the F1 mice, the body weight histogram of the *Obese-10* N2 mice were clearly deviated toward overweight (Fig. 4a, Mann-Whitney U test, $p < 0.0001$). The N2 mice of this *Obese10* pedigree were used for the linkage analysis. The initial linkage analysis was performed by using 23 N2 male mice and identified a high QTL (quantitative trait locus) peak on chromosome 18 with an LOD score 3.94 according to the body weight of 18 weeks (Fig. 4b). These N2 mice also showed a LOD score 2.44 (Fig. 4c) which was measured according to the body weight of 26 weeks. These 23 N2 mice also showed a high LOD score 3.94 on chromosome 2 which was measured according the body weight of 18 weeks (Fig. 4b), but it was gone near the base level when measured according to the body weight of 26 weeks (Fig. 4c). The reason of change of LOD score is due the change of body weight values of some mice (which have very close body weight values exhibited a variation comparing with one another) that was measured at 18th week and 26th week. Further analysis was focused only on the chromosome 18 using a larger number (n=206) of N2 mice (females, n = 99; males, n = 107), which exhibited a high LOD score (10.7 for males, 13.3 for females; 16.4 for total,) between rs13483369 (Chr18: 54774495) and rs29690544 (Chr18: 84686237) (Fig. 4e, f). Within this region, about 147 protein-coding genes are located, among them, the *Mc4r* gene exhibited a well known role in relation to the pathogenesis of human obesity[231–234] and rodents[235,236]. Throughout the MGI (Mouse genome informatics) data base analysis, we found that except *Mc4r* gene, the other genes are not associated with causing obesity but we can not deny the possibility. Through the whole-exome sequencing, we also found some genes mutations in different chromosomes (except

chromosome 18) of *Obese-10* pedigree. We did not find any established report of these genes for association with causing obesity. According to the linkage analysis, the QTL peaks in this region is not so high (under the suggestive value), which assumed that the gene mutations within this region does not create a strong association to cause obesity.

In addition, through the whole-exome sequencing we also did not find any common gene at chromosome 2, between the two sequenced mice sample. One of the mice showed mutation in *Xirp2* gene and *Lrp2* gene (Fig. 4d). But these genes are not associated with obesity. Actually, this QTL peak was associated with low body weight and the peak was near to the base level when measured according to the body weight of 26 weeks (Fig. 4c). Subsequently, through the direct sequencing of the entire *Mc4r* gene we have identified a single nucleotide substitution from thymine to adenine only in the obese mice of the *Obese-10* pedigree (Fig. 5a). This mutation caused a translation of amino acid from tyrosine to stop codon (Tyr-41-Stop) on the codon 41 of the peptide. This amino acid (tyrosine) is located at the beginning of the first transmembrane domain of the MC4R protein (Y41X) (Fig. 5b). According to the result of whole-exome sequencing of two obese mice (Body weight 56.3 g and 54.5 g at the age of 26 weeks old) of the *Obese-10* pedigree, the substitution of nucleotide thymine to adenine in the *Mc4r* gene (Chr18: 66859918) is located within the chromosome 18 region linked to the obese phenotype (Table 2, Fig. 4e). On the other hand, the two obese mice of the *Obese-13* pedigree did not show any mutation in *Mc4r* gene (Table 2). Thus, the mutation (Y41X) of the *Mc4r* gene is considered to be responsible gene for causing obesity in the *Obese-10* pedigree. In addition, the two mice (the last column in Fig. 4f), of *Obese-10* pedigree showed obesity without having the B6J/N haplotype. By direct sequencing, we also confirmed that these mice are devoid of any mutation in the *Mc4r* gene. This result, demonstrates that the effects of any other mutations or by other unknown factors may cause the obesity in these mice.

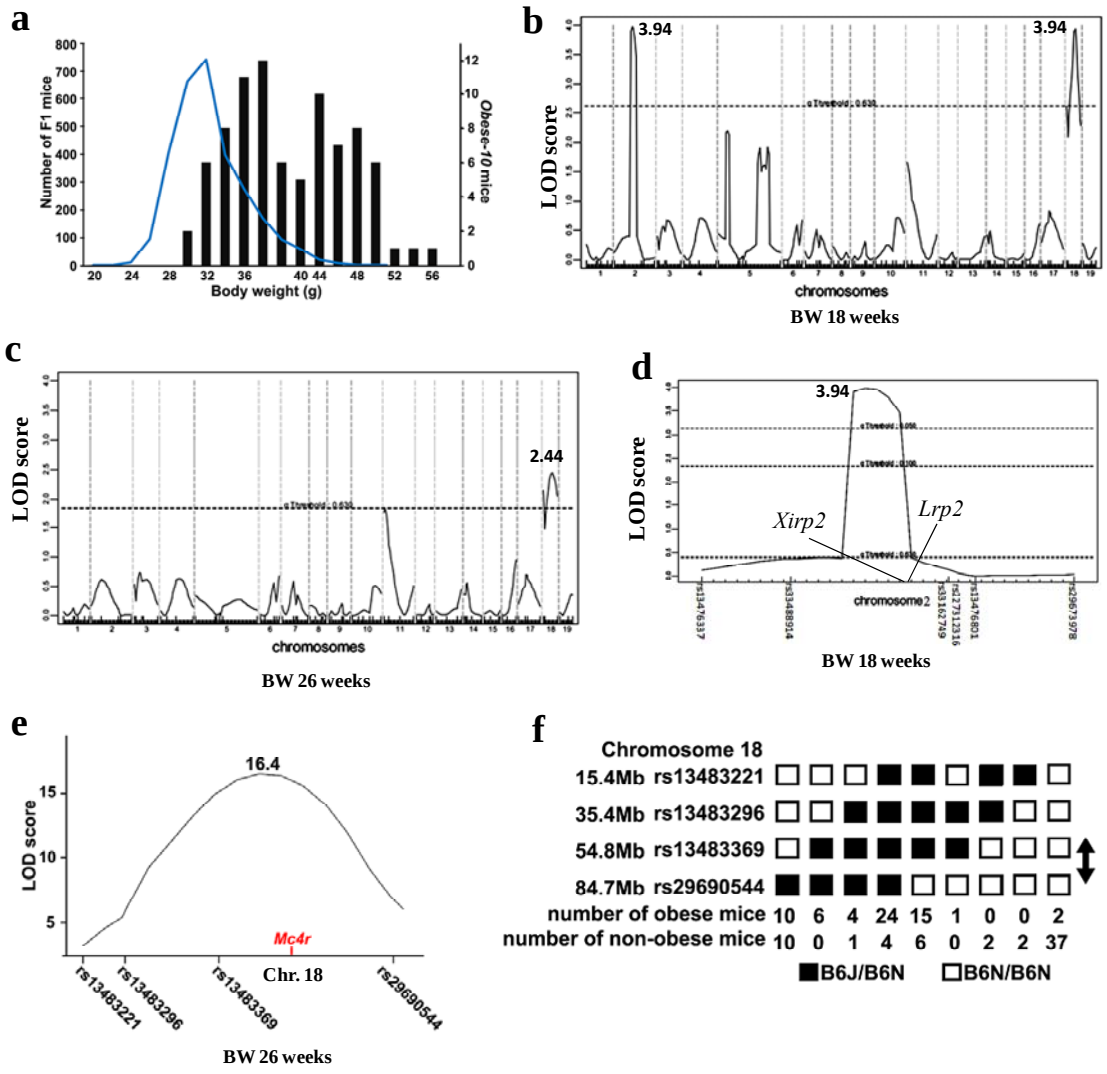

Figure 4. Mapping and analysis of sample mice of *Obese-10* pedigree[225]**.** (a) The body weight histogram of F1 mice and N2 littermates (bars) of *Obese-10* pedigree. Here, the body weights of N2 littermates are deviated toward overweight compared with the body weight distribution of the screened F1 mice. (b) QTL analysis of the *Obese-10* pedigree according to the body weight of 18 weeks (n=23) showed a high LOD score peak associated with high body weight on chromosome 18 associated with low body weight on chromosome 2. (c) QTL analysis of the *Obese-10* pedigree according to the body weight of 26 weeks (n=23) showed a high LOD score peak associated with high body weight on chromosome 18. (d) The results of QTL analysis of the *Obese-10* pedigree (n = 23) according to the body weight of 18

weeks exhibited a single peak of LOD score between rs33488914 and rs33622749 on chromosome 2. (e) The results of QTL analysis of the *Obese-10* pedigree (n = 206) for body weight exhibited a single peak of LOD score between rs13483369 and rs29690544 on chromosome 18. (f) The results of haplotype analysis of *Obese-10* N2 mice indicate that the mutation falls between rs13483369 and rs29690544 (arrow) on chromosome 18.

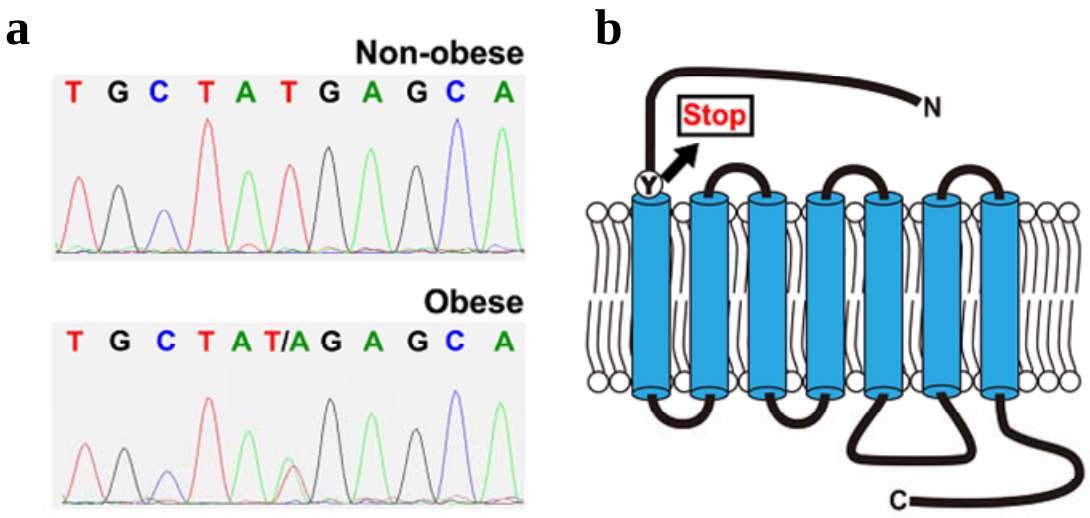

Figure 5. Identification of a single nucleotide substitution of the *Mc4r* gene in *Obese-10* pedigree[225] (a) Through the direct sequencing of the *Mc4r* gene identified a substitution of thymine-to-adenine specific to obese mice of the *Obese-10* pedigree. (b) The mutation in the *Mc4r* gene results in a premature stop codon, which is located at the beginning of the first transmembrane domain of the MC4R, a G-protein coupled receptor.

4.3.2. *Mc4r*$^{Y41X/+}$ mice exhibited higher *Mc4r* mRNA[225]

To investigate *Mc4r* mRNA level through qPCR analysis, the cDNA was synthesized from hypothalamic tissue of mice at 12 weeks of age. The *Mc4r* mRNA content of *Mc4r*$^{Y41X/+}$ mice was significantly higher than that of *Mc4r*$^{+/+}$ mice (Fig. 6d).

4.3.3. *Mc4r*$^{Y41X/+}$ mice generated severe obesity[225]

The mice were kept in the single cage, fed a normal diet and the body weight was measured weekly. The N2 mice were weighed from the age of 10 weeks to the age of 26 weeks and the N3 mice were weighed from 6 to 11 weeks. The body weight of both N2 male and female *Mc4r*$^{Y41X/+}$ mice were significantly ($p<0.001$) greater than those of *Mc4r*$^{+/+}$ mice (Fig. 6a,b). Besides, the body weight analysis of N3 mice of *Obese-10* pedigree exhibited a significant increase of body weight of *Mc4r*$^{Y41X/+}$ mice as early as 6 weeks of age (Fig. 6c). To measure the weight of epididymal fat we had dissected the intra-abdominal white adipose tissue (WAT) at 12 weeks of age. An excessive accumulation of white adipose tissue was found in *Mc4r*$^{Y41X/+}$ mice. The epididymal fat mass of *Mc4r*$^{Y41X/+}$ mice was significantly larger than that of *Mc4r*$^{+/+}$ mice at the age of 12 weeks (Fig. 6e). To investigate serum leptin level blood serum was collected at 12 weeks of age. Consistent with a larger fat mass, *Mc4r*$^{Y41X/+}$ mice had a higher serum leptin level compared with *Mc4r*$^{+/+}$ mice (Fig. 6f).

4.3.4. *Mc4r*$^{Y41X/+}$ mice were hyperphagic[225]

In order to measure the amount of food intake at the age of 8 weeks of N3 mice, we allowed the mice to take powdered food form a small food jar. After one week of habituation of feeding, at the age of 9 weeks the daily food intake was measured in every 24 hours for seven consecutive days. The *Mc4r*$^{Y41X/+}$ mice had a significantly ($p<0.001$) increased daily food intake compared with the *Mc4r*$^{+/+}$ mice (Fig. 6g).

4.3.5. *Mc4r*$^{Y41X/+}$ mice were pre-diabetic[225]

At the age of 9 weeks of N3 mice, the blood glucose level was measured by collecting blood from the tail vein. Though the blood glucose level seems to be higher in *Mc4r*$^{Y41X/+}$ mice than the *Mc4r*$^{+/+}$ mice, but statistically did not reach at significance (Fig. 6h). To investigate serum insulin level blood serum was collected at the age 12 weeks of N3 mice. As for glucose metabolism, where both *Mc4r*$^{Y41X/+}$ mice and *Mc4r*$^{+/+}$ mice had almost similar blood

glucose levels, but the serum insulin level of *Mc4r*$^{Y41X/+}$ mice was significantly higher than that of *Mc4r*$^{+/+}$ mice (Fig. 6i). The similar blood glucose level in obese pedigrees may be the result of compensation by the high insulin level.

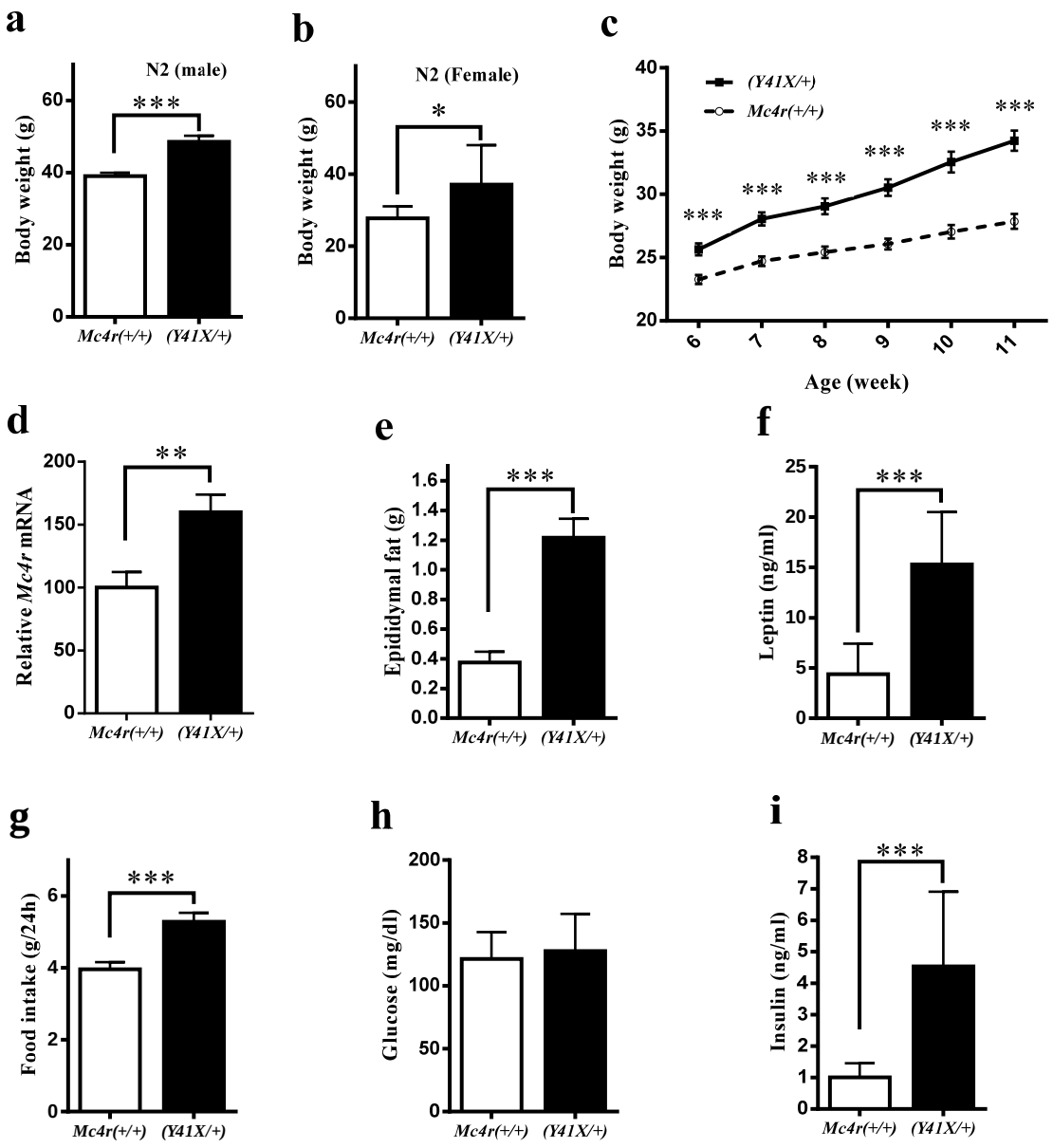

Figure 6. Metabolic phenotypes of *Mc4r* mutant mice[225]**.** (a) At the age of 26 weeks, the N2 generation of *Mc4r*$^{Y41X/+}$ male mice (n = 11) showed higher body weight than *Mc4r*$^{+/+}$ male mice (n = 11). (b) At the age of 26 weeks, the N2 generation of *Mc4r*$^{Y41X/+}$ female

mice (n = 4) also showed higher body weights than *Mc4r*$^{+/+}$ female mice (n = 8). (c) The increased body weight of N3 mice indicates early-onset obesity in *Mc4r*$^{Y41X/+}$ mice (n = 16) relative to *Mc4r*$^{+/+}$ (n = 16) mice. *** $p < 0.001$, one-way repeated ANOVA followed by Tukey's post-hoc test. (d) Increased level of *Mc4r* mRNA of *Mc4r*$^{Y41X/+}$ mice (n = 8) was observed than the *Mc4r*$^{+/+}$ mice (n = 6).) (e) The *Mc4r*$^{Y41X/+}$ mice (n = 6) exhibited increased epididymal fat weights than the *Mc4r*$^{+/+}$ mice (n = 6). (f) Increased serum leptin level was found in *Mc4r*$^{Y41X/+}$ mice (n = 8) in comparison to the *Mc4r*$^{+/+}$ mice (n = 8). (g) The amount of daily food intake of *Mc4r*$^{Y41X/+}$ mice (n = 6) was higher than that of *Mc4r*$^{+/+}$ mice (n = 6). (h) Both the *Mc4r*$^{+/+}$ mice (n = 16) and *Mc4r*$^{Y41X/+}$ mice (n = 16) exhibited almost similar blood glucose level. (i) The *Mc4r*$^{Y41X/+}$ mice (n = 8) exhibited higher serum insulin levels than *Mc4r*$^{+/+}$ mice (n = 8). * $p < 0.05$, ** $p < 0.01$, *** $p < 0.001$, two-tailed *t*-test. Data are shown as the mean + s.e.m.

4.4. *Sim1* mutation of the *Obese-13* pedigree

4.4.1. Identification of single point mutation on *Sim1* gene in the *Obese-13* pedigree[225]

The founder F1 mouse of the *Obese-13* pedigree weighted 47 g at the age of 10 weeks and within the increase of age the body also increased and exhibited severe obesity showing body weight 55.5 g at 18th week and 63.5 at the age of 26th week. Subsequently, relative to the body weight distribution of the F1 mice, the body weight histogram of the N2 mice of this obese pedigree showed a deviation toward the overweight (Fig. 7a, Mann-Whitney U test, $p < 0.0001$). These N2 mice were subjected for the linkage analysis. Initially, we performed linkage disequilibrium analysis of 49 N2 mice (25 males, 24 females) of this *Obese-13* pedigree and found a single and strong quantitative trait locus on chromosome 10 with a high LOD score 7.19 measured according to the body weight of 26 weeks (Fig. 7b). Further linkage disequilibrium analysis focusing only on chromosome 10, using 172 N2 mice of this pedigree (male, n = 106; female, n = 66), exhibited a very high LOD score (25.6 for total,

22.8 for males, 10.0 for females) between rs13480575 (Chr10: 33372829) and rs13480619 (Chr10: 57472268) (Fig. 7c, d). Within this region, About 96 protein-coding genes are located, but, only the *Sim1* gene exhibited a well known role in the pathogenesis of obesity in humans[237–239] and rodents[207,215,219,240,241]. Throughout the MGI (Mouse genome informatics) data base analysis, we found that, except *Sim1* gene, the other genes are not associated with causing obesity, but we can not deny their possibility. Through the whole-exome sequencing, we found some genes mutations in different chromosomes (except chromosome 10) of *Obese-13* pedigree. We did not find any established report of these genes for association with causing obesity. According to the linkage analysis the QTL peaks in this region is not so high (under the suggestive value), which assumed that the gene mutations within this region does not create a strong association to cause obesity. In chromosome18 of *Obese-13* pedigree have suggestive LOD score about 3 (Fig. 7b) that is associated with low body weight, but we did not find any gene mutation through whole exome sequencing. The reason is that, Whole exome sequencing strategy can sequenced only the protein coding regions (exons). The mutation may be located in the region of introns. Thus, we did not find the mutation by whole exome sequencing. To identify the gene mutation in this region, it is necessary to perform whole genome sequencing. Subsequently, through the direct sequencing of all 11 exons of the *Sim1* gene we have identified a single nucleotide substitution in exon 4 specific to obese mice of the *Obese-13* pedigree, which results the transversion of amino acid from methionine to lysine (Fig. 8a,b).

According to the result of whole-exome sequencing of two severely obese N2 mice (Body weight 62.5 g and 60.6 g at the age of 26 weeks old) of the *Obese-13* pedigree, both of the obese N2 mice showed heterozygous non-synonymous mutations in the *Sim1*gene (Chr10: 50908536) as well as in *Sec63* gene (Chr10: 42816394). We also performed whole-exome sequencing of two severely obese N2 mice of the *Obese-10* pedigree, but they did not show

any mutation in *Sim1* or *Sec63* gene (Table 2). Both mutated genes *Sim1* and *Sec63* found in the *Obese-13 pedigree*, were located within the mapped chromosomal region (Fig. 7c) of chromosome 10 and no other non-synonymous mutations were found in that region. In order to the additional confirmation, about the segregation of these two mutations in the obese phenotype, we performed direct sequencing analysis of the *Sim1* and *Sec63* genes in five obese mice having chromosomal recombination between rs13480575 and rs13480619 (the fifth column in Fig. 7d) and found that all of the obese mice showed mutations in both *Sim1* and *Sec63* genes. We also performed direct sequencing of randomly selected five non-obese mice, but the non-obese mice did not show any mutation in *Sim1* or *Sec63* gene. This result suggested that due to the reason of proximity the mutations in the *Sec63* and *Sim1* genes were co-segregated. In addition, one mouse (the second column from the last in Fig. 7d), of *Obese-13* pedigree showed obesity without having the B6J/N haplotype. By direct sequencing, we also confirmed that the mouse is devoid of any mutation in the *Sim1* and *Sec63* genes. This result, demonstrates that the effects of any other mutations or by other unknown factors may cause the obesity in this mouse.

SIM1 is a transcriptional factor which belongs to the basic helix–loop–helix-PER-ARNT-SIM (bHLH-PAS) transcription factor family[209]. The mutation in *Sim1* gene resulted in an amino acid substitution from methionine to lysine (M136K), which is located on the PAS A domain of the SIM1 protein (Fig. 8c). The substituted methionine is located in the Fα helix (Fig. 8d) of PAS A domain that is composed of five helices and five strands[210]. The α-helix sequence of PAS A domains exerts almost common structural modules of amino acids in all kingdoms of life. This high conservation of α-helix sequence of PAS A domains suggests a strong evolutionary conservation in functional features and involved in signal transduction in a wide range of individuals.

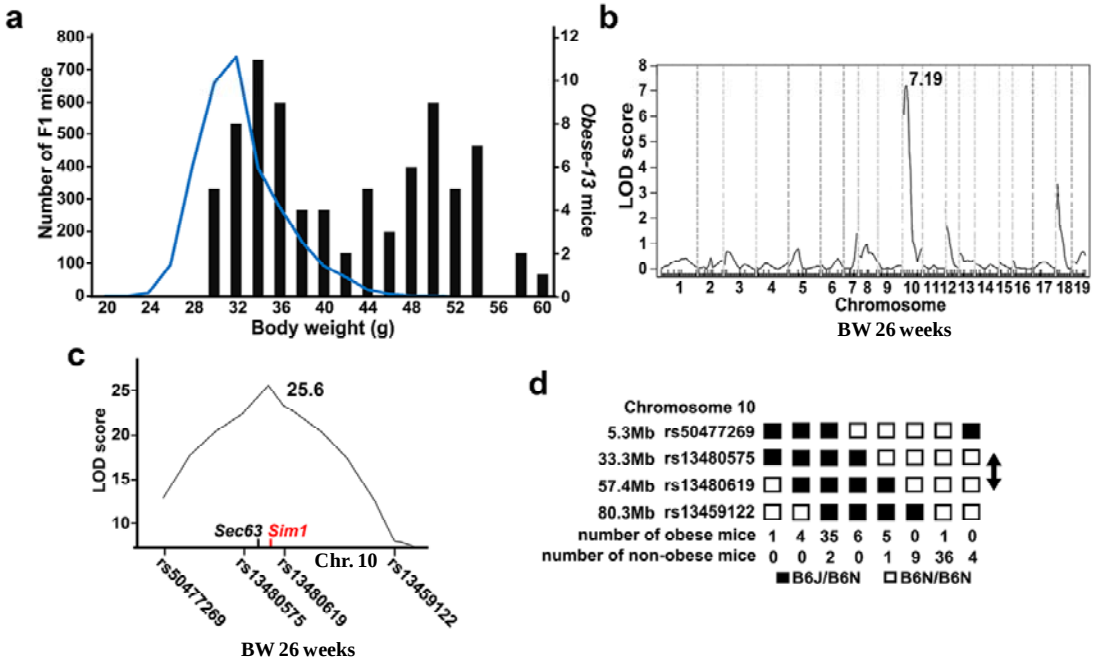

Figure 7. Mapping and analysis of sample mice of *Obese-13* pedigree[225]. (a) The body weight histogram of F1 mice and N2 littermates (bars) of *Obese-13* pedigree. Here the body weights of N2 littermates are deviated toward overweight compared with the body weight distribution of the screened F1 mice. (b) The results of QTL analysis of the *Obese-13* pedigree (n = 49) for body weight exhibited a single peak of LOD score on chromosome 10. (c) Additional QTL analysis focusing only on chromosome 10 using 172 N2 mice indicates a single peak (LOD score, 25.6) located between rs13480575 and rs13480619. (d) The haplotype analysis of *Obese-13* N2 mice shows that the mutation falls between rs13480575 and rs13480619 (arrow) on chromosome 10.

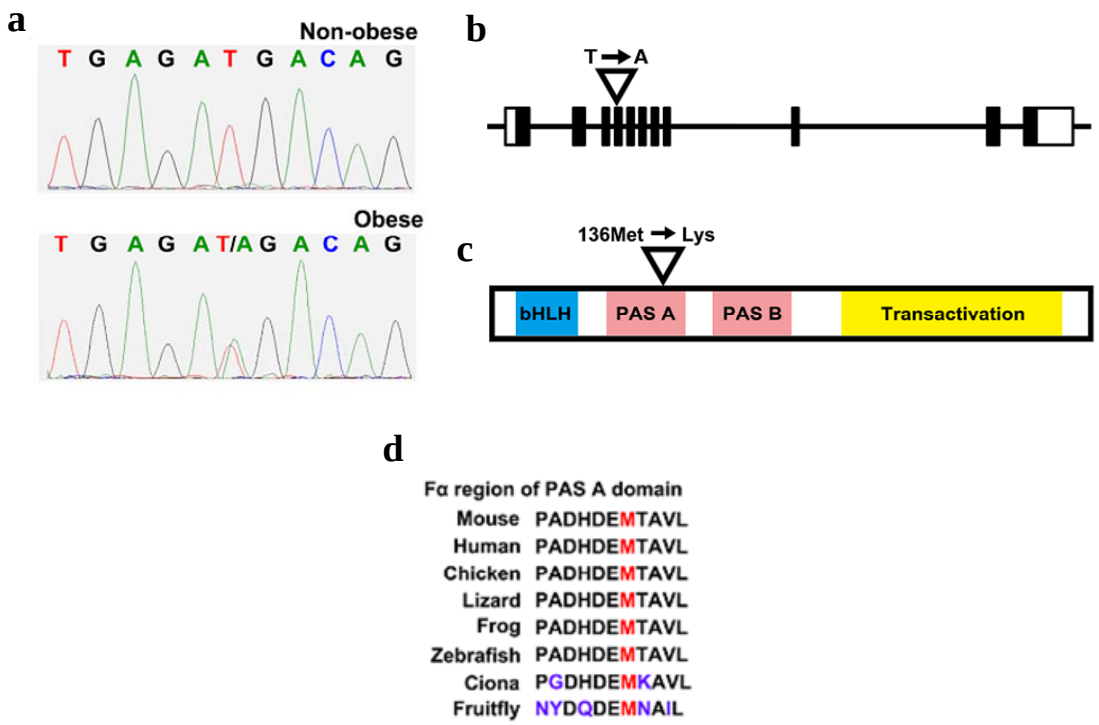

Figure 8. Identification of a single nucleotide substitution of the *Sim1* gene in *Obese-13* pedigree[225] (a) Through the direct sequencing of the *Sim1* gene identified a substitution of thymine-to-adenine specific to obese mice of the *Obese-13* pedigree. (b) The substitution of nucleotide thymine (T)-to-adenine (A) is located in exon 4 of the *Sim1* gene. Here, the coding regions are indicated by black box, while the non-coding regions are indicated by white box. (c) The 136th methionine residue located in the PAS A domain that is substituted to lysine. (d) The 136th methionine is well-conserved among vertebrates and invertebrates. The Fα region of the PAS A domain is indicated.

4.4.2. SIM1(M136K) exhibited a significant decrease in transcriptional activity[225]

The effect of the mutations on SIM1 transcriptional activity was evaluated by *In vitro* luciferase reporter assay. As SIM1 and other bHLH-PAS members form a heterodimer with ARNT2 via the PAS domain to induce transcription of target genes[209,210], we measured the effect of transcriptional activity of SIM1 wild-type protein, SIM1(M136K) protein and

SIM1:ARNT2 dimer through luciferase assay. In consistent with the previous reports[227], in this assay, we observed that the wild-type SIM1 protein singly exhibited a very low transcriptional activity, but, a strong transcriptional activity was seen when the SIM1 protein is co-transfected with ARNT2 (Fig. 9a). On the other hand, the co-transfection of SIM1(M136K) with ARNT2 did not show any transcriptional activity. We further performed the Luciferase assay to observe whether SIM1(M136K) interferes with the activity of wild-type SIM1 by transfecting SIM1, ARNT2 and SIM1(M136K) together. The presence of SIM1(M136K) did not alter the transcriptional activity of the SIM1:ARNT2 dimer (Fig. 9a), resulting that SIM1(M136K) did not show any dominant negative effect on the wild-type SIM1 protein. Further, we assayed the transcriptional activity by increasing the SIM1 content, where the ARNT2 content remaining stable, the result reveals that the luciferase units increased in a dose-dependent manner (Fig. 9b). However, we did not find any change in luciferase units at the increased amount of SIM1(M136K) with ARNT2. Thus, the mutation in the *Sim1* gene produces SIM1(M136K) protein, which totally lacks its transcriptional activity.

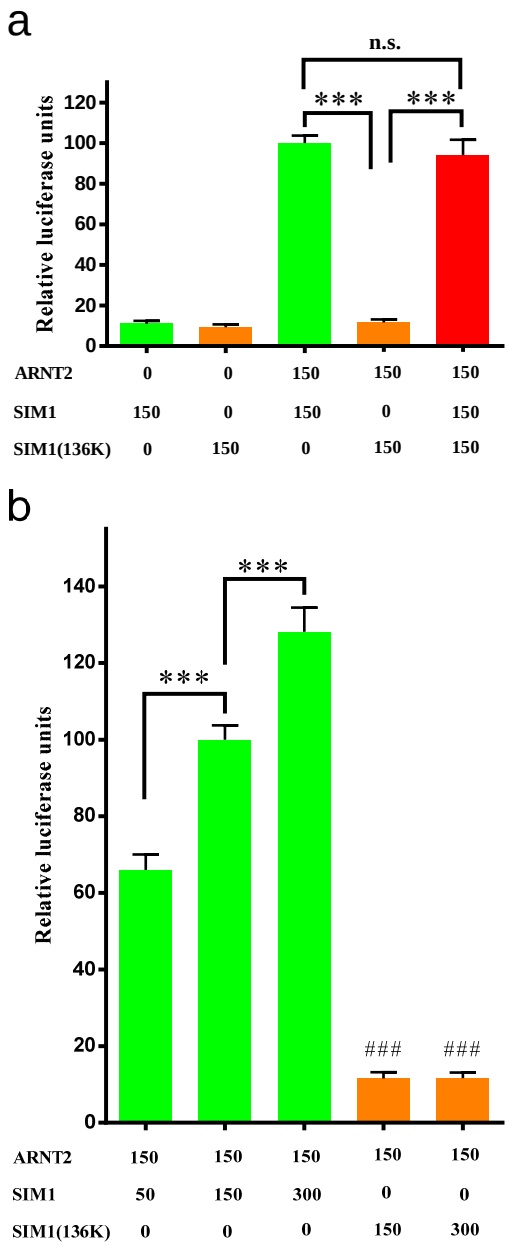

Figure 9. Luciferase assay of SIM1 protein[225]. (a, b)The HEK293 cells were used for transient transfection with ARN2 expression plasmids, SIM1 wild-type and/or SIM1(M136K) expression plasmids, luciferase reporter plasmids and Renilla luciferase plasmids for the compensation of transfection efficiency. Bars indicate firefly/Renilla luciferase activity values relative to the mean firefly/Renilla values of the wild-type SIM1 (a, 150 ng; b, 50 ng)-

and ARNT2-transfected cells. *** $p < 0.001$, ### $p < 0.001$ vs. any of the SIM1 groups, one-way ANOVA followed by Tukey's post-hoc test. Data are shown as the mean + s.e.m.

4.4.3. *Sim1*$^{M136K/+}$ mice exhibited lower *Sim1* mRNA[225]

To investigate *Sim1* mRNA level through qPCR analysis, the cDNA was synthesized from hypothalamic tissue of mice at 12 weeks of age. The *Sim1* mRNA content of *Sim1*$^{M136K/+}$ mice was significantly lower than that of *Sim1*$^{+/+}$ mice (Fig. 10d).

4.4.4. *Sim1*$^{M136K/+}$ mice generated severe obesity[225]

The mice were kept in the single cage, fed a normal diet and the body weight was measured weekly. The N2 mice were weighed from the age of 10 weeks to the age of 26 weeks and the N3 mice were weighed from 6 to 11 weeks. The body weights of both N2 male and female *Sim1*$^{M136K/+}$ mice were significantly ($p<0.001$) greater than those of *Sim1*$^{+/+}$ mice (Fig. 10a,b). Besides, the body weight analysis of N3 mice of *Obese-13* pedigree exhibited a significant increase of body weight of *Sim1*$^{M136K/+}$ mice as early as 6 weeks of age (Fig. 10c). To measure the weight of epididymal fat we dissected the intra-abdominal white adipose tissue (WAT) of N3 mice at 12 weeks of age. An excessive accumulation of white adipose tissue was found in *Sim1*$^{M136K/+}$ mice. The epididymal fat mass of *Sim1*$^{M136K/+}$ mice was higher than that of *Sim1*$^{+/+}$ mice at the age of 12 weeks (Fig. 10e). To investigate the serum leptin level of N3 mice, the blood serum was collected at 12 weeks of age. Consistent with a larger fat mass, *Sim1*$^{M136K/+}$ mice had higher serum leptin levels when compared with *Sim1*$^{+/+}$ mice (Fig. 10f).

4.4.5. *Sim1*$^{M136K/+}$ mice were hyperphagic[225]

In order to measure the amount of food intake at the age of 8 weeks of N3 mice, we allowed the mice to take powdered food form a small food jar. After one week of habituation of feeding, at the age of 9 weeks the daily food intake was measured in every 24 hours for seven

consecutive days. The *Sim1*$^{M136K/+}$ mice exhibited a significantly ($p<0.001$) increased daily food intake compared with *Sim1*$^{+/+}$ mice (Fig. 10g).

4.4.6. *Sim1*$^{M136K/+}$ mice were pre-diabetic[225]

At the age of 9 weeks of N3 mice, the blood glucose level was measured by collecting blood from the tail vein. Though the blood glucose level seems to be higher in *Sim1*$^{M136K/+}$ mice than the *Sim1*$^{+/+}$ mice, but statistically did not reach at significance (Fig. 10h). To investigate the serum insulin level blood serum was collected at the age 12 weeks of N3 mice. As for glucose metabolism, whereas *Sim1*$^{M136K/+}$ and *Sim1*$^{+/+}$ mice had almost similar blood glucose levels, but the serum insulin level of *Sim1*$^{M136K/+}$ mice was significantly higher than that of *Sim1*$^{+/+}$ mice (Fig. 10i). The similar blood glucose level in obese pedigrees may be the result of compensation by the high insulin level.

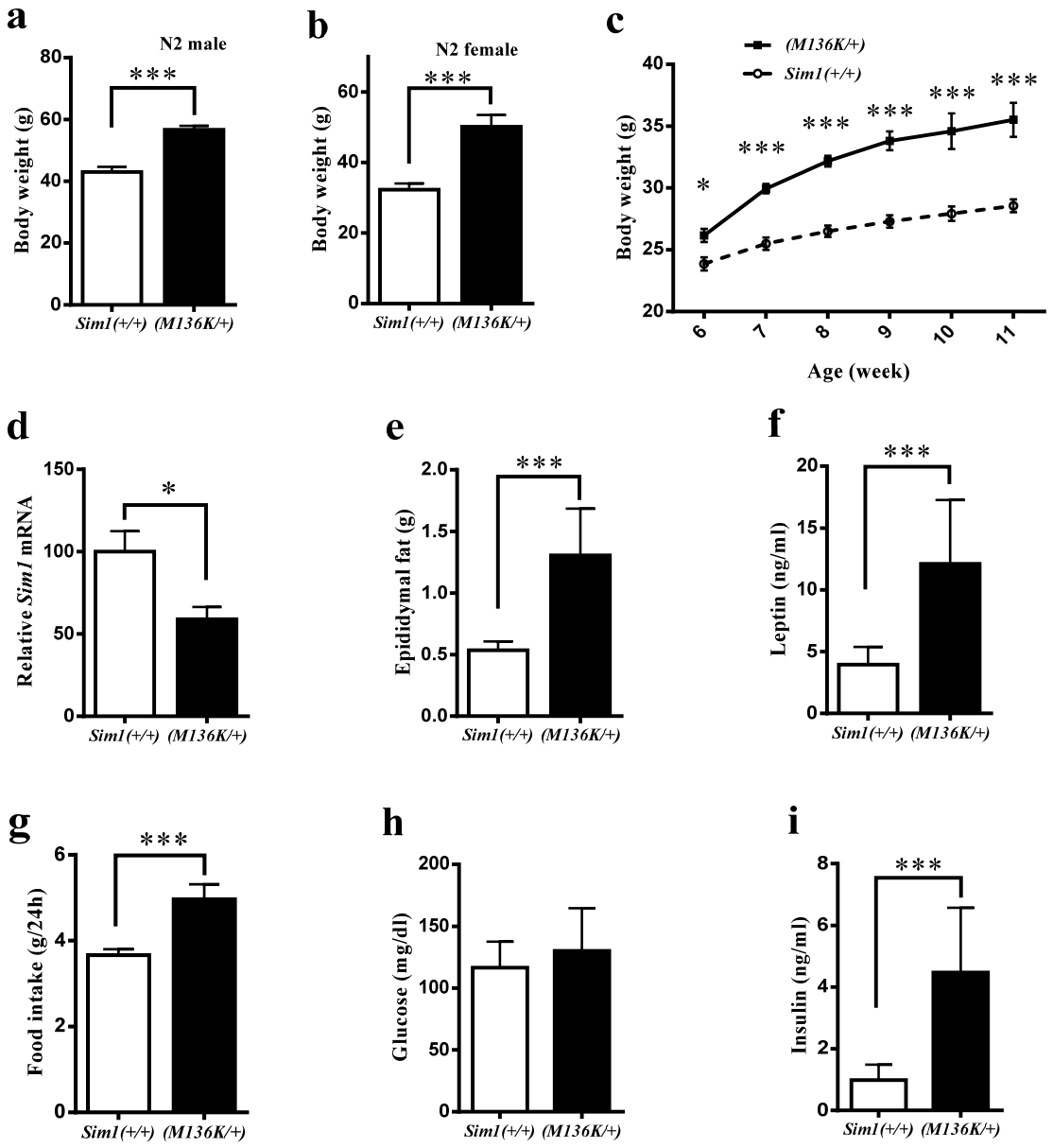

Figure 10. Metabolic phenotypes of *Sim1* mutant mice[225]. (a) At the age of 26 weeks, the N2 generation of $Sim1^{M136K/+}$ male mice (n = 13) showed higher body weight than $Sim1^{+/+}$ male mice (n = 12). (b) At the age of 26 weeks, the N2 generation of $Sim1^{M136K/+}$ female mice (n = 11) showed higher body weight than $Sim1^{+/+}$ female mice (n = 13). (b) The increased body weight of N3 mice indicates early-onset obesity in $Sim1^{M136K/+}$ mice (n=10) than the $Sim1^{+/+}$mice (n = 19). * $p < 0.05$, *** $p < 0.001$, one-way repeated ANOVA followed by Tukey's post-hoc test. (d) Decreased level of *Sim1* mRNA of $Sim1^{M136K/+}$ mice (n

= 6) was observed than the *Sim1*$^{+/+}$mice (n = 6).) (e) The *Sim1*$^{M136K/+}$ mice (n = 6) exhibited Increased epididymal fat weights than the *Sim1*$^{+/+}$ mice (n = 6). (f) Increased serum leptin level was found in *Sim1*$^{M136K/+}$ mice (n = 8) in comparing to the *Sim1*$^{+/+}$ mice (n = 8). (g) The amount of daily food intake of *Sim1*$^{M136K/+}$ mice (n = 6) was higher than that of *Sim1*$^{+/+}$ mice (n = 6). (h) Both the *Sim1*$^{+/+}$mice (n = 19) and *Sim1*$^{M136K/+}$ mice (n = 10) exhibited almost similar blood glucose level. (i) The *Sim1*$^{M136K/+}$ mice (n = 8) exhibited higher serum insulin levels than *Sim1*$^{+/+}$mice (n = 8). * $p < 0.05$, ** $p < 0.01$, *** $p < 0.001$, two-tailed *t*-test. Data are shown as the mean + s.e.m.

Table 2. Whole exome sequencing identifies non synonymous mutations within the mapped chromosomal regions[225].

Mouse ID	**Obese-10 A**		**Obese-10 B**		**Obese-13 A**		**Obese-13 B**	
Body weight (26 weeks)	56.3 g		54.5 g		62.5 g		60.6 g	
Total reads	85,845,404	100.0%	74,370,332	100.0%	78,108,258	100.0%	84,534,362	100.0%
Mapped reads	76,972,358	89.7%	66,530,500	89.5%	68,763,865	88.0%	73,595,915	87.1%
Not mapped reads	8,873,046	10.3%	7,839,832	10.5%	9,344,393	12%	10,938,447	12.9%
Average coverage of capture target regions	93		80		81		86	
Minimum coverage of capture target regions								
5 X		97.2%		96.1%		96.3%		96.8%
10 X		93.4%		90.7%		91.0%		92.3%
20 X		81.3%		75.2%		75.8%		78.7%
40 X		54.3%		46.4%		47.0%		50.3%
80 X		25.6%		21.6%		22.0%		23.4%
100 X		19.9%		17.1%		17.4%		18.3%
Variants called	8,693	100.0%	7,393	100.0%	7,453	100.0%	7,818	100.0%
After filtering against control	626	7.2%	457	6.2%	443	5.9%	535	6.8%
With amino acid change	40	0.5%	31	0.4%	21	0.3%	29	0.4%
Sec63 (chr 10: 42816394)	A/A		A/A		A/G		A/G	
Sim1 (chr 10: 50908536)	T/T		T/T		T/A		T/A	
Mc4r (chr:18: 66859918)	A/T		A/T		A/A		A/A	

4.5. Quantitation of hypothalamic gene expression[225]

In the assay of hypothalamic gene expression, we compared the levels of hypothalamic neuropeptide gene expressions of *Sim1*$^{M136K/+}$ mice and *Mc4r* $^{Y41X/+}$ mice with those of mice with diet-induced obesity (DIO). This assay was done to find out if there were changes in gene expression common to these three mouse models of obesity. The diet induced obesity (DIO) mice and control mice were fed a high-fat diet as well as a regular chow diet, respectively, for 9 weeks, starting at the age of 3 weeks (DIO mice, body weight 30.2 ± 0.4 g), n = 9; chow mice, body weight 24.7 ± 0.3 g, n = 9). In this study, we examined the mRNAs of the following genes: *Agrp, Avp*, *Crh*, *Ghrh, Mch, Npy, Orexin, Oxytocin, Pacap, Pomc, Somatostatin* and *Trh*. A significant reduction of *Avp* mRNA expression was seen in all of the obese groups, whereas, there was no change in the expression of *Crh, Mch*, *Npy, Pomc,* and *Somatostatin* mRNAs levels (Fig. 11a,b) in comparing to their wild-type littermates. A reduced mRNA expression of *Agrp* was found in both *Sim1*$^{M136K/+}$ mice and DIO mice than their wild-type littermates. The *Sim1*$^{M136K/+}$ mice exhibited a significant reduction in *Orexin*, *Oxytocin* and *Trh* mRNAs in comparing to the *Sim1*$^{+/+}$ mice. Particularly, a drastic reduction (90%) of *Oxytocin* mRNA was observed in *Sim1*$^{M136K/+}$ mice than the *Sim1*$^{+/+}$ mice. Whereas, a significantly reduced level in *Ghrh* and *Pacap* mRNAs were found only in DIO mice (Fig. 11a,b).

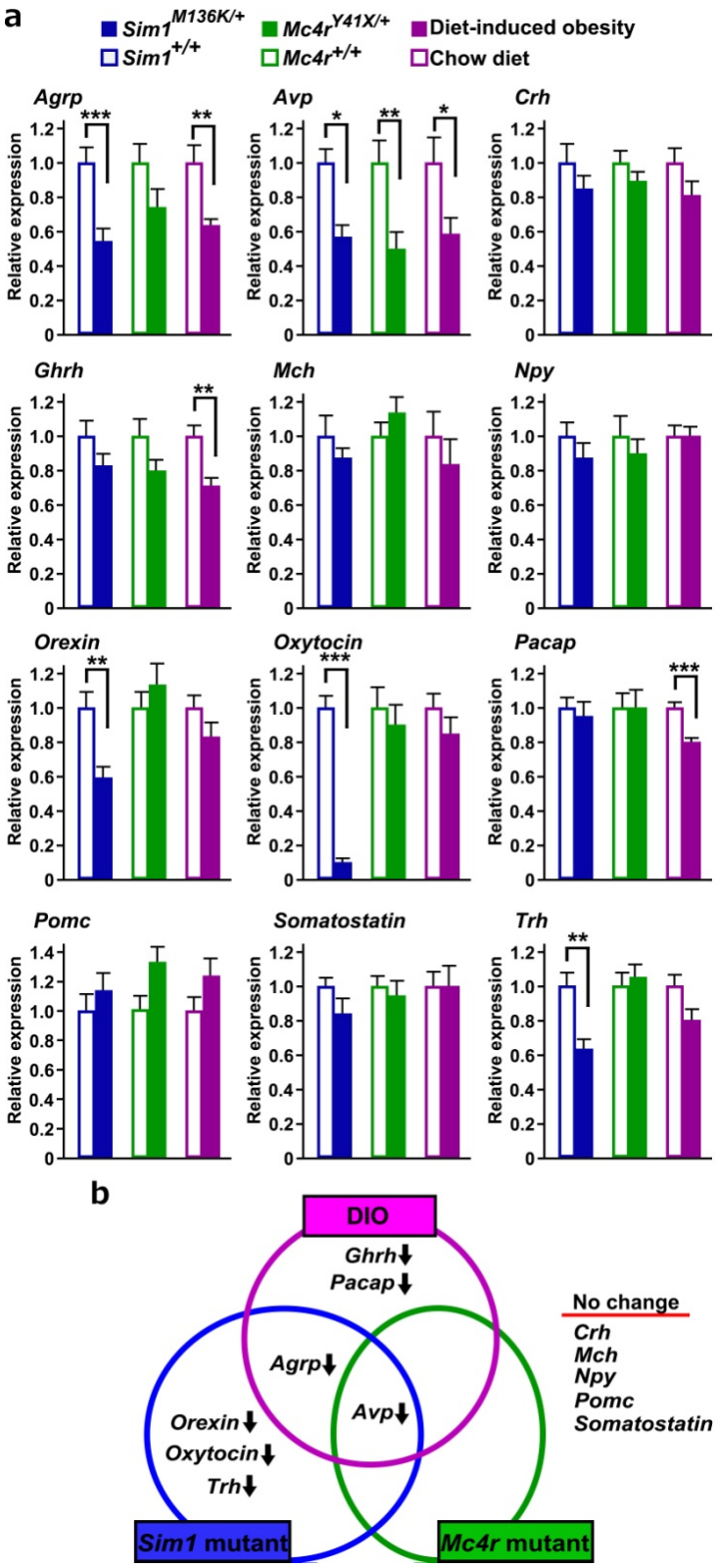

Figure 11. Hypothalamic neuropeptide/gene expression in three mouse models of obesity[225]. (a) Measurement of hypothalamic neuropeptide gene expression in *Mc4r*$^{+/+}$ (n =

9), *Mc4r*$^{Y41X/+}$ (n = 9), *Sim1*$^{+/+}$ (n = 9), *Sim1*$^{M136K/+}$ (n = 9), along with high-fat-diet-induced obesity (DIO) mice (n = 9) and mice fed a regular chow diet (n = 9). For each comparison values are indicated as compared to the average of the control groups. (b) Altered profiles of neuropeptide gene expression of the three models of mouse obesity. * $p < 0.05$, ** $p < 0.01$, *** $p < 0.001$, two-tailed *t*-test with Bonferroni correction for multiple comparisons. Data are shown as the mean + s.e.m.

Chapter 5.
Discussion

In this forward genetic study, in parallel with the screening of ENU-mutagenized mice for sleep/wake disorder, we have screened the mice to identify any genetic mutation responsible for obesity. This study was performed through the dominant screening, using C57BL/6 substrains. Throughout the screening of more than 5000 mutagenized G1/F1 mice, we have successfully established two different obese pedigrees i.e., *Obese-10* and *Obese-13*, having a single point mutation in *Mc4r* gene and *Sim1*gene respectively. Though, several ENU-mutagenesis process were succeed to establish obesity pedigree[39,85,86] through the recessive screening, but there is no recognized evidence of successful dominant screening to establish an obesity pedigree. Thus, this is the first successful dominant screening for obesity.

One of the main reasons of success of this dominant screening may be the mating mouse strains. In this dominant screening, we used ENU induced B6J male and counter strain B6J/B6N wild-type female to generate G1/F1 mice. As each individual G1/F1 animal was heterozygous for a unique set of induced mutations, dominant phenotypes were then identified in N2 mice by further breeding using B6N wild-type female as a counter strain. The parent mating mice (B6J and B6N) of F1 mice have almost same QTLs in relation to body weight, same genetic backgrounds, metabolic characteristics and almost phenotypes are similar among the strains[40,224]. Thus, it has a high possibility to cause a clear phenotypic difference between mutant group and wild-type group and seems to be easy to identify the single candidate mutation caused by ENU mutagenesis through the dominant screening for obesity. Consequently, this very simple and efficient dominant mating scheme rapidly provides genome-wide coverage for dominant mutations and gives useful information for forward genetics that is difficult to obtain with reverse genetics approaches.

The obese mice are allied with infertility and it is difficult to produce new progeny through natural mating using obese mice. In a dominant screening, the dominantly inherited obesity mice exhibits severe obesity, also suffered from infertility and unable to produce progeny through the natural mating[48,242]. If the mating mice are suffering from low fertility, the in vitro fertilization method is necessary to use for the production of new progeny[48]. As the obese mice of *Obese-10* and *Obese-13* were mostly unable to perform natural mating, we have used in vitro fertilization method to generate the next generation. The subsequent linkage analysis and whole exome sequencing easily helps to detect the mutations in the chromosomal region of the target phenotype. According to and the number of non-synonymous mutations and available mutation rates[87,243] the ENU treated mice progeny exhibit 50-70 mutations. Accordingly, we found 20-40 non-synonymous mutations in the N2 progeny of *Obese-10* as well as *Obese-13* pedigrees (Table 2). Thus, this dominant screening of obesity showed an opportunity in forward genetics strategy using C57BL/6 substrains for mutagenized and counter strain, in vitro fertilization method for the production of new progeny and whole exome sequencing to identify mutations in the chromosomal region of a target phenotype. The number of non-synonymous mutations in the N2 progeny of *Obese-10* as well as *Obese-13* pedigrees (Table 2) would be decreased, if we could perform a fine linkage analysis. The finesse of linkage analysis within the mapped chromosomal region linked to the target phenotypes depend upon number of SNPs marker that is used. Though there has been 17,000 SNPs between B6J and B6N[41] but we were able to use only 4 SNPs markers within the target region of chromosome 18 (*Obese-10*) and 6 SNPs markers within target region of chromosome 10 (*Obese-13*). If we can increase the number SNPs markers within the mapped region, it may more helpful to perform more successful linkage analysis.

Among the 13 most obese G1/F1 mice, those have been selected to test the heritability of obesity, only two pedigrees successfully established heritability of obesity. Though the other

11 G1/F1 mice had overweight, but they could not establish the heritable obesity. The reason may be the lacking of availability of any strong obesogenic effect caused by a single gene mutation[35]. Moreover, it can be hypothesized that the obesity of the other 11 G1/F1 mice was developed by chance or may be associated with the combined effects of weak obesogenic mutations or due to the random fluctuations in body weight. On supporting to this evidence we found that the distribution of body weight of the G1/F1 mice tends to skew toward overweight (Fig. 3b).

Further, the funders F1 mice of *Obese-10* pedigree as well as the *Obese-13* pedigree were the two heaviest mice among the 5000 mice that we have screened. Though, we cannot indicate these body weight as a standard scale at which dominant screening will be succeeded but, we can assume that the mutation of their (F1 mice of *Obese-10* pedigree and *Obese-13* pedigree) candidate gene may be affected strongly to generate obesity than the other relevant causes. Otherwise, it is very difficult to detect gene mutations throughout a dominant screening, in case of moderate or weak obesity.

In this research, the single point mutation in *Mc4r* gene, occurred in the $Mc4r^{R41X/+}$ mice of *Obese-10* pedigree, caused the transversion of amino acid tyrosine to a premature stop codon (Tyr-41-Stop), generated a loss of function of *Mc4r* gene and contributed to increase body weight of $Mc4r^{R41X/+}$ mice. Mutation of the *Mc4r* gene plays a major role in generating obesity both in rodents and human[211,244,245]. Heterozygous *Mc4r* null mutant mice exhibit obesity phenotype associated with hyperphagia and hyperleptinemia[235].

Leptin is secreted from the high amount of adipose tissue and hyperleptinemia is commonly observed in human obesity and animal models[246–248]. The increased level of serum leptin is correlated with the increased adipose mass[249]. The increased daily food intake in obese mice proposes the resistance of leptin mediated energy expenditure[250]. With the increase of body weight, insulin secretion also increases in the basal state[251]. Heterozygous *Mc4r* null mutant

also reveals obesity phenotype allied with hyperinsulinemia[235]. Thus, the increased metabolic characteristics in the *Mc4r*$^{R41X/+}$ mice of *Obese-10* pedigree, showed a correlation with the *Mc4r* mutant human and rodents. Besides, the increased insulin level, but no change in blood glucose level in *Mc4r*$^{R41X/+}$ mice suggests for maintaining normal blood glucose levels by compensating with increased insulin levels.

In order to measure the protein level we have performed western blotting for brain homogenates using MC4R antibodies from two companies (Abcam #ab24233; Alomone labs #AMR-024), but it turned out that both antibodies cross-react a variety of brain proteins so that it is very difficult to examine MC4R protein in brain homogenates due to too many background bands. In general and based on our experience, there are few good antibodies for GPCR such as MC4R protein. Actually, there have been no report of western blot for MC4R of MC4R-deficient mice.

Sim1 is expressed in the paraventricular (PVN), supraoptic (SON), and anterior periventricular (aPV) nuclei of the hypothalamus for terminal migration and differentiation of the neurons in these region. Thus, the disruption of *Sim1* affects the development of several neurosecretory lineages in the region of SON, PVN, and aPV[207]. Mice homozygous for a null allele of Sim1 (*Sim1*$^{-/-}$) die perinatally due to the failure of forming PVN, SON and aPV[220]. Where as *Sim1*$^{+/-}$ mice are viable but carrying developmental defect of PVN associated with early onset obesity, hyper leptinemia and insulinemia, increased linear growth[240].We can detect this defect in *Sim1*$^{+/-}$ mice comparing with the wild-type littermates through quantitative histological analysis at the age of 8 weeks. A quantitative histological analysis demonstrates a 24% fewer cells of PVN in *Sim1*$^{+/-}$ mice compare to the wild-type littermates[240]. The in situ hybridization can detect the SIM1 transcript or the immunocytochemistry using a polyclonal SIM1 antiserum can detect SIM1 protein in the hypothalamic SON, PVN, and aPV[207]. Mutation of *Sim1* gene produced in adult mice also

develop obesity. Conditional inactivation of Sim1 gene in the region of hypothalamic neurons of adult mice was generated using a neural specific Cre transgene (*CaMK-CreER*^{T2}), which is induced by Tamoxifen and observed that the hypothalamic circuit involve in the increase of body weight in high fat diet feeding condition with no change of energy expenditure[220]. The neuropeptides of paraventricular nucleus in the conditional Sim1 mutant adult mice exhibits a similar change to those of heterozygous Sim1 mutant (*Sim1*$^{+/-}$) mice[216].

In this study, the other single point mutation in *Sim1* gene, occurred in the *Sim1*$^{M136K/+}$ mice of *Obese-13* pedigree, caused the transversion of amino acid from methionine to lysine (Met-136-Lys), located in the exon 4 of *Sim1* gene in obese mice. This change of amino acid generated a change of its protein structure and produced SIM1 (M136K) protein having total lacks of transcriptional activity and contributed to increase body weight of *Sim1*$^{M136K/+}$ mice. *Sim1* haploinsufficiency, both in human and mice is associated with severe obesity[212,240,252,253]. Obesity generated by *Sim1* deficiency is hyperphagic and showed a critical regulatory effect on energy expenditure[215,241,254]. Hyperleptinemia is correlated with increased adipose tissue and is associated with *Sim1* haploinsufficient mice[240]. Hyperinsulinemia is correlated with *Sim1* haploinsufficiency mice[240]. Thus, the increased metabolic characteristics in the *Sim1*$^{M136K/+}$ mice of *Obese-13* pedigree, exhibited a correlation with the results of *Sim1* mutant human and rodents. Besides, the increased insulin level, but no alteration in blood glucose level in *Sim1*$^{M136K/+}$ mice suggests for maintaining the normal blood glucose level by compensating with increased insulin levels.

Due to the presence of bHLH (basic helix-loop-helix) and PAS (Per-Arnt-Sim) domain SIM1 acts as a critical transcriptional factor and strongly expressed in the development of the PVN[207]. By using the PAS domain wild-type SIM1 binds with ARNT2 to form a hetero-dimer and exerts a strong transcriptional activity for functioning in the development of the hypothalamus[208]. The function of the PAS domain in regulation of the dimerization activity

of the bHLH domain. If any change or mutation in any member of PAS domain it loses its functional activity. Mutant SIM1 protein exhibits a decrease in transcriptional activity[228]. Accordingly, the SIM1(M136K) protein in *Sim1*$^{M136K/+}$ mice of *Obese-13* pedigree exhibited its loss of function in the luciferase reporter assay. Besides, the SIM1(M136K) protein failed to change the transcriptional activity of the SIM1 wild-type:ARNT2 dimer suggests that the SIM1(M136K) protein does not have a dominant negative effect. With the increase amount of wild-type SIM1 protein, it exhibits an increased transcriptional activity, but the SIM1(M136K) protein did not. This finding demonstrates that, the SIM1 (M136K) protein completely loses its transcriptional activity.

In the *Obese-13* pedigree, along with the *Sim1* gene mutation, we also found a non-synonymous heterozygous mutation in *Sec63* gene in the obese mice. The gene *Sec63* works with the *Sec61* translocon and HSPA5 in facilitating the "cotranslational" translocation across the endoplasmic reticulum (ER) membrane[255]. The *Sec61* complex is known as the central component of the protein translocation apparatus of the endoplasmic reticulum membrane. In addition, the *Sec61-Sec62-Sec63* complex may perform post-translational protein translocation into the endoplasmic reticulum[256]. Mutations of *Sec63* gene have been associated with autosomal dominant polycystic liver disease[229]. Liver or kidney specific inactivation of *Sec63* gene resulted in liver or polycystic kidney disease, respectively. Knockout mice of *Sec63* gene increased the severity of cyst formation[255]. But, we did not find any liver and kidney dysfunction or cyst formation in the obese mice of this *Obese-13* pedigree. Although several studies have been done, but, none of these literature explained any relation of *Sec63* gene mutation with the obesity. Though, we cannot refute the possibility of having any effect of *Sec63* gene mutation in causing obesity, but there is no any evidence behind the genetic links between obesity and *Sec63* gene.

Many of hypothalamic genes/neuropeptides play an important role in food intake and energy expenditure[106]. The *Mc4r* gene also expressed in a number of hypothalamic sites, including the dorsomedial, lateral, ventromedial and paraventricular nuclei[198] and contributes in regulating feeding behavior[192]. A significant reduction of *Avp* mRNA expression was found in the hypothalamus of $Mc4r^{R41X/+}$ mice, along with the $Sim1^{M136K/+}$ mice and DIO mice. The reduced *Avp* mRNA level in all three obese groups may be due to the hypothalamic posterior pituitary dysfunction caused by abnormal endogenous opioids[257] or due to the any other secondary effect of obesity such as increased leptin and insulin level in obese mice[258].

Sim1 gene is necessary for the development of PVH neurons and developmental defects in PVN results obesity in *Sim1* haploinsufficient mice[207,240]. As the SIM1 is a transcription factor and haploinsufficiency of SIM1 may affect the transcription level of target genes[207]. The decreased mRNAs expression of *Oxytocin, Trh, Avp & Agrp* in $Sim1^{M136K/+}$ mice may be due to the lack of transcriptional activity, which is consistent with of SIM1 haploinsufficient mice[215,216,220,259]. As *Orexin* is expressed in the LHA, and SIM1 does not express in LHA. Thus the decreased expression of *Orexin* mRNA in $Sim1^{M136K/+}$ mice may not be the direct results of disrupted transcriptional activity of the mutant SIM1 protein. Instead, it may be due to the high leptin level or due to a secondary change based on the tight reciprocal fiber connections between the maldeveloped PVN of $Sim1^{M136K/+}$ mice and *Orexin* neurons[260].

In order to confirm the change of hypothalamic gene expression due to the obesogenic effect, we used high fat diet induced B6J male mice. The DIO male B6J mice are a suitable model for investigating non-genetic mechanisms of obesity, as well as for recognizing the major changes in the hypothalamic expression of genes[261]. Besides, the DIO mice would be a nice model for human obesity in which high-calorie food is intensely used. Long time use of high-fat diet in mice generates leptin-resistance[85,262]. No change in expression of *Pomc* mRNA but a significant reduction of *Ghrh* mRNA and *Agrp* mRNA expression was found in high fat

diet feeding mice[263–266]. This result is consistent with reduction of *Ghrh* mRNA and *Agrp* mRNA expression in our DIO mice. Thus, the common changes of *Agrp* mRNA expression between the *Sim1*$^{M136K/+}$ mice and the DIO mice may be the result of the secondary obesogenic effect associated with the increased insulin and leptin levels[258]. As we know, ghrelin stimulates *Ghrh* secretion from the hypothalamus[267] and obesity is characterized by markedly decreased of ghrelin. The significant reduction of *Ghrh* in obese as compared to lean controls is due to the ghrelin resistance in obese individuals[268,269]. Again, the high fat diet also changes the behavioral activity beside the generation of obesity[270]. Thus, the change of *Pacap* and *Ghrh* mRNAs can be considered the result of behavioral changes beyond the metabolic changes in DIO mice. Therefore, it can be suggests that, through a different pattern of hypothalamic gene expression, each obesity models of this study represents the involvement of their hypothalamic genes in generating obesity.

Chapter 6.
Conclusion

In summary, through the dominant screening of forward genetic study using ENU-mutagenesis and C57BL/6 substrains, we have identified *Sim1* and *Mc4r* gene mutations among very few genes, which cause obesity via haploinsufficiency. In most cases the human obesity caused by gene mutation is dominantly inherited[194,271]. Therefore, the knockout mice of *Sim1* and *Mc4r* gene cannot be the complete model of obesity that is found in human because, the knockout mice are completely lacking of protein of the target gene. Instead, identification as well as characterization of mutations produced by ENU-mutagenesis in mice will direct, the better understanding of the obesity associated with human gene mutation[39]. Thus, the dominant screening of forward genetic strategy using the C57BL/6 substrains as an ENU mutagenized and counter strain would be a good choice to identify the responsible gene in obesity research as well as in the research of any other disease, which is caused by gene mutation.

Chapter 7.
References

1 Moresco EMY, Li X, Beutler B. Going forward with genetics: Recent technological advances and forward genetics in mice. American Journal of Pathology. 2013; **182**: 1462–1473.

2 Russ A, Stumm G, Augustin M, Sedlmeier R, Wattler S, Nehls M. Random mutagenesis in the mouse as a tool in drug discovery. Drug Discovery Today. 2002; **7**: 1175–1183.

3 Nguyen D, Xu T. The expanding role of mouse genetics for understanding human biology and disease. *Disease Models & Mechanisms* 2008; **1**: 56–66.

4 Zhang Y, Proenca R, Maffei M, Barone M, Leopold L, Friedman JM. Positional cloning of the mouse obese gene and its human homologue. *Nature* 1994; **372**: 425–32.

5 Guénet JL. Chemical mutagenesis of the mouse genome: An overview. In: *Genetica*. 2004, pp 9–24.

6 Cordes SP. N-ethyl-N-nitrosourea mutagenesis: boarding the mouse mutant express. *Microbiology and molecular biology reviews : MMBR* 2005; **69**: 426–39.

7 Russell LB, Hunsicker PR, Cacheiro NL, Bangham JW, Russell WL, Shelby MD. Chlorambucil effectively induces deletion mutations in mouse germ cells. *Proceedings of the National Academy of Sciences of the United States of America* 1989; **86**: 3704–8.

8 Russell WL, Kelly EM, Hunsicker PR, Bangham JW, Maddux SC, Phipps EL.

Specific-locus test shows ethylnitrosourea to be the most potent mutagen in the mouse. *Proceedings of the National Academy of Sciences of the United States of America* 1979; **76**: 5818–5819.

9 Favor J, Neuhäuser-Klaus A, Ehling UH. The effect of dose fractionation on the frequency of ethylnitrosourea-induced dominant cataract and recessive specific locus mutations in germ cells of the mouse. *Mutation Research - Fundamental and Molecular Mechanisms of Mutagenesis* 1988; **198**: 269–275.

10 Russell WL, Kelly EM. Specific-locus mutation frequencies in mouse stem-cell spermatogonia at very low radiation dose rates. *Proceedings of the National Academy of Sciences of the United States of America* 1982; **79**: 539–41.

11 Justice MJ, Bode VC. Genetic analysis of mouse t haplotypes using mutations induced by ethylnitrosourea mutagenesis: the order of T and qk is inverted in t mutants. *Genetics* 1988; **120**: 533–543.

12 Stottmann RW, Beier DR. Using ENU mutagenesis for phenotype-driven analysis of the mouse. *Methods in Enzymology* 2010; **477**: 329–348.

13 Singer B, Dosanjh MK. Site-directed mutagenesis for quantitation of base-base interactions at defined sites. *Mutation Research - Fundamental and Molecular Mechanisms of Mutagenesis* 1990; **233**: 45–51.

14 Noveroske JK, Weber JS, Justice MJ. The mutagenic action of N-ethyl-N-nitrosourea in the mouse. *Mammalian genome : official journal of the International Mammalian Genome Society* 2000; **11**: 478–83.

15 Bielas JH, Heddle J a. Proliferation is necessary for both repair and mutation in transgenic mouse cells. *Proceedings of the National Academy of Sciences of the United*

States of America 2000; **97**: 11391–11396.

16 Justice MJ, Noveroske JK, Weber JS, Zheng B, Bradley A. Mouse ENU mutagenesis. Human Molecular Genetics. 1999; **8**: 1955–1963.

17 Arnold CN, Barnes MJ, Berger M, Blasius AL, Brandl K, Croker B *et al.* ENU-induced phenovariance in mice: inferences from 587 mutations. *BMC Research Notes* 2012; **5**: 577.

18 O'Neill JP. DNA damage, DNA repair, cell proliferation, and DNA replication: how do gene mutations result? *Proceedings of the National Academy of Sciences of the United States of America* 2000; **97**: 11137–11139.

19 Takahasi KR, Sakuraba Y, Gondo Y. Mutational pattern and frequency of induced nucleotide changes in mouse ENU mutagenesis. *BMC Molecular Biology* 2007; **8**: 52.

20 Augustin M, Sedlmeier R, Peters T, Huffstadt U, Kochmann E, Simon D *et al.* Efficient and fast targeted production of murine models based on ENU mutagenesis. *Mammalian Genome* 2005; **16**: 405–413.

21 Balling R. ENU mutagenesis: analyzing gene function in mice. *Annual review of genomics and human genetics* 2001; **2**: 463–492.

22 Russell LB, Hunsicker PR, Russell WL. Comparison of the genetic effects of equimolar doses of ENU and MNU: while the chemicals differ dramatically in their mutagenicity in stem-cell spermatogonia, both elicit very high mutation rates in differentiating spermatogonia. *Mutation research* 2007; **616**: 181–95.

23 Weber JS, Salinger A, Justice MJ. Optimal N-ethyl-N-nitrosourea (ENU) doses for inbred mouse strains. *Genesis* 2000; **26**: 230–233.

24 Hitotsumachi S, Carpenter DA, Russell WL. Dose-repetition increases the mutagenic effectiveness of N-ethyl-N-nitrosourea in mouse spermatogonia. *Proceedings of the National Academy of Sciences of the United States of America* 1985; **82**: 6619–6621.

25 Justice MJ, Carpenter DA, Favor J, Neuhauser-Klaus A, Hrabé De Angelis M, Soewarto D *et al.* Effects of ENU dosage on mouse strains. *Mammalian Genome* 2000; **11**: 484–488.

26 Boles MK, Wilkinson BM, Maxwell A, Lai L, Mills A a, Nishijima I *et al.* A mouse chromosome 4 balancer ENU-mutagenesis screen isolates eleven lethal lines. *BMC genetics* 2009; **10**: 12.

27 Acevedo-Arozena A, Wells S, Potter P, Kelly M, Cox RD, Brown SDM. ENU mutagenesis, a way forward to understand gene function. *Annual review of genomics and human genetics* 2008; **9**: 49–69.

28 Gondo Y. Trends in large-scale mouse mutagenesis: from genetics to functional genomics. *Nature reviews Genetics* 2008; **9**: 803–810.

29 Pulst SM. Genetic linkage analysis. *Archives of neurology* 1999; **56**: 667–672.

30 Lander E, Kruglyak L. Genetic dissection of complex traits: guidelines for interpreting and reporting linkage results. *Nature Genetics* 1995; **11**: 241–247.

31 Kwon JM, Goate a M. The candidate gene approach. *Alcohol research & health : the journal of the National Institute on Alcohol Abuse and Alcoholism* 2000; **24**: 164–168.

32 Lander ES, Linton LM, Birren B, Nusbaum C, Zody MC, Baldwin J *et al.* Initial sequencing and analysis of the human genome. *Nature* 2001; **409**: 860–921.

33 Waterston RH, Lindblad-Toh K, Birney E, Rogers J, Abril JF, Agarwal P *et al.* Initial

sequencing and comparative analysis of the mouse genome. *Nature* 2002; **420**: 520–562.

34 Ott J, Wang J, Leal SM. Genetic linkage analysis in the age of whole-genome sequencing. *Nature Reviews Genetics* 2015; **16**: 275–284.

35 Takahashi JS, Shimomura K, Kumar V. Searching for genes underlying behavior: lessons from circadian rhythms. *Science (New York, NY)* 2008; **322**: 909–912.

36 Inoue M, Sakuraba Y, Motegi H, Kubota N, Toki H, Matsui J *et al.* A series of maturity onset diabetes of the young, type 2 (MODY2) mouse models generated by a large-scale ENU mutagenesis program. *Human Molecular Genetics* 2004; **13**: 1147–1157.

37 Hong CJ, Tsai PJ, Cheng CY, Chou CK, Jheng HF, Chuang YC *et al.* ENU mutagenesis identifies mice with morbid obesity and severe hyperinsulinemia caused by a novel mutation in leptin. *PLoS ONE* 2010; **5**. doi:10.1371/journal.pone.0015333.

38 Furuse T, Wada Y, Hattori K, Yamada I, Kushida T, Shibukawa Y *et al.* Phenotypic characterization of a new Grin1 mutant mouse generated by ENU mutagenesis. *European Journal of Neuroscience* 2010; **31**: 1281–1291.

39 Meehan TP, Tabeta K, Du X, Woodward LS, Firozi K, Beutler B *et al.* Point mutations in the melanocortin-4 receptor cause variable obesity in mice. *Mammalian Genome* 2006; **17**: 1162–1171.

40 Keane TM, Goodstadt L, Danecek P, White MA, Wong K, Yalcin B *et al.* Mouse genomic variation and its effect on phenotypes and gene regulation. *Nature* 2011; **477**: 289–94.

41 Kumar V, Kim K, Joseph C, Kourrich S, Yoo S-H, Huang HC *et al.* C57BL/6N mutation in Cytoplasmic FMRP interacting protein 2 regulates cocaine response. *Science (New York, NY)* 2013; **342**: 1508–12.

42 Alexander J, Chang G, Dourmashkin J, Leibowitz S. Distinct phenotypes of obesity-prone AKR/J, DBA2J and C57BL/6J mice compared to control strains. *International Journal of Obesity advance online publication* 2005; : 1–10.

43 Collino S, Martin F-PJ, Montoliu I, Barger JL, Da Silva L, Prolla TA *et al.* Transcriptomics and Metabonomics Identify Essential Metabolic Signatures in Calorie Restriction (CR) Regulation across Multiple Mouse Strains. *Metabolites* 2013; **3**: 881–911.

44 Lin C, Fesi BD, Marquis M, Bosak NP, Theodorides ML, Avigdor M *et al.* Body Composition QTLs Identified in Intercross Populations Are Reproducible in Consomic Mouse Strains. *PloS one* 2015; **10**: e0141494.

45 Kay VJ, Barratt CLR. Male obesity: impact on fertility. *The British Journal of Diabetes & Vascular Disease* 2009; **9**: 237–241.

46 Best D, Bhattacharya S. Obesity and fertility. Hormone Molecular Biology and Clinical Investigation. 2015; **24**: 5–10.

47 Van Loendersloot LL, Van Wely M, Repping S, Bossuyt PMM, Van Der Veen F. Individualized decision-making in IVF: Calculating the chances of pregnancy. *Human Reproduction* 2013; **28**: 2972–2980.

48 Ghanayem BI, Bai R, Kissling GE, Travlos G, Hoffler U. Diet-induced obesity in male mice is associated with reduced fertility and potentiation of acrylamide-induced reproductive toxicity. *Biology of reproduction* 2010; **82**: 96–104.

49 Tabor HK, Risch NJ, Myers RM. Candidate-gene approaches for studying complex genetic traits: practical considerations. *Nature reviews Genetics* 2002; **3**: 391–397.

50 Cardon LR, Bell JI. Association study designs for complex diseases. *Nature reviews Genetics* 2001; **2**: 91–99.

51 Malhotra AK, Goldman D. Benefits and pitfalls encountered in psychiatric genetic association studies. Biological Psychiatry. 1999; **45**: 544–550.

52 Ng SB, Turner EH, Robertson PD, Flygare SD, Bigham AW, Eichler EE *et al.* Targeted capture and massively parallel sequencing of 12 human exomes. *Nature* 2009; **461**: 272–6.

53 Ng SB, Buckingham KJ, Lee C, Bigham AW, Tabor HK, Dent KM *et al.* Exome sequencing identifies the cause of a mendelian disorder. *Nature genetics* 2010; **42**: 30–35.

54 Rabbani B, Tekin M, Mahdieh N. The promise of whole-exome sequencing in medical genetics. *Journal of human genetics* 2014; **59**: 5–15.

55 Ng M, Fleming T, Robinson M, Thomson B, Graetz N, Margono C *et al.* Global, regional, and national prevalence of overweight and obesity in children and adults during 1980-2013: A systematic analysis for the Global Burden of Disease Study 2013. *The Lancet* 2014; **384**: 766–781.

56 Lobstein T. Prevalence and costs of obesity. *Medicine (United Kingdom)* 2015; **43**: 77–79.

57 Lim SS, Vos T, Flaxman AD, Danaei G, Shibuya K, Adair-Rohani H *et al.* A comparative risk assessment of burden of disease and injury attributable to 67 risk

factors and risk factor clusters in 21 regions, 1990-2010: a systematic analysis for the Global Burden of Disease Study 2010. *Lancet* 2012; **380**: 2224–60.

58 de Sousa AGP, Cercato C, Mancini MC, Halpern A. Obesity and obstructive sleep apnea-hypopnea syndrome. *Obesity reviews : an official journal of the International Association for the Study of Obesity* 2008; **9**: 340–354.

59 Felson DT, Anderson JJ, Naimark A, Walker AM, Meenan RF. Obesity and knee osteoarthritis. The Framingham Study. *Annals of Internal Medicine* 1988; **109**: 18–24.

60 Chan JM, Rimm EB, Colditz GA, Stampfer MJ, Willett WC. Obesity, fat distribution, and weight gain as risk factors for clinical diabetes in men. *Diabetes Care* 1994; **17**: 961–969.

61 Colditz GA, Willett WC, Rotnitzky A, Manson JE. Weight gain as a risk factor for clinical diabetes mellitus in women. *Annals of Internal Medicine* 1995; **122**: 481–486.

62 Stampfer MJ, Maclure KM, Colditz GA, Manson JE, Willett WC. Risk of symptomatic gallstones in women with severe obesity. *American Journal of Clinical Nutrition* 1992; **55**: 652–658.

63 Ratziu V, Giral P, Charlotte F, Bruckert E, Thibault V, Theodorou I *et al.* Liver fibrosis in overweight patients. *Gastroenterology* 2000; **118**: 1117–23.

64 Seidell JC, Verschuren WM, van Leer EM, Kromhout D. Overweight, underweight, and mortality. A prospective study of 48,287 men and women. *Archives of internal medicine* 1996; **156**: 958–963.

65 Chen J-L, Weiss S, Heyman MB, Lustig R. Risk factors for obesity and high blood pressure in Chinese American children: maternal acculturation and children's food

choices. *Journal of immigrant and minority health / Center for Minority Public Health* 2011; **13**: 268–75.

66 Lew EA. Mortality and weight: Insured lives and the American Cancer Society studies. *Annals of Internal Medicine* 1985; **103**: 1024–1029.

67 Manson JE, Willett WC, Stampfer MJ, Colditz GA, Hunter DJ, Hankinson SE *et al.* Body weight and mortality among women. *The New England journal of medicine* 1995; **333**: 677–85.

68 Franks PW, Hanson RL, Knowler WC, Sievers ML, Bennett PH, Looker HC. Childhood obesity, other cardiovascular risk factors, and premature death. *New England Journal of Medicine* 2010; **362**: 485–493.

69 Wang Y, Lobstein T. Worldwide trends in childhood overweight and obesity. *International Journal of Pediatric Obesity* 2006; **1**: 11–25.

70 Allison DB, Fontaine KR, Manson JE, Stevens J, VanItallie TB. Annual Deaths Attributable to Obesity in the United States. *JAMA* 1999; **282**: 1530–1538.

71 Calle EE, Thun MJ, Petrelli JM, Rodriguez C, Heath CW. Body-mass index and mortality in a prospective cohort of U.S. adults. *The New England journal of medicine* 1999; **341**: 1097–105.

72 Jousilahti P, Tuomilehto J, Vartiainen E, Pekkanen J, Puska P. Body Weight, Cardiovascular Risk Factors, and Coronary Mortality : 15-Year Follow-up of Middle-aged Men and Women in Eastern Finland. *Circulation* 1996; **93**: 1372–1379.

73 Stevens J, Cai J, Pamuk ER, Williamson DF, Thun MJ, Wood JL. The effect of age on the association between body-mass index and mortality. *The New England journal of*

medicine 1998; **338**: 1–7.

74 Wei M, Kampert JB, Barlow CE, Nichaman MZ, Gibbons LW, Paffenbarger RS *et al.* Relationship between low cardiorespiratory fitness and mortality in normal-weight, overweight, and obese men. *JAMA : the journal of the American Medical Association* 1999; **282**: 1547–1553.

75 Lau DCW, Douketis JD, Morrison KM, Hramiak IM, Sharma AM, Ur E. 2006 Canadian clinical practice guidelines on the management and prevention of obesity in adults and children. *Canadian Medical Association Journal* 2007; **176**: s1–s13.

76 Bleich S, Cutler D, Murray C, Adams A. Why is the developed world obese? *Annual review of public health* 2008; **29**: 273–295.

77 Drewnowski A, Specter SE. Poverty and obesity: the role of energy density and energy costs. *The American Journal of Clinical Nutrition* 2004; **79**: 6–16.

78 James WPT. The fundamental drivers of the obesity epidemic. In: *Obesity Reviews*. 2008, pp 6–13.

79 Nestle M, Jacobson MF. Halting the obesity epidemic: a public health policy approach. *Public health reports* 2000; **115**: 12–24.

80 Keith SW, Redden DT, Katzmarzyk PT, Boggiano MM, Hanlon EC, Benca RM *et al.* Putative contributors to the secular increase in obesity: exploring the roads less traveled. *International journal of obesity (2005)* 2006; **30**: 1585–94.

81 Winter Y, Sankowski R, Back T. Genetic Determinants of Obesity and Related Vascular Diseases. *Vitamins and Hormones* 2013; **91**: 29–48.

82 Hebebrand J, Bammann K, Hinney A. Genetic determinants of obesity. Current issues.

Bundesgesundheitsblatt, Gesundheitsforschung, Gesundheitsschutz 2010; **53**: 674–80.

83 Shawky RM, Sadik DI. Genetics of obesity. *Egyptian Journal of Medical Human Genetics* 2012; **13**: 11–17.

84 Speakman J, Hambly C, Mitchell S, Król E. The contribution of animal models to the study of obesity. *Laboratory animals* 2008; **42**: 413–32.

85 Friedman J. Leptin at 20: An overview. Journal of Endocrinology. 2014; **223**: T1–T8.

86 Grosse J, Tarnow P, Römpler H, Schneider B, Sedlmeier R, Huffstadt U *et al.* N-ethyl-N-nitrosourea-based generation of mouse models for mutant G protein-coupled receptors. *Physiological genomics* 2006; **26**: 209–17.

87 Andrews TD, Whittle B, Field MA, Balakishnan B, Zhang Y, Shao Y *et al.* Massively parallel sequencing of the mouse exome to accurately identify rare, induced mutations: an immediate source for thousands of new mouse models. *Open biology* 2012; **2**: 120061.

88 Chan JL, Heist K, DePaoli AM, Veldhuis JD, Mantzoros CS. The role of falling leptin levels in the neuroendocrine and metabolic adaptation to short-term starvation in healthy men. *Journal of Clinical Investigation* 2003; **111**: 1409–1421.

89 Cowley M a, Smart JL, Rubinstein M, Cerdán MG, Diano S, Horvath TL *et al.* Leptin activates anorexigenic POMC neurons through a neural network in the arcuate nucleus. *Nature* 2001; **411**: 480–484.

90 Vong L, Ye C, Yang Z, Choi B, Chua S, Lowell BB. Leptin Action on GABAergic Neurons Prevents Obesity and Reduces Inhibitory Tone to POMC Neurons. *Neuron* 2011; **71**: 142–154.

91 Bayer L, Jacquemard C, Fellmann D, Griffond B. Survival of rat MCH (melanin-concentrating hormone) neurons in hypothalamus slice culture: Histological, pharmacological and molecular studies. *Cell and Tissue Research* 1999; **297**: 23–33.

92 Yamanaka A, Beuckmann CT, Willie JT, Hara J, Tsujino N, Mieda M *et al.* Hypothalamic orexin neurons regulate arousal according to energy balance in mice. *Neuron* 2003; **38**: 701–713.

93 Segal-Lieberman G, Bradley RL, Kokkotou E, Carlson M, Trombly DJ, Wang X *et al.* Melanin-concentrating hormone is a critical mediator of the leptin-deficient phenotype. *Proceedings of the National Academy of Sciences of the United States of America* 2003; **100**: 10085–10090.

94 Clément K, Vaisse C, Lahlou N, Cabrol S, Pelloux V, Cassuto D *et al.* A mutation in the human leptin receptor gene causes obesity and pituitary dysfunction. *Nature* 1998; **392**: 398–401.

95 Farooqi IS, Wangensteen T, Collins S, Kimber W, Matarese G, Keogh JM *et al.* Clinical and molecular genetic spectrum of congenital deficiency of the leptin receptor. *The New England journal of medicine* 2007; **356**: 237–247.

96 Halaas JL, Gajiwala KS, Maffei M, Cohen SL, Chait BT, Rabinowitz D *et al.* Weight reducing effects of the plasma protein encoded by the Obese gene. *Science* 1995; **269**: 543–546.

97 Farooqi I, Jebb S, Langmack G, Lawrence E, Cheetham C, Prentice A *et al.* Effects of recombinant leptin therapy in a child with congenital leptin deficiency. *New England Journal of Medicine* 1999; **341**: 879–884.

98 Woods SC, Seeley RJ. Adiposity signals and the control of energy homeostasis. In:

Nutrition. 2000, pp 894–902.

99 Brown LM, Clegg DJ, Benoit SC, Woods SC. Intraventricular insulin and leptin reduce food intake and body weight in C57BL/6J mice. *Physiology and Behavior* 2006; **89**: 687–691.

100 Cheung CC, Clifton DK, Steiner RA. Proopiomelanocortin neurons are direct targets for leptin in the hypothalamus. *Endocrinology* 1997; **138**: 4489–4492.

101 Konner AC, Janoschek R, Plum L, Jordan SD, Rother E, Ma X *et al.* Insulin Action in AgRP-Expressing Neurons Is Required for Suppression of Hepatic Glucose Production. *Cell Metabolism* 2007; **5**: 438–449.

102 Lin H V., Plum L, Ono H, Gutiérrez-Juárez R, Shanabrough M, Borok E *et al.* Divergent regulation of energy expenditure and hepatic glucose production by insulin receptor in agouti-related protein and POMC neurons. *Diabetes* 2010; **59**: 337–346.

103 Claret M, Smith MA, Batterham RL, Selman C, Choudhury AI, Fryer LGD *et al.* AMPK is essential for energy homeostasis regulation and glucose sensing by POMC and AgRP neurons. *Journal of Clinical Investigation* 2007; **117**: 2325–2336.

104 Bruning JC. Role of Brain Insulin Receptor in Control of Body Weight and Reproduction. *Science* 2000; **289**: 2122–2125.

105 Ellacott KLJ, Cone RD. The central melanocortin system and the integration of short- and long-term regulators of energy homeostasis. *Recent progress in hormone research* 2004; **59**: 395–408.

106 Schwartz MW, Woods SC, Porte D, Seeley RJ, Baskin DG. Central nervous system control of food intake. *Nature* 2000; **404**: 661–671.

107 Cone RD. Anatomy and regulation of the central melanocortin system. *Nature neuroscience* 2005; **8**: 571–578.

108 Elmquist JK, Coppari R, Balthasar N, Ichinose M, Lowell BB. Identifying hypothalamic pathways controlling food intake, body weight, and glucose homeostasis. In: *Journal of Comparative Neurology*. 2005, pp 63–71.

109 Mineur YS, Abizaid A, Rao Y, Salas R, DiLeone RJ, Gündisch D *et al.* Nicotine decreases food intake through activation of POMC neurons. *Science (New York, NY)* 2011; **332**: 1330–2.

110 Krude H, Biebermann H, Luck W, Horn R, Brabant G, Grüters a. Severe early-onset obesity, adrenal insufficiency and red hair pigmentation caused by POMC mutations in humans. *Nature genetics* 1998; **19**: 155–157.

111 Bäckberg M, Madjid N, Ögren SO, Meister B. Down-regulated expression of agouti-related protein (AGRP) mRNA in the hypothalamic arcuate nucleus of hyperphagic and obese tub/tub mice. *Molecular Brain Research* 2004; **125**: 129–139.

112 Ollmann MM, Wilson BD, Yang Y-KY, Kerns JA, Chen Y, Gantz I *et al.* Antagonism of Central Melanocortin Receptors in Vitro and in Vivo by Agouti-Related Protein. *Science* 1997; **278**: 135–138.

113 Shutter JR, Graham M, Kinsey AC, Scully S, Luthy R, Stark KL. Hypothalamic expression of ART, a novel gene related to agouti, is up-regulated in obese and diabetic mutant mice. *Genes & Development* 1997; **11**: 593–602.

114 Hagan MM, Rushing PA, Pritchard LM, Schwartz MW, Strack AM, Van Der Ploeg LH *et al.* Long-term orexigenic effects of AgRP-(83---132) involve mechanisms other than melanocortin receptor blockade. *American journal of physiology Regulatory,*

integrative and comparative physiology 2000; **279**: R47--52.

115 Rossi M, Kim MS, Morgan DGA, Small CJ, Edwards CMB, Sunter D *et al.* A C-terminal fragment of Agouti-related protein increases feeding and antagonizes the effect of alpha-melanocyte stimulating hormone in vivo. *Endocrinology* 1998; **139**: 4428–4431.

116 Morton GJ, Schwartz MW. The NPY/AgRP neuron and energy homeostasis. *International journal of obesity and related metabolic disorders : journal of the International Association for the Study of Obesity* 2001; **25 Suppl 5**: S56-62.

117 Bäckberg M, Collin M, Ovesjö ML, Meister B. Chemical coding of GABAB receptor-immunoreactive neurones in hypothalamic regions regulating body weight. Journal of Neuroendocrinology. 2003; **15**: 1–14.

118 Lin S, Boey D, Herzog H. NPY and Y receptors: Lessons from transgenic and knockout models. Neuropeptides. 2004; **38**: 189–200.

119 Schwartz MW, Baskin DG, Bukowski TR, Kuijper JL, Foster D, Lasser G *et al.* Specificity of leptin action on elevated blood glucose levels and hypothalamic neuropeptide Y gene expression in ob/ob mice. *Diabetes* 1996; **45**: 531–535.

120 Stephens TW, Basinski M, Bristow PK, Bue-Valleskey JM, Burgett SG, Craft L *et al.* The role of neuropeptide Y in the antiobesity action of the obese gene product. Nature. 1995; **377**: 530–532.

121 Glenn Stanley B, Kyrkouli SE, Lampert S, Leibowitz SF. Neuropeptide Y chronically injected into the hypothalamus: A powerful neurochemical inducer of hyperphagia and obesity. *Peptides* 1986; **7**: 1189–1192.

122 Zarjevski N, Cusin I, Vettor R, Rohner-Jeanrenaud F, Jeanrenaud B. Chronic intracerebroventricular neuropeptide-Y administration to normal rats mimics hormonal and metabolic changes of obesity. *Endocrinology* 1993; **133**: 1753–1758.

123 Erickson JC, Hollopeter G, Palmiter RD. Attenuation of the obesity syndrome of ob/ob mice by the loss of neuropeptide Y. *Science (New York, NY)* 1996; **274**: 1704–1707.

124 Bittencourt JC, Presse F, Arias C, Peto C, Vaughan J, Nahon JL *et al.* The melanin-concentrating hormone system of the rat brain: An immuno- and hybridization histochemical characterization. *Journal of Comparative Neurology* 1992; **319**: 218–245.

125 Skofitsch G, Jacobowitz DM, Zamir N. Immunohistochemical localization of a melanin concentrating hormone-like peptide in the rat brain. *Brain Research Bulletin* 1985; **15**: 635–649.

126 Marsh DJ, Weingarth DT, Novi DE, Chen HY, Trumbauer ME, Chen AS *et al.* Melanin-concentrating hormone 1 receptor-deficient mice are lean, hyperactive, and hyperphagic and have altered metabolism. *Proceedings of the National Academy of Sciences of the United States of America* 2002; **99**: 3240–3245.

127 Lalonde R, Qian S. Exploratory activity, motor coordination, and spatial learning in Mchr1 knockout mice. *Behavioural Brain Research* 2007; **178**: 293–304.

128 Shimada M, Tritos NA, Lowell BB, Flier JS, Maratos-Flier E. Mice lacking melanin-concentrating hormone are hypophagic and lean. *Nature* 1998; **396**: 670–674.

129 Ludwig DS, Tritos NA, Mastaitis JW, Kulkarni R, Kokkotou E, Elmquist J *et al.* Melanin-concentrating hormone overexpression in transgenic mice leads to obesity and insulin resistance. *The Journal of clinical investigation* 2001; **107**: 379–86.

130 Qu D, Ludwig DS, Gammeltoft S, Piper M, Pelleymounter M a, Cullen MJ *et al.* A role for melanin-concentrating hormone in the central regulation of feeding behaviour. Nature. 1996; **380**: 243–247.

131 Sakurai T, Amemiya A, Ishii M, Matsuzaki I, Chemelli RM, Tanaka H *et al.* Orexins and orexin receptors: A family of hypothalamic neuropeptides and G protein-coupled receptors that regulate feeding behavior. *Cell* 1998; **92**: 573–585.

132 Nair SG, Golden S a, Shaham Y. Differential effects of the hypocretin 1 receptor antagonist SB 334867 on high-fat food self-administration and reinstatement of food seeking in rats. *British journal of pharmacology* 2008; **154**: 406–16.

133 Thorpe AJ, Cleary JP, Levine AS, Kotz CM. Centrally administered orexin A increases motivation for sweet pellets in rats. *Psychopharmacology* 2005; **182**: 75–83.

134 Baird JP, Choe A, Loveland JL, Beck J, Mahoney CE, Lord JS *et al.* Orexin-a hyperphagia: Hindbrain participation in consummatory feeding responses. *Endocrinology* 2009; **150**: 1202–1216.

135 Jankowski M, Hajjar F, Kawas SA, Mukaddam-Daher S, Hoffman G, McCann SM *et al.* Rat heart: a site of oxytocin production and action. *Proceedings of the National Academy of Sciences of the United States of America* 1998; **95**: 14558–63.

136 Rosen GJ, de Vries GJ, Goldman SL, Goldman BD, Forger NG. Distribution of oxytocin in the brain of a eusocial rodent. *Neuroscience* 2008; **155**: 809–817.

137 Yamashita M, Takayanagi Y, Yoshida M, Nishimori K, Kusama M, Onaka T. Involvement of Prolactin-Releasing Peptide in the Activation of Oxytocin Neurones in Response to Food Intake. *Journal of Neuroendocrinology* 2013; **25**: 455–465.

138 Blevins JE, Ho JM. Role of oxytocin signaling in the regulation of body weight. *Reviews in Endocrine & Metabolic Disorders* 2013; **14**: 311–29.

139 Insel TR. The challenge of translation in social neuroscience: a review of oxytocin, vasopressin, and affiliative behavior. *Neuron* 2010; **65**: 768–79.

140 Chaves VE, Tilelli CQ, Brito NA, Brito MN. Role of oxytocin in energy metabolism. Peptides. 2013; **45**: 9–14.

141 Deblon N, Veyrat-Durebex C, Bourgoin L, Caillon A, Bussier AL, Petrosino S *et al.* Mechanisms of the anti-obesity effects of oxytocin in diet-induced obese rats. *PLoS ONE* 2011; **6**. doi:10.1371/journal.pone.0025565.

142 Leng G, Onaka T, Caquineau C, Sabatier N, Tobin VA, Takayanagi Y. Oxytocin and appetite. Progress in Brain Research. 2008; **170**: 137–151.

143 Wu Z, Xu Y, Zhu Y, Sutton AK, Zhao R, Lowell BB *et al.* An Obligate Role of Oxytocin Neurons in Diet Induced Energy Expenditure. *PLoS ONE* 2012; **7**. doi:10.1371/journal.pone.0045167.

144 Parker JA, Bloom SR. Hypothalamic neuropeptides and the regulation of appetite. Neuropharmacology. 2012; **63**: 18–30.

145 Olszewski PK, Klockars A, Schi??th HB, Levine AS. Oxytocin as feeding inhibitor: Maintaining homeostasis in consummatory behavior. Pharmacology Biochemistry and Behavior. 2010; **97**: 47–54.

146 Nishimori K, Takayanagi Y, Yoshida M, Kasahara Y, Young LJ, Kawamata M. New aspects of oxytocin receptor function revealed by knockout mice: sociosexual behaviour and control of energy balance. Progress in Brain Research. 2008; **170**: 79–

90.

147 Takayanagi Y, Kasahara Y, Onaka T, Takahashi N, Kawada T, Nishimori K. Oxytocin receptor-deficient mice developed late-onset obesity. *Neuroreport* 2008; **19**: 951–955.

148 Amico JA, Vollmer RR, Cai H, Miedlar JA, Rinaman L, Janet A *et al.* Enhanced initial and sustained intake of sucrose solution in mice with an oxytocin gene deletion. *{AJP:} Regulatory, Integrative and Comparative Physiology* 2005; **289**: R1798–R1806.

149 Zhang G, Bai H, Zhang H, Dean C, Wu Q, Li J *et al.* Neuropeptide Exocytosis Involving Synaptotagmin-4 and Oxytocin in Hypothalamic Programming of Body Weight and Energy Balance. *Neuron* 2011; **69**: 523–535.

150 Rosskamp R. [Growth hormone releasing hormone. Review]. *Klinische Padiatrie* 1988; **200**: 81–88.

151 Boron, W; Boulpaep EL, Walter F, Boron. *Medical Physiology: A Cellular and Molecular Approaoch.* 2003http://books.google.com/books?id=HlMJRw08ihgC&printsec=frontcover.

152 Grossman a, Savage MO, Besser GM. Growth hormone releasing hormone. *Clinics in endocrinology and metabolism* 1986; **15**: 607–27.

153 Lechan RM, Fekete C. Chapter 12: The TRH neuron: a hypothalamic integrator of energy metabolism. Progress in Brain Research. 2006; **153**: 209–235.

154 JACKSON IMD, REICHLIN S. Brain thyrotrophin-releasing hormone is independent of the hypothalamus. *Nature* 1977; **267**: 853–854.

155 Chiamolera MI, Wondisford FE. Thyrotropin-Releasing Hormone and the Thyroid

Hormone Feedback Mechanism. *Endocrinology* 2009; **150**: 1091–1096.

156 Bowers CY, Friesen HG, Hwang P, Guyda HJ, Folkers K. Prolactin and thyrotropin release in man by synthetic pyroglutamyl-histidyl-prolinamide. *Biochemical and Biophysical Research Communications* 1971; **45**: 1033–1041.

157 Wilber JF, Utiger RD. In vitro studies on mechanism of action of thyrotropin releasing factor. *Proceedings of the Society for Experimental Biology and Medicine Society for Experimental Biology and Medicine (New York, NY)* 1968; **127**: 488–90.

158 Horita A. An update on the CNS actions of TRH and its analogs. In: *Life Sciences*. 1998, pp 1443–1448.

159 Steward C a, Horan TL, Schuhler S, Bennett GW, Ebling FJP. Central administration of thyrotropin releasing hormone (TRH) and related peptides inhibits feeding behavior in the Siberian hamster. *Neuroreport* 2003; **14**: 687–691.

160 Suzuki T, Kohno H, Sakurada T, Tadano T, Kisara K. Intracranial injection of thyrotropin releasing hormone (TRH) suppresses starvation-induced feeding and drinking in rats. *Pharmacology, Biochemistry and Behavior* 1982; **17**: 249–253.

161 Morley JE. The neuroendocrine control of appetite: The role of the endogenous opiates, cholecystokinin, TRH, gamma-amino-butyric-acid and the diazepam receptor. *Life Sciences* 1980; **27**: 355–368.

162 Vijayan E, McCann SM. Suppression of feeding and drinking activity in rats following intraventricular injection of thyrotropin releasing hormone (TRH). *Endocrinology* 1977; **100**: 1727–1729.

163 Vogel RA, Cooper BR, Barlow TS, Prange AJ, Mueller RA, Breese GR. Effects of

thyrotropin-releasing hormone on locomotor activity, operant performance and ingestive behavior. *The Journal of pharmacology and experimental therapeutics* 1979; **208**: 161–8.

164 Choi YH, Hartzell D, Azain MJ, Baile CA. TRH decreases food intake and increases water intake and body temperature in rats. *Physiology and Behavior* 2002; **77**: 1–4.

165 Castañeda TR, Jürgens H, Wiedmer P, Pfluger P, Diano S, Horvath TL *et al.* Obesity and the neuroendocrine control of energy homeostasis: the role of spontaneous locomotor activity. *The Journal of nutrition* 2005; **135**: 1314–1319.

166 Ervin GN, Schmitz SA, Nemeroff CB, Prange AJ. Thyrotropin-releasing hormone and amphetamine produce different patterns of behavioral excitation in rats. *European Journal of Pharmacology* 1981; **72**: 35–43.

167 Wei E, Sigel S, Loh H, Way EL. Thyrotrophin releasing hormone and shaking behavior in rat. *Nature* 1975; **253**: 739–740.

168 Zhang X, van den Pol a. N. Thyrotropin-Releasing Hormone (TRH) Inhibits Melanin-Concentrating Hormone Neurons: Implications for TRH-Mediated Anorexic and Arousal Actions. *Journal of Neuroscience* 2012; **32**: 3032–3043.

169 Brownstein MJ, Russell JT, Gainer H. Synthesis, transport, and release of posterior pituitary hormones. *Science (New York, NY)* 1980; **207**: 373–378.

170 Caldwell H, Iii WY. Oxytocin and Vasopressin: Genetics and Behavioral Implications. *Handbook of Neurochemistry and Molecular Neurobiology* 2006; : 573–607.

171 Nielsen S, Chou CL, Marples D, Christensen EI, Kishore BK, Knepper MA. Vasopressin increases water permeability of kidney collecting duct by inducing

translocation of aquaporin-CD water channels to plasma membrane. *Proceedings of the National Academy of Sciences of the United States of America* 1995; **92**: 1013–7.

172 Meyer AH, Langhans W, Scharrer E. Vasopressin reduces food intake in goats. *Quarterly journal of experimental physiology (Cambridge, England)* 1989; **74**: 465–473.

173 Miyata A, Arimura A, Dahl RR, Minamino N, Uehara A, Jiang L *et al.* Isolation of a novel 38 residue-hypothalamic polypeptide which stimulates adenylate cyclase in pituitary cells. *Biochemical and Biophysical Research Communications* 1989; **164**: 567–574.

174 Vaudry D, Falluel-Morel A, Bourgault S, Basille M, Burel D, Wurtz O *et al.* Pituitary adenylate cyclase-activating polypeptide and its receptors: 20 years after the discovery. *Pharmacological reviews* 2009; **61**: 283–357.

175 Vaudry D, Gonzalez BJ, Basille M, Yon L, Fournier a, Vaudry H. Pituitary adenylate cyclase-activating polypeptide and its receptors: from structure to functions. *Pharmacological reviews* 2000; **52**: 269–324.

176 Morley JE, Horowitz M, Morley PMK, Flood JF. Pituitary adenylate cyclase activating polypeptide (PACAP) reduces food intake in mice. *Peptides* 1992; **13**: 1133–1135.

177 Mizuno Y, Kondo K, Terashima Y, Arima H, Murase T, Oiso Y. Anorectic effect of pituitary adenylate cyclase activating polypeptide (PACAP) in rats: Lack of evidence for involvement of hypothalamic neuropeptide gene expression. *Journal of Neuroendocrinology* 1998; **10**: 611–616.

178 Chance WT, Thompson H, Thomas I, Fischer JE. Anorectic and neurochemical effects of pituitary adenylate cyclase activating polypeptide in rats. *Peptides* 1995; **16**: 1511–

1516.

179 Tachibana T, Saito S, Tomonaga S, Takagi T, Saito ES, Boswell T *et al.* Intracerebroventricular injection of vasoactive intestinal peptide and pituitary adenylate cyclase-activating polypeptide inhibits feeding in chicks. *Neuroscience Letters* 2003; **339**: 203–206.

180 Matsuda K. Recent advances in the regulation of feeding behavior by neuropeptides in fish. In: *Annals of the New York Academy of Sciences*. 2009, pp 241–250.

181 Vale W, Spiess J, Rivier C, Rivier J. Characterization of a 41-residue ovine hypothalamic peptide that stimulates secretion of corticotropin and beta-endorphin. *Science (New York, NY)* 1981; **213**: 1394–1397.

182 Hillebrand JJG, de Wied D, Adan R a. H. Neuropeptides, food intake and body weight regulation: a hypothalamic focus. *Peptides* 2002; **23**: 2283–2306.

183 Matsuda K. Regulation of feeding behavior and psychomotor activity by corticotropin-releasing hormone (CRH) in fish. *Frontiers in Neuroscience* 2013. doi:10.3389/fnins.2013.00091.

184 Finley JCW, Maderdrut JL, Roger LJ, Petrusz P. The immunocytochemical localization of somatostatin-containing neurons in the rat central nervous system. *Neuroscience* 1981; **6**: 2173–2192.

185 Viollet C, Lepousez G, Loudes C, Videau C, Simon A, Epelbaum J. Somatostatinergic systems in brain: Networks and functions. *Molecular and Cellular Endocrinology* 2008; **286**: 75–87.

186 Beranek L, Hajdu I, Gardi J, Taishi P, Obál F, Krueger JM. Central administration of

the somatostatin analog octreotide induces captopril-insensitive sleep responses. *The American journal of physiology* 1999; **277**: R1297-304.

187 Feifel D, Vaccarino FJ. Central somatostatin: a re-examination of its effects on feeding. *Brain Research* 1990; **535**: 189–194.

188 Rezek M, Havlicek V, Hughes KR, Friesen H. Central site of action of somatostatin (SRIF): Role of hippocampus. *Neuropharmacology* 1976; **15**: 499–504.

189 Cummings SL, Truong BG, Gietzen DW. Neuropeptide Y and somatostatin in the anterior piriform cortex alter intake of amino acid-deficient diets. *Peptides* 1998; **19**: 527–535.

190 Nakahara K, Takata S, Ishii A, Nagao K, Bannai M, Takahashi M *et al.* Somatostatin is involved in anorexia in mice fed a valine-deficient diet. *Amino Acids* 2012; **42**: 1397–1404.

191 Tannenbaum GS, Patel YC. On the fate of centrally administered somatostatin in the rat: massive hypersomatostatinemia resulting from leakage into the peripheral circulation has effects on growth hormone secretion and glucoregulation. *Endocrinology* 1986; **118**: 2137–43.

192 Bray GA. Nutrient intake is modulated by peripheral peptide administration. *Obesity research* 1995; **3 Suppl 4**: 569S–572S.

193 Stengel A, Karasawa H, Taché Y. The role of brain somatostatin receptor 2 in the regulation of feeding and drinking behavior. *Hormones and Behavior* 2015; **73**: 15–22.

194 Yeo GS, Farooqi IS, Aminian S, Halsall DJ, Stanhope RG, O'Rahilly S. A frameshift mutation in MC4R associated with dominantly inherited human obesity. *Nature*

genetics 1998; **20**: 111–112.

195 Gantz I, Miwa H, Konda Y, Shimoto Y, Tashiro T, Watson SJ *et al.* Molecular cloning, expression, and gene localization of a fourth melanocortin receptor. *Journal of Biological Chemistry* 1993; **268**: 15174–15179.

196 Vergoni AV, Bertolini A. Role of melanocortins in the central control of feeding. In: *European Journal of Pharmacology*. 2000, pp 25–32.

197 Cone RD. The central melanocortin system and energy homeostasis. Trends in Endocrinology and Metabolism. 1999; **10**: 211–216.

198 Mountjoy KG, Mortrud MT, Low MJ, Simerly RB, Cone RD. Localization of the melanocortin-4 receptor (MC4-R) in neuroendocrine and autonomic control circuits in the brain. *Molecular endocrinology* 1994; **8**: 1298–1308.

199 Balthasar N, Dalgaard LT, Lee CE, Yu J, Funahashi H, Williams T *et al.* Divergence of melanocortin pathways in the control of food intake and energy expenditure. *Cell* 2005; **123**: 493–505.

200 Ahima RS, Flier JS. Leptin. *Annu Rev Physiol* 2000; **62**: 413–437.

201 Elias CF, Aschkenasi C, Lee C, Kelly J, Ahima RS, Bjorb??k C *et al.* Leptin differentially regulates NPY and POMC neurons projecting to the lateral hypothalamic area. *Neuron* 1999; **23**: 775–786.

202 Fan W, Boston B a, Kesterson R a, Hruby VJ, Cone RD. Role of melanocortinergic neurons in feeding and the agouti obesity syndrome. Nature. 1997; **385**: 165–168.

203 Seeley RJ, Yagaloff K a, Fisher SL, Burn P, Thiele TE, van Dijk G *et al.* Melanocortin receptors in leptin effects. *Nature* 1997; **390**: 349.

204 Ghamari-Langroudi M, Digby GJ, Sebag JA, Millhauser GL, Palomino R, Matthews R *et al.* G-protein-independent coupling of MC4R to Kir7.1 in hypothalamic neurons. *Nature* 2015; **520**: 94–98.

205 Garfield AS, Li C, Madara JC, Shah BP, Webber E, Steger JS *et al.* A neural basis for melanocortin-4 receptor-regulated appetite. *Nature neuroscience* 2015; **18**: 863–871.

206 Ward MP, Mosher JT, Crews ST. Regulation of bHLH-PAS protein subcellular localization during Drosophila embryogenesis. *Development (Cambridge, England)* 1998; **125**: 1599–1608.

207 Michaud JL, Rosenquist T, May NR, Fan CM. Development of neuroendocrine lineages requires the bHLH-PAS transcription factor SIM1. *Genes and Development* 1998; **12**: 3264–3275.

208 Michaud JL, Derossi C, May NR, Holdener BC, Fan CM. ARNT2 acts as the dimerization partner of SIM1 for the development of the hypothalamus. *Mechanisms of Development* 2000; **90**: 253–261.

209 Bersten DC, Sullivan AE, Peet DJ, Whitelaw ML. bHLH-PAS proteins in cancer. *Nature reviews Cancer* 2013; **13**: 827–41.

210 Wu D, Potluri N, Lu J, Kim Y, Rastinejad F. Structural integration in hypoxia-inducible factors. *Nature* 2015; **524**: 303–8.

211 Farooqi I, Rahilly SO. Monogenic Obesity in Humans. *Annual Review of Medicine* 2005; **56**: 443–56.

212 Holder JL, Butte NF, Zinn a R. Profound obesity associated with a balanced translocation that disrupts the SIM1 gene. *Human molecular genetics* 2000; **9**: 101–

108.

213 Xu C, Fan C-M. Allocation of paraventricular and supraoptic neurons requires Sim1 function: a role for a Sim1 downstream gene PlexinC1. *Molecular endocrinology (Baltimore, Md)* 2007; **21**: 1234–1245.

214 Leibowitz SF, Hammer NJ, Chang K. Hypothalamic paraventricular nucleus lesions produce overeating and obesity in the rat. *Physiology and Behavior* 1981; **27**: 1031–1040.

215 Tolson KP, Gemelli T, Gautron L, Elmquist JK, Zinn AR, Kublaoui BM. Postnatal Sim1 deficiency causes hyperphagic obesity and reduced Mc4r and oxytocin expression. *The Journal of neuroscience : the official journal of the Society for Neuroscience* 2010; **30**: 3803–3812.

216 Kublaoui BM, Gemelli T, Tolson KP, Wang Y, Zinn AR. Oxytocin deficiency mediates hyperphagic obesity of Sim1 haploinsufficient mice. *Molecular endocrinology (Baltimore, Md)* 2008; **22**: 1723–1734.

217 Blevins JE, Eakin TJ, Murphy JA, Schwartz MW, Baskin DG. Oxytocin innervation of caudal brainstem nuclei activated by cholecystokinin. *Brain Research* 2003; **993**: 30–41.

218 Xu Y, Wu Z, Sun H, Zhu Y, Kim ER, Lowell BB *et al.* Glutamate mediates the function of melanocortin receptor 4 on Sim1 neurons in body weight regulation. *Cell Metabolism* 2013; **18**: 860–870.

219 Kublaoui BM, Holder JL, Tolson KP, Gemelli T, Zinn AR. SIM1 overexpression partially rescues agouti yellow and diet-induced obesity by normalizing food intake. *Endocrinology* 2006; **147**: 4542–4549.

220 Tolson KP, Gemelli T, Meyer D, Yazdani U, Kozlitina J, Zinn AR. Inducible neuronal inactivation of Sim1 in adult mice causes hyperphagic obesity. *Endocrinology* 2014; **155**: 2436–2444.

221 Kohler SW, Provost GS, Fieck a, Kretz PL, Bullock WO, Sorge J a *et al.* Spectra of spontaneous and mutagen-induced mutations in the lacI gene in transgenic mice. *Proceedings of the National Academy of Sciences of the United States of America* 1991; **88**: 7958–7962.

222 Masuya H, Nakai Y, Motegi H, Niinaya N, Kida Y, Kaneko Y *et al.* Development and implementation of a database system to manage a large-scale mouse ENU-mutagenesis program. Mammalian Genome. 2004; **15**: 404–411.

223 Provost GS, Short JM. Characterization of mutations induced by ethylnitrosourea in seminiferous tubule germ cells of transgenic B6C3F1 mice. *Proceedings of the National Academy of Sciences of the United States of America* 1994; **91**: 6564–8.

224 Mekada K, Abe K, Murakami A, Nakamura S, Nakata H, Moriwaki K *et al.* Genetic differences among C57BL/6 substrains. *Experimental animals* 2009; **58**: 141–149.

225 Hossain MS, Asano F, Fujiyama T, Miyoshi C, Sato M, Ikkyu A *et al.* Identification of mutations through dominant screening for obesity using C57BL/6 substrains. *Scientific Reports* 2016; **6**: 32453.

226 Wharton K a, Franks RG, Kasai Y, Crews ST. Control of CNS midline transcription by asymmetric E-box-like elements: similarity to xenobiotic responsive regulation. *Development (Cambridge, England)* 1994; **120**: 3563–3569.

227 Moffett P, Pelletier J. Different transcriptional properties of mSim-1 and mSim-2. *FEBS Letters* 2000; **466**: 80–86.

228 Zegers D, Beckers S, Hendrickx R, Van Camp JK, de Craemer V, Verrijken a *et al.* Mutation screen of the SIM1 gene in pediatric patients with early-onset obesity. *International Journal of Obesity* 2014; **38**: 1000–1004.

229 Davila S, Furu L, Gharavi AG, Tian X, Onoe T, Qian Q *et al.* Mutations in SEC63 cause autosomal dominant polycystic liver disease. *Nature genetics* 2004; **36**: 575–7.

230 Zimmermann R, M??ller L, Wullich B. Protein transport into the endoplasmic reticulum: mechanisms and pathologies. *Trends in Molecular Medicine* 2006; **12**: 567–573.

231 Loos RJF. The genetic epidemiology of melanocortin 4 receptor variants. European Journal of Pharmacology. 2011; **660**: 156–164.

232 Locke A, Kahali B, Berndt S, Justice A, Pers T. Genetic studies of body mass index yield new insights for obesity biology. *Nature* 2015; **518**: 197–206.

233 Thorleifsson G, Walters GB, Gudbjartsson DF, Steinthorsdottir V, Sulem P, Helgadottir A *et al.* Genome-wide association yields new sequence variants at seven loci that associate with measures of obesity. *Nature genetics* 2009; **41**: 18–24.

234 Willer CJ, Speliotes EK, Loos RJF, Li S, Lindgren CM, Heid IM *et al.* Six new loci associated with body mass index highlight a neuronal influence on body weight regulation. *Nature genetics* 2009; **41**: 25–34.

235 Huszar D, Lynch CA, Fairchild-Huntress V, Dunmore JH, Fang Q, Berkemeier LR *et al.* Targeted Disruption of the Melanocortin-4 Receptor Results in Obesity in Mice. *Cell* 1997; **88**: 131–141.

236 Tao YX. The melanocortin-4 receptor: Physiology, pharmacology, and

pathophysiology. Endocrine Reviews. 2010; **31**: 506–543.

237 Bonnefond A, Raimondo A, Stutzmann F, Ghoussaini M, Ramachandrappa S, Bersten DC *et al.* Loss-of-function mutations in SIM1 contribute to obesity and Prader-Willi-like features. *Journal of Clinical Investigation* 2013; **123**: 3037–3041.

238 Ramachandrappa S, Raimondo A, Cali AMG, Keogh JM, Henning E, Saeed S *et al.* Rare variants in single-minded 1 (SIM1) are associated with severe obesity. *Journal of Clinical Investigation* 2013; **123**: 3042–3050.

239 Montagne L, Raimondo A, Delobel B, Duban-Bedu B, Noblet FS, Dechaume A *et al.* Identification of two novel loss-of-function SIM1 mutations in two overweight children with developmental delay. *Obesity* 2014; **22**: 2621–2624.

240 Michaud JL, Boucher F, Melnyk a, Gauthier F, Goshu E, Lévy E *et al.* Sim1 haploinsufficiency causes hyperphagia, obesity and reduction of the paraventricular nucleus of the hypothalamus. *Human molecular genetics* 2001; **10**: 1465–1473.

241 Holder JL, Zhang L, Kublaoui BM, DiLeone RJ, Oz OK, Bair CH *et al.* Sim1 gene dosage modulates the homeostatic feeding response to increased dietary fat in mice. *American journal of physiology Endocrinology and metabolism* 2004; **287**: E105–E113.

242 De Luca C, Kowalski TJ, Zhang Y, Elmquist JK, Lee C, Kilimann MW *et al.* Complete rescue of obesity, diabetes, and infertility in db/db mice by neuron-specific LEPR-B transgenes. *Journal of Clinical Investigation* 2005; **115**: 3484–3493.

243 Wang T, Zhan X, Bu C-H, Lyon S, Pratt D, Hildebrand S *et al.* Real-time resolution of point mutations that cause phenovariance in mice. *Proceedings of the National Academy of Sciences* 2015; **112**: E440–E449.

244 Yeo GSH. Mutations in the human melanocortin-4 receptor gene associated with severe familial obesity disrupts receptor function through multiple molecular mechanisms. *Human Molecular Genetics* 2003; **12**: 561–574.

245 Trevaskis JL, Butler AA. Double leptin and melanocortin-4 receptor gene mutations have an additive effect on fat mass and are associated with reduced effects of leptin on weight loss and food intake. *Endocrinology* 2005; **146**: 4257–4265.

246 Bates SH, Myers MG. The role of leptin receptor signaling in feeding and neuroendocrine function. Trends in Endocrinology and Metabolism. 2003; **14**: 447–452.

247 Cohen P, Zhao C, Cai X, Montez JM, Rohani SC, Feinstein P *et al.* Selective deletion of leptin receptor in neurons leads to obesity. *Journal of Clinical Investigation* 2001; **108**: 1113–1121.

248 Sadaf Farooqi I, O'Rahilly S. Leptin: A pivotal regulator of human energy homeostasis. In: *American Journal of Clinical Nutrition*. 2009 doi:10.3945/ajcn.2008.26788C.

249 Friedman JM, Halaas JL. Leptin and the regulation of body weight in mammals. *Nature* 1998; **395**: 763–770.

250 Ste Marie L, Miura GI, Marsh DJ, Yagaloff K, Palmiter RD. A metabolic defect promotes obesity in mice lacking melanocortin-4 receptors. *Proceedings of the National Academy of Sciences of the United States of America* 2000; **97**: 12339–44.

251 Polonsky KS, Given BD, Van Cauter E. Twenty-four-hour profiles and pulsatile patterns of insulin secretion in normal and obese subjects. *Journal of Clinical Investigation* 1988; **81**: 442–448.

252 Varela MC, Simões-Sato AY, Kim CA, Bertola DR, De Castro CIE, Koiffmann CP. A new case of interstitial 6q16.2 deletion in a patient with Prader-Willi-like phenotype and investigation of SIM1 gene deletion in 87 patients with syndromic obesity. *European Journal of Medical Genetics* 2006; **49**: 298–305.

253 Bonaglia MC, Ciccone R, Gimelli G, Gimelli S, Marelli S, Verheij J *et al.* Detailed phenotype-genotype study in five patients with chromosome 6q16 deletion: narrowing the critical region for Prader-Willi-like phenotype. *European journal of human genetics : EJHG* 2008; **16**: 1443–1449.

254 Kublaoui BM, Holder JL, Gemelli T, Zinn AR. Sim1 haploinsufficiency impairs melanocortin-mediated anorexia and activation of paraventricular nucleus neurons. *Molecular endocrinology (Baltimore, Md)* 2006; **20**: 2483–2492.

255 Fedeles S V, Tian X, Gallagher A-R, Mitobe M, Nishio S, Lee SH *et al.* A genetic interaction network of five genes for human polycystic kidney and liver diseases defines polycystin-1 as the central determinant of cyst formation. *Nature genetics* 2011; **43**: 639–647.

256 Lang S, Benedix J, Fedeles S V., Schorr S, Schirra C, Schauble N *et al.* Different effects of Sec61 , Sec62 and Sec63 depletion on transport of polypeptides into the endoplasmic reticulum of mammalian cells. *Journal of Cell Science* 2012; **125**: 1958–1969.

257 Coiro V, Capretti L, Speroni G, Castelli A, Bianconi L, Cavazzini U *et al.* Increase by naloxone of arginine vasopressin and oxytocin responses to insulin-induced hypoglycemia in obese men. *Journal of Endocrinological Investigation: Official Journal of the Italian Society of Endocrinology* 1990; **13**: 757–763.

258 Fujikawa T, Chuang J-C, Sakata I, Ramadori G, Coppari R. Leptin therapy improves insulin-deficient type 1 diabetes by CNS-dependent mechanisms in mice. *Proceedings of the National Academy of Sciences of the United States of America* 2010; **107**: 17391–17396.

259 Xi D, Gandhi N, Lai M, Kublaoui BM. Ablation of Sim1 neurons causes obesity through hyperphagia and reduced energy expenditure. *PLoS ONE* 2012; **7**. doi:10.1371/journal.pone.0036453.

260 Sakurai T. The role of orexin in motivated behaviours. *Nature Reviews Neuroscience* 2014; **15**: 719–731.

261 Koza RA, Nikonova L, Hogan J, Rim JS, Mendoza T, Faulk C *et al.* Changes in gene expression foreshadow diet-induced obesity in genetically identical mice. *PLoS Genetics* 2006; **2**: 769–780.

262 Funato H, Tsai AL, Willie JT, Kisanuki Y, Williams SC, Sakurai T *et al.* Enhanced Orexin Receptor-2 Signaling Prevents Diet-Induced Obesity and Improves Leptin Sensitivity. *Cell Metabolism* 2009; **9**: 64–76.

263 Huang XF, Han M, South T, Storlien L. Altered levels of POMC, AgRP and MC4-R mRNA expression in the hypothalamus and other parts of the limbic system of mice prone or resistant to chronic high-energy diet-induced obesity. *Brain research* 2003; **992**: 9–19.

264 Ross AW, Russell L, Helfer G, Thomson LM, Dalby MJ, Morgan PJ. Photoperiod regulates lean mass accretion, but not adiposity, in growing F344 rats fed a high fat diet. *PLoS ONE* 2015; **10**. doi:10.1371/journal.pone.0119763.

265 Yasrebi A, Hsieh A, Mamounis KJ, Krumm EA, Yang JA, Magby J *et al.* Differential

gene regulation of GHSR signaling pathway in the arcuate nucleus and NPY neurons by fasting, diet-induced obesity, and 17β-estradiol. *Molecular and Cellular Endocrinology* 2016; **422**: 42–56.

266 Yu Y, Deng C, Huang XF. Obese reversal by a chronic energy restricted diet leaves an increased Arc NPY/AgRP, but no alteration in POMC/CART, mRNA expression in diet-induced obese mice. *Behavioural Brain Research* 2009; **205**: 50–56.

267 Wren AM, Small CJ, Fribbens C V., Neary NM, Ward HL, Seal LJ *et al.* The hypothalamic mechanisms of the hypophysiotropic action of ghrelin. *Neuroendocrinology* 2002; **76**: 316–324.

268 Ahmad I, Finkelstein JA, Downs TR, Frohman LA. Obesity-associated decrease in growth hormone-releasing hormone gene expression: a mechanism for reduced growth hormone mRNA levels in genetically obese Zucker rats. *Neuroendocrinology* 1993; **58**: 332–337.

269 Iwakura H, Akamizu T, Ariyasu H, Irako T, Hosoda K, Nakao K *et al.* Effects of ghrelin administration on decreased growth hormone status in obese animals. *American journal of physiology Endocrinology and metabolism* 2007; **293**: E819–E825.

270 Takase K, Tsuneoka Y, Oda S, Kuroda M, Funato H. High-fat diet feeding alters olfactory-, social-, and reward-related behaviors of mice independent of obesity. *Obesity* 2016; **24**: 886–894.

271 Vaisse C, Clement K, Guy-grand B, Froguel P. A frameshift mutation in human MC4R is associated with a dominant form of obesity. *Nature genetics* 1998; **20**: 113–114.

参 考 論 文 (**Reference paper)**

1. Hossain, M.S., Asano, F., Fujiyama, T., Miyoshi, C., Sato, M., Ikkyu, A., Kanno, S., Hotta, N., Kakizaki, M., Honda, T., Kim, S.J., Komiya, H., Miura, I., Suzuki, T., Kobayashi, K., Kaneda, H., Kumar, V., Takahashi, J.S., Wakana, S., Funato, H., Yanagisawa, M. Identification of mutations through dominant screening for obesity using C57BL/6 substrains. *Scientific Reports* 2016; **6**: 32453.